

OPTICAL QUANTAL ANALYSIS OF EVOKED AND SPONTANEOUS SINGLE-
VESICLE FUSION

APPROVED BY SUPERVISORY COMMITTEE

Donald Hilgemann, Ph.D

Ege Kavalali, Ph.D

Robin Hiesinger, Ph.D

Joseph Albanesi, Ph.D

DEDICATION

I would like to thank the members of my Graduate Committee, my family, my significant other, my friends, all of my teachers, and so on and so forth.

OPTICAL QUANTAL ANALYSIS OF EVOKED AND SPONTANEOUS SINGLE-
VESICLE FUSION

by

JEREMY THOMAS SHENG LEITZ

DISSERTATION

Presented to the Faculty of the Graduate School of Biomedical Sciences

The University of Texas Southwestern Medical Center at Dallas

In Partial Fulfillment of the Requirements

For the Degree of

DOCTOR OF PHILOSOPHY

The University of Texas Southwestern Medical Center at Dallas

Dallas, Texas

August 2014

Copyright

by

Jeremy Thomas Sheng Leitz, 2014

All Rights Reserved

OPTICAL QUANTAL ANALYSIS OF EVOKED AND SPONTANEOUS SINGLE-
VESICLE FUSION

Publication No. _____

Jeremy Thomas Sheng Leitz, Ph.D.

The University of Texas Southwestern Medical Center at Dallas, 2014

Supervising Professor: Ege Kavalali, Ph.D.

Synaptic vesicle recycling is critical for the maintenance and proper function of neurotransmission. Neurotransmission can proceed through action-potential evoked vesicle fusion where, upon depolarization, Ca^{2+} enters the nerve terminal through voltage-gated channels, interacts with vesicle-associated proteins to promote fusion with the terminal membrane, and causes release of vesicle contents. Neurotransmission can also occur spontaneously in the absence of stimulation, although this process is still Ca^{2+} -dependent. Regardless of the mode of vesicle fusion, the vesicle lipids and protein components must be removed from the terminal membrane; the vesicle must be reconstituted and re-filled with

neurotransmitter, so that it may ultimately be reused. Uncoupling the roles of Ca^{2+} in synaptic vesicle fusion and retrieval has been difficult to date as studies have relied on measurements of bulk synaptic vesicle retrieval. Here, to dissect the role of Ca^{2+} in these processes, we utilized low signal-to-noise pHluorin-tagged vesicular probes to monitor single synaptic vesicle recycling of both action-potential evoked and spontaneous fusion vesicles in rat hippocampal neurons.

We show that during stimulation, increasing extracellular Ca^{2+} increases synaptic vesicle fusion probability, but decreases the rate of synaptic vesicle retrieval. This negative regulation of synaptic vesicle retrieval is blocked by the Ca^{2+} chelation as well as inhibition of calcineurin, a Ca^{2+} -calmodulin-dependent phosphatase. Indeed, the slow time course of aggregate synaptic vesicle retrieval detected during repetitive activity can be explained by a progressive decrease in the rate of synaptic vesicle retrieval during the stimulation train. These results indicate Ca^{2+} entry during single action potentials slows the pace of subsequent synaptic vesicle recycling. Conversely, we found that synaptic vesicles that undergo spontaneous fusion are retrieved very rapidly and this retrieval time is Ca^{2+} -independent. Interestingly, we found that within a single synaptic bouton, the rate of spontaneous neurotransmission is independent of evoked fusion probability, suggesting there are fundamental regulatory differences between these forms of neurotransmission. Moreover, we found that the glycoprotein Reelin can act presynaptically to enhance spontaneous neurotransmission without affecting evoked neurotransmission by mobilizing a molecularly specific subset of synaptic vesicles. These data illustrate fundamental differences in vesicle recycling between modes of neurotransmission at the single-vesicle level.

TABLE OF CONTENTS

DEDICATION	<i>iii</i>
ABSTRACT	<i>vi</i>
TABLE OF CONTENTS	<i>vii</i>
PRIOR PUBLICATIONS	<i>xiv</i>
LIST OF FIGURES	<i>xv</i>
LIST OF DEFINITIONS	<i>xviii</i>
CHAPTER 1: GENERAL INTRODUCTION	1
1.1 ULTRASTRUCTURE OF THE SYNAPSE	1
1.2 THE SYNAPTIC VESICLE	2
1.2.1 MOLECULAR ANATOMY OF A SYNAPTIC VESICLE	2
1.2.2 SYNAPTIC VESICLE POOLS	4
1.3 MODES OF SYNAPTIC VESICLE FUSION	5
1.3.1 SYNCHRONOUS FUSION	6
1.3.2 ASYNCHRONOUS FUSION	9
1.3.3 SPONTANEOUS FUSION	12
1.3.4 FULL-COLLAPSE AND KISS-AND-RUN FUSION MODES	16
1.4 SYNAPTIC VESICLE RETRIEVAL	18
1.4.1 CALCIUM TRIGGERS ENDOCYTOSIS	19
1.4.2 CALCIUM MODULATES THE RATE OF ENDOCYTOSIS	22
1.4.3 ENDOCYTOSIS AT THE SINGLE VESICLE LEVEL	26

CHAPTER 2: CALCIUM INFLUX SLOWS SINGLE SYNAPTIC VESICLE

ENDOCYTOSIS	30
2.1 BACKGROUND	30
2.2 METHODS	32
2.2.1 DISSOCIATED CULTURES.....	32
2.2.2 CALCIUM CHELATION AND CLACINEURIN INHIBITION	32
2.2.3 FLUORESCENCE IMAGING.....	33
2.2.4 FLUORESCENCE ANALYSIS.....	33
2.2.5 STIMULATION PROTOCOL	33
2.2.6 RECONSTRUCTION OF ENDOCYTIC RETREIVAL DURING 1 HZ STIMULATION	34
2.3 RESULTS	34
2.3.1 DETECTION OF SYNAPTIC VESICLE FUSION AND RETRIEVAL DURING LOW-FREQUENCY STIMULATION	34
2.3.2 CALCIUM-DEPENDENT REGULATION OF SINGLE SYNAPTIC VESICLE FUSION PROBABILITY	38
2.3.3 THE EFFECT OF CALCIUM ON MULTIVESICULAR RELEASE	41
2.3.4 THE EFFECT OF CALCIUM ON SINGLE SYNAPTIC VESICLE RETRIEVAL	43
2.3.5 THE RELATION BETWEEN PROBABILITY OF SYNAPTIC VESICLE FUSION AND SYNAPTIC VESICLE TRAFFICKING.....	44

2.3.6 INTRASYNAPTIC CALCIUM ACTS TO MODULATE VESICLE ENDOCYTOSIS	47
2.3.7 INTRASYNAPTIC CALCIUM ACTS VIA CALCINEURIN TO MODULATE VESICLE ENDOCYTOSIS.....	47
2.3.8 ESTIMATING SINGLE-VESICLE RETRIEVAL DURING HIGHER- FREQUENCY STIMULATION	50
2.4 DISCUSSION.....	53
2.4.1 SINGLE VESICLE ENDOCYTOSIS IS RAPID	53
2.4.2 CALCIUM INCREASES VESICLE FUSION PROBABILITY AND SLOWS RETRIEVAL.....	54
2.4.3 ENDOCYTOSIS PROGRESSIVELY SLOWS DURING HIGH FREQUENCY STIMULATION	56
CHAPTER 3: FAST RETRIEVAL AND AUTONOMOUS REGULATION OF SINGLE SPONTANEOUSLY RECYCLING SYNAPTIC VESICLES	58
3.1 BACKGROUND	58
3.2 METHODS	60
3.2.1 CELL CULTURE	60
3.2.2 LENTIVIRAL PREPARATIONS.....	60
3.2.3 VGLUT1-PHLUORIN IMAGING AND ANALYSIS	61
3.2.4 SYPHATOMATO/PSD95-GCAMP5K IMAGING AND ANALYSIS	62
3.2.5 MULTIVESICULAR DECAY ANALYSIS.....	63

3.3 RESULTS	64
3.3.1 SYNAPTIC VESICLES THAT FUSE SPONTANEOUSLY RECYCLE RAPIDLY	64
3.3.2 DUAL COLOR IMAGING SHOWS THAT SPONTANEOUSLY FUSING VESICLES ELICIT POSTSYNAPTIC CALCIUM SIGNALS	67
3.3.3 INCREASING EXTRACELLULAR TRIGGERS MULTIPLE SPONTANEOUS FUSION EVENTS	71
3.3.4 CALCIUM DOES NOT ALTER THE KINETICS OF FLUOREESCENCE TRANSIENTS ORIGINATING FROM SPONTANEOUS FUSION EVENTS	75
3.3.5 INCREASING EXTRACELLULAR CALCIUM CONCENTRATION INCREASES THE FREQUENCY OF FAST SPONTANEOUS VESICLE FUSION AND RETRIEVAL	79
3.3.6 THE RATE OF SPONTANEOUS SYNAPTIC VESICLE FUSION AND THE PROBABILITY OF STIMULATION-EVOKED FUSION DO NOT CORRELATE WITHIN A GIVEN SYNAPSE	81
3.4 DISCUSSION	83
CHAPTER 4: REELIN MOBILIZES A VAMP7-DEPENDENT SYNAPTIC VESICLE POOL AND SELECTIVELY AUGMENTS SPONTANEOUS NEUROTRANSMISSION.....	88

4.1 BACKGROUND	88
4.2 METHODS	90
4.2.1 CELL CULTURE AND MOUSE LINES	90
4.2.2 LENTIVIRAL PREPARATIONS	91
4.2.3 ELECTROPHYSIOLOGY	92
4.2.4 REELIN AND PHARMACOLOGY	93
4.2.5 SINGLE COLOR IMAGING	94
4.2.6 DUAL COLOR IMAGING	95
4.2.7 STATISTICAL ANALYSIS	95
4.2.8 APOER2 AND SYNAPSIN IMMUNOCYTOCHEMISTRY	96
4.3 RESULTS	96
4.3.1 REELIN CAUSES AN INCREASE IN SPONTANEOUS NEUROTRANSMITTER RELEASE	96
4.3.2 REELIN SELECTIVELY AUGMENTS SPONTANEOUS TRANSMISSION.....	100
4.3.3 REELIN-DEPENDENT FACILITATION OF SPONTANEOUS TRANSMISSION REQUIRES SNAP-25 BUT NOT SYB2	104
4.3.4 REELIN FACILITATES TRAFFICKING OF VAMP7-EXPRESSING SYNAPTIC VESICLES	106
4.3.5 REELIN SELECTIVELY ACTS ON VAMP7 EXPRESSING SYNAPTIC VESICLES WITHIN AN INDIVIDUAL SYNAPTIC TERMINAL	108
4.3.6 VAMP7 KNOCKDOWN ABOLISHES THE EFFECT OF REELIN.....	110

4.4 DISCUSSION.....	111
CHAPTER 5: CONCLUSIONS AND FUTURE DIRECTIONS	117
5.1 CALCIUM CONTROLS THE RATE OF ENDOCYTOSIS.....	117
5.2 RETRIEVAL OF STIMULATION-EVOKED VS SPONTANEOUSLY TRAFFICKING SYNAPTIC VESICLES	119
5.3 A MOLECULAR DEFINITION OF VESICLE POOLS.....	123
5.4 SPONTANEOUS NOISE VS. SPONTANEOUS SIGNALING.....	125
BIBLIOGRAPHY.....	128

PRIOR PUBLICATIONS

Leitz J. and Kavalali E.T. (*submitted*) Fast retrieval and autonomous regulation of spontaneously recycling synaptic vesicles

Manjot B.*, Leitz J.*, Reese A.L., Ramirez D.M., Durakoglulugil M., Herz J., Monteggia L.M. and Kavalali E.T. (2013) Reelin mobilizes a VAMP7-dependent synaptic vesicle pool and selectively augments spontaneous neurotransmission. *Neuron* **80**, 934-46

Leitz J and Kavalali ET (2011) Ca²⁺ influx slows single synaptic vesicle endocytosis. *J. Neuroscience* **31**, 16318-28

Kavalali ET, Chung C, Khvotchev M, Leitz J, Nosyreva E, Raingo J, Ramirez DM. (2011) Spontaneous neurotransmission: an independent pathway for neuronal signaling? *Physiology (Bethesda)* 26: 45-53

Chung C, Barylko B, Leitz J, Kavalali ET. (2010) Acute dynamin inhibition dissects synaptic vesicle recycling pathways that drive spontaneous and evoked neurotransmission. *J. Neurosci.* 30: 1363-76

*Equal contribution

LIST OF FIGURES

2.1 SINGLE-VESICLE FUSION EVENTS ARE DISTINGUISHABLE FROM NOISE AND DECAY RAPIDLY	36
2.2 INCREASING CALCIUM CAUSES AN INCREASE IN PR	40
2.3 INCREASING EXTRACELLULAR CALCIUM PROMOTES MULTIVESICULAR RELEASE, SLOWS DECAY TIME, INCREASES PROPENSITY FOR A VESICLE TO DWELL, AND INCREASES THAT DWELL TIME.....	42
2.4 THE PROBABILITY OF SYNAPTIC VESICLE FUSION CORRELATES WITH THE PROPENSITY OF MULTIVESICULAR FUSION AND A LONGER SINGLE VESICLE RETRIEVAL TIME.....	46
2.5 THE RATE OF ENDOCYTOSIS IS CONTROLLED BY INTRACELLULAR CALCIUM INFLUX	48
2.6 INTRACELLULAR CALCIUM ACTIVATES CALCINEURIN TO CONTROL THE RATE OF ENDOCYTOSIS	49
2.7 MODELING OF 1 HZ STIMULATION REQUIRES A SERIAL SLOWING IN ENDOCYTOSIS KINETICS.....	52
3.1 SPONTANEOUS INCREASES IN VGLUT1-PHLUORIN FLUORESCENCE DECAY RAPIDLY	65
3.2 DUAL COLOR IMAGING OF CELLS EXPRESSING SYPHATOMATO AND PSD-95-GCAMP5K SHOW SPONTANEOUS INCREASES IN FLUORESCENCE THAT ARE ANALOGOUS TO THOSE OBSERVED IN VGLUT1-PHLUORIN	69

3.3 INCREASING EXTRACELLULAR CALCIUM INCREASES MULTIVESICULAR RELEASE	73
3.4 INCREASING EXTRACELLULAR CALCIUM INCREASES THE AMPLITUDE OF SPONTANEOUS EVENTS IN BOTH SYPHTOMATO AND PSD-95-GCAMP5K	74
3.5 INCREASING EXTRACELLULAR CALCIUM DOES NOT ALTER FLUORESCENCE DECAY TIMES	76
3.6 INCREASING EXTRACELLULAR CALCIUM DOES NOT ALTER DECAY TIME OF SPONTANEOUS INCREASES IN SYPHTOMATO FLUORESCENCE	78
3.7 INCREASING EXTRACELLULAR CALCIUM INCREASES SPONTANEOUS RELEASE RATE.....	78
3.8 SPONTANEOUS VESICLE FUSION RATE AND STIMULATION-EVOKED FUSION PROBABILITY DO NOT CORRELATE AT A GIVEN SYNAPSE.....	82
4.1 REELIN INCREASES THE FREQUENCY OF SPONTANEOUS NEUROTRANSMISSION	99
4.2 REELIN SELECTIVELY AUGMENTS SPONTANEOUS SYNAPTIC VESICLE TRAFFICKING WITHOUT ALTERING THE PROPERTIES OF EVOKED NEUROTRANSMISSION	103
4.3 REELIN-INDUCED INCREASE IN SPONTANEOUS RELEASE REQUIRES SNAP- 25 BUT NOT SYB2	105
4.4 REELIN SELECTIVELY MOBILIZES A POOL OF VESICLES TAGGED WITH VAMP7	107

4.5 DUAL COLOR ANALYSIS OF VESICULAR SNARE TRAFFICKING REVEALS
THAT VAMP7 SPECIFICALLY RESPONDS TO REELIN APPLICATION 109

LIST OF DEFINITIONS

AMPA – α -Amino-3-hydroxy-5-methyl-4-isoxazolepropionic acid

AMPA – AMPA receptor

AP – action potential

AP-5 – 2-amino-5-phosphonopentanoic acid

CNS – central nervous system

CNQX – 6-cyano-7-nitroquinoxaline-2,3-dione

div – days in vitro

EGTA – ethylene glycol tetraacetic acid

EM – electronmicrographs

EPSC – excitatory postsynaptic current

GABA – gamma-aminobutyric acid

GFP – green fluorescent protein

Het – heterozygous mouse

Homo – homozygous mouse

Hz – hertz

IPSC – inhibitory postsynaptic current

KD – knockdown

KO – knockout

mEPSC – miniature excitatory postsynaptic current

mIPSC – miniature inhibitory postsynaptic current

NMDA – N-methyl-D-aspartate

NMDAR – NMDA receptor

PSD – postsynaptic density

SV – Synaptic vesicle

Syb2 – synaptobrevin 2

synaptopHluorin – synaptophysin-pHluorin

sypH – synaptobrevin-pHluorin

Syt1 – synaptotagmin 1

Syt7 – synaptotagmin 7

TTX – tetrodotoxin

WT – wild-type

CHAPTER ONE

GENERAL INTRODUCTION

“The central nervous system evolved to shepherd the gonads through the hazards of the environment.” – Dr. Steven Arch

Ultrastructure of the Synapse

Chemical neurotransmission is achieved by the fusion of neurotransmitter-containing synaptic vesicles with the presynaptic terminal membrane. Upon fusion, neurotransmitters in the lumen of the synaptic vesicle disperse into the extracellular space and act on the receptors of the postsynaptic cell. This junction between pre- and postsynaptic cells was first observed in 1862 by Wilhelm Kuhne at the end-plate of the frog neuromuscular junction. Yet, it was not until 1889 that the junction between two neurons was observed by Santiago Ramon y Cajal and still eight more years, in 1897, until this junction would receive the name “the synapse” from Charles Sherrington (with the aid of classicist Arthur Verrall). If Cajal was the first to observe the physical structure of the neuronal synapse as being the junction between two cells, it was Sherrington who first noted its potential functional significance as barrier to electrical conduction through a neuron circuit.

Over one hundred years later, the synapse has come to be a central area of study in the field of neuroscience. The synapse between neurons can be broken down into three distinct components: the presynaptic terminal, the postsynaptic specialization and the synaptic cleft that separates them. For the purposes of this dissertation, and the data presented here, the following information is particular to excitatory hippocampal neurons.

The presynaptic neuron contains hundreds of 40-50 nm diameter synaptic vesicles that package neurotransmitter. Of these hundreds of vesicles only a subset resides near the synaptic terminal and at any given time only a few (8-10 vesicles) associate very closely to the synaptic terminal membrane (Schikorski and Stevens, 1997, 2001). These synaptic vesicles release their neurotransmitter contents by fusing with the plasma membrane of the presynaptic terminal in the process of exocytosis. Synaptic vesicle fusion occurs at precise locations within the presynaptic terminal immediately adjacent to the synaptic cleft (Palade and Palay, 1954; Palay, 1956; Gray, 1959). These active zones contain numerous cytoskeletal proteins (discussed below and reviewed in Dresbach et al., 2001; Jahn et al., 2003) that facilitate and support vesicles fusion. When a vesicle fuses, the neurotransmitters in the lumen disperse into the 15-20 nm wide synaptic cleft that separates pre- and postsynaptic neurons, to act on receptors on the postsynaptic cell. In excitatory synapses, postsynaptic receptors are clustered in an area called the post-synaptic density (PSD) and these receptors are activated in presence of glutamate to allow ions to move into the cell or initiate a protein signaling cascade. The form and extent of this postsynaptic signal relies on the amplitude, and frequency, of neurotransmitter release from the presynaptic neuron which in turn relies on the fusion, retrieval and reuse of synaptic vesicles.

The Synaptic Vesicle

Molecular anatomy of a synaptic vesicle

The synaptic vesicle is a remarkably complex small (40-50 nm diameter) organelle that packages and transports neurotransmitter. It has a variety of proteins (>80 different

proteins) on its surface and in some cases contains many copies of a single protein, for example ~70 copies of the SNARE synaptobrevin 2 (syb2 aka VAMP2) (Takamori et al., 2006), although the quantity of some of these proteins, such as syb2, can be quite variable (Mutch et al., 2011). Furthermore, only a few of these proteins may actually be required for function (reviewed in van den Bogaart and Jahn, 2011). Synaptic vesicles fuse with the terminal membrane to release neurotransmitter and this fusion is triggered by Ca^{2+} via Ca^{2+} sensor proteins such as, synaptotagmin1. Synaptotagmin 1 (syt1) is the canonical Ca^{2+} sensor that is required for synchronous neurotransmission in hippocampal excitatory synapses (Fernandez-Chacon et al., 2001; Xu et al., 2009 and discussed in detail below). The prototypical synaptic vesicle of a glutamatergic neurons also contains 1-2 copies of the vesicular ATPase (vATPase) which is responsible for generating and maintaining a pH gradient between the vesicle lumen (pH 5.6) and the cytosol (pH 7.4) (Forgacs, 2007). This pH gradient is used to fill synaptic vesicles with neurotransmitter through several (6 to 9) copies of the vesicular glutamate transporter 1 (VGLUT1). Vesicles contain several Rab proteins that act to target synaptic vesicles to the axon terminal and to tether or dock synaptic vesicles at the active zone prior to fusion (Jahn et al., 2003). Synaptic vesicle-associated phosphoproteins synapsins also act to tether the synaptic vesicles to the terminal cytoarchitecture and phosphorylation of these proteins can control the number of synaptic vesicles that are available to fuse (Menegon et al., 2006). In addition, there are a wide variety of cytosolic proteins that promote or inhibit synaptic vesicle fusion, retrieval, and trafficking. Together these vesicular and cytosolic proteins work in concert to endow a large degree of dynamism to a small organelle.

Synaptic vesicle pools

While synaptic vesicles appear to be physically homogeneous in electron microscopy studies, they are not operationally identical. Only a small population of synaptic vesicles is fusion-competent at any given time (Harata et al., 2001). Indeed, even after prolonged stimulation, a substantial number of vesicles do not participate in neurotransmission (Sudhof, 2000). Vesicles that do participate in exocytosis make up the recycling pool of synaptic vesicles, while vesicles that are immobile compose the resting pool (although this pool may participate in other forms of neurotransmission such as spontaneous neurotransmitter release (Fredj and Burrone, 2009; Hua et al., 2011; Bal et al., 2013)). The recycling pool of vesicles can be further divided into the readily-releasable pool (vesicles that fuse immediately) and the reserve pool. In hippocampal neurons the readily releasable pool is approximately 4-8 vesicles while the reserve pool is composed of 17-20 vesicles that serve to replenish the readily-releasable pool during activity (Murthy and Stevens, 1999). The differences between these pools are deeper than simple spatial proximity to the active zone since the pools have been shown to intermingle using styrl dye labeling combined with electron microscopy (Rizzoli and Betz, 2004). Movement between these pools is facilitated by cytosolic factors that act on synaptic vesicle proteins. For example, synaptic vesicles are mobilized from the resting pool to the recycling pool by phosphorylation of the synaptic vesicle proteins synapsins (Chi et al., 2001; Menegon et al., 2006). The relative size of these pools varies between cell types and because the very definition of these pools is operational, there have been conflicting reports on the size of these pools within cell types (reviewed in Sudhof, 2004). Several recent studies, however, have extended the functional definitions of these

pools and proposed a potential molecular definition of pool identity: the vSNARE composition of synaptic vesicles (Ramirez and Kavalali, 2012).

Modes of Synaptic Vesicle Fusion

Synaptic vesicles fuse under a variety of circumstances. Vesicles fuse during neuronal activity and this fusion can be either tightly coupled to Ca^{2+} influx (synchronous neurotransmission) or loosely coupled to Ca^{2+} influx (asynchronous neurotransmission). Vesicles can also fuse in the absence of activity, or when activity is pharmacologically inhibited (spontaneous neurotransmission). Relatively recent work has shown that these different forms of neurotransmission may be due, at least in part, to different molecular profiles of synaptic vesicles, specifically vSNAREs heterogeneity. Classically, vesicle fusion relies on the formation of the SNARE complex composed of SNAP-25, syntaxin-1 and the vesicular SNARE, syb2. But it has become clear that this is not the only requirement for vesicle fusion. In syb2 knockout neurons, synchronous neurotransmission is severely attenuated, but spontaneous neurotransmission persists (Schoch et al., 2001). In SNAP-25 knockout neurons, synchronous neurotransmission is again abolished but spontaneous neurotransmission remains (although less than in wild type) (Bronk et al., 2007). Moreover, α -latrotoxin can increase spontaneous neurotransmission independent of syb2, SNAP-25 or Munc13 (the specific roles of these proteins to be discussed below) (Deak et al., 2009). Synchronous, asynchronous and spontaneous neurotransmission can be differentially regulated by phorbol esters (Waters and Smith, 2000; Virmani et al., 2005). Therefore, it has been proposed that these different forms of neurotransmission may utilize alternate Ca^{2+}

sensors (Sun et al., 2007; Groffen et al., 2010; Pang et al., 2011; Yao et al., 2011), may be derived from different vesicle populations (Sara et al., 2005 reviewed in Ramirez and Kavalali, 2012), and may utilize divergent recycling pathways (Deak et al., 2004; Chung et al., 2010 and the data presented here). However, this notion that alternate synaptic vesicles pools contribute to alternate forms of neurotransmission is not without controversy as several studies have show that all neurotransmission originates from a single pool of synaptic vesicles (Groemer and Klingauf, 2007; Hua et al., 2010; Wilhelm et al., 2010).

Regardless, it is accepted that the importance of these divergent forms of neurotransmission extends beyond the presynaptic terminal to differentially activation of postsynaptic receptors and thus divergent postsynaptic signaling cascades. For example, spontaneous and synchronous neurotransmission activate non-overlapping populations of postsynaptic receptors (Atasoy et al., 2008) although exactly how this is achieved remains uncertain, although spatial separation seems most likely (discussed below). Furthermore, blocking spontaneous neurotransmission initiates a form of homeostatic synaptic plasticity that is distinct from classical activity-dependent Hebbian potentiation (Frank et al., 2006; Sutton et al., 2006; Sutton et al., 2007; Autry et al., 2011; Nosyreva et al., 2013). But operationally, how are these modes of neurotransmission defined? And what factors might lend themselves to a molecular definition of these pools of neurotransmission?

Synchronous fusion

Synchronous synaptic vesicle fusion is the best characterized form of exocytosis, as it can be triggered with relative ease. Operationally it is defined as synaptic vesicle fusion that

occurs within hundreds of microseconds of Ca^{2+} entry (Sabatini and Regehr, 1996). In preparation for this fast synchronous synaptic fusion, a small cohort of synaptic vesicles are docked to the terminal plasma membrane through the formation of a protein complex composed of Rab3 and Rab27 on the synaptic vesicle and the cytosolic proteins Rab3-interacting molecule (RIM (Wang et al., 1997)), RIM interacting molecule (RIM-BP) (Wang et al., 2000) and Munc13 (Brose et al., 1995 reviewed in Sudhof, 2013). RIM and RIM-BP proteins tether vesicles to Ca^{2+} channels (Gracheva et al., 2008) while Munc13 catalyzes the conformational switch of the SNARE protein, syntaxin-1 from the closed to open state (Augustin et al., 1999). When either RIM, RIM-BP, or Munc13-1 are knocked out, synaptic transmission can still occur, but it is no longer tightly coupled to Ca^{2+} influx (Kaesler et al., 2011, Liu et al., 2011, Augustin et al., 1999, respectively). With syntaxin 1 open, a four-helical *trans*-complex is able to form between syntaxin-1 (which contributes two helices), SNAP-25 and the vSNARE synaptobrevin-2 (syb2 also known as VAMP2) (Sollner et al., 1993; Hanson et al., 1997; Poirier et al., 1998 reviewed in Sudhof, 2013). Formation of this SNARE complex primes synaptic vesicles for release but also requires Munc18-1 (Hata et al., 1993), which binds to the assembled SNARE complex (as well as closed syntaxin-1) (Khvotchev et al., 2007; Deak et al., 2009b; Zhou et al., 2013). Although the precise role of Munc18-1 in exocytosis remains enigmatic, its importance is undeniable as it is the only protein whose deletion abrogates all forms of vesicle fusion (Verhage et al., 2000). In preparation for fast synchronous release, the cytosolic protein complexin also binds to the fully assembled SNARE complex (McMahon et al., 1995; Giraudo et al., 2006) to further

prime vesicles for release and prevent vesicles from undergoing spontaneous vesicle fusion (Reim et al., 2001; Cai et al., 2008).

When an action potential arrives at the synaptic terminal, Ca^{2+} influx is rapid but short-lived due to high Ca^{2+} buffering (Schneppenburger and Neher, 2000; Meinrenken et al., 2002). Synaptic vesicles sense Ca^{2+} entry through the vesicle protein synaptotagmin-1 (syt1). Syt1 which has two cytoplasmic C2 domains (Perin et al., 1990; Perin et al., 1991) that bind Ca^{2+} (Brose et al., 1992) to promote vesicle fusion (Fernandez-Chacon et al., 2001). Syt1 is required for fast vesicle fusion (Geppert et al., 1994) as genetic deletion of syt1 (Xu et al., 2009) or mutations that augment Ca^{2+} binding (Mackler et al., 2002; Shin et al., 2009) severely hinder synchronous neurotransmission. Despite the deficit in synchronous transmission, syt1 knockout facilitates spontaneous synaptic vesicle fusion (Xu et al., 2009; Lee et al., 2013). Interestingly, complexin knockout neurons (Cai et al., 2008; Maximov et al., 2009; Kaeser-Woo et al., 2012), phenocopy synaptotagmin knockouts (Reim et al., 2001; Giraudo et al., 2006).

Exactly how the SNARE complex, syt1, complexin and Munc18-1 act to open a fusion pore between the synaptic vesicle lumen and the extracellular environment is still unknown. Syt1 contains both phospholipid-binding domains as well as SNARE interaction domains. Therefore, Ca^{2+} binding to syt1 might produce enough of positive electrostatic force to pull the vesicle towards the negatively charged phospholipid terminal membrane. Alternatively, Syt1 may act on the SNARE complex directly to mechanically force the SNARE complex away from the vesicle, which draws the transmembrane domains together as the SNARE complex shifts from a *trans* configuration to *cis* (reviewed in Sudhof, 2013).

This second model is supported by experiments increasing the distance between the SNARE motif of syb2 (Deak et al., 2006) or syntaxin-1 (Zhou et al., 2013) where vesicle fusion is impaired. But when the transmembrane domain of syntaxin-1 is replaced by lipid-anchors, fusion is unaffected (Zhou et al., 2013). These data suggest just the mechanical push and not the formation of a *cis*-transmembrane domain is required for fusion.

Operationally, the fast synchronous synaptic vesicle pool is defined as the subset of synaptic vesicles that fuse in less than 200 μsec of Ca^{2+} influx. But another molecular definition is becoming apparent. The vSNARE protein syb2 is required for fast synchronous release but in syb2 knockout neurons transmission is not all together absent, although this deficiency leads to lethality at birth. In these syb2 deficient neurons, spontaneous transmission and a loosely Ca^{2+} -coupled form of neurotransmission persist (Schoch et al., 2001; Deak et al., 2004; Deak et al., 2006). This incomplete abolition of neurotransmission is the common outcome for a variety of synaptic vesicle protein deficiencies (i.e. synaptotagmin-1, complexin, Munc13-1). Thus there may be an underlying molecular heterogeneity of synaptic vesicles that determine the forms of neurotransmission.

Asynchronous fusion

Although synchronous synaptic vesicle fusion is the predominant form of fusion at mammalian central synapses, it is not the only form of Ca^{2+} -dependent fusion. Initial experiments describing the kinetics of neurotransmitter release at the frog neuromuscular junction found that there were two phases of transmitter release: a fast component (synchronous vesicle fusion) and a slow delayed component that was not closely tied to

stimulation (Barrett and Stevens, 1972). This asynchronous neurotransmission was then functionally defined as neurotransmission that persists more than 1 second after Ca^{2+} influx ceased (Barrett and Stevens, 1972; Goda and Stevens, 1994). During trains of neuronal activity, Ca^{2+} builds in the synaptic terminal and promotes asynchronous neurotransmission. Given that neuronal activity *in vivo* occurs as trains of action potentials (Hubel, 1959), asynchronous transmission is a physiologically relevant form of neurotransmission. In some neurons, such as GABAergic interneurons of the hippocampus, asynchronous vesicle fusion dominates over synchronous neurotransmitter release and may be responsible for preventing spontaneous excitatory activity (Lu and Trussell, 2000; Hefft and Jonas, 2005). Conversely, asynchronous neurotransmission is nearly absent in calyx of Held (Sun et al., 2007). Separating synchronous and asynchronous neurotransmission is a significant challenge as their definitions are somewhat qualitative. However, these two components could be separated to some extent by their sensitivity to Sr^{2+} which acts primarily facilitates asynchronous transmission (Goda and Stevens, 1994). Genetic deletion of the SNARE components SNAP-25 (Washbourne et al., 2002; Bronk et al., 2007), syntaxin-1 or synaptobrevin 2 (Schoch et al., 2001), or removal of SNARE proteins via tetanus and botulinum toxin cleavage (Ashton and Dolly, 2000) severely disrupts synchronous transmission, but leaves some form of Ca^{2+} dependent asynchronous vesicle fusion intact. A similar phenotype can be generated by mutation (Geppert et al., 1994) or deletion of synaptotagmin 1 (Maximov and Sudhof, 2005).

To date, two lines of investigation lend insight into the molecular mechanisms that might differentiate asynchronous from synchronous neurotransmission: a disparate Ca^{2+}

sensitivities between the two forms of neurotransmission and the limited overlap and preferential trafficking of the vSNARE VAMP4 over syb2 (Raingo et al., 2012).

Focusing on the Ca^{2+} sensors, it was shown that the deletion of either syt1 or syt7 had similar effects on exocytosis but double deletion of both Ca^{2+} sensors dramatically reduced overall exocytosis in chromaffin cells (Schonn et al., 2008). This data suggested a partially redundant role of syt1 and 7. In agreement, one year later, it was shown that constitutive knockout of either syt1 or 7 in mice did not alter vesicle fusion kinetics (Maximov et al., 2009). However, when either syt7 or syt1 was acutely knocked-down, in a complementary constitutive knockout background, there was a severe loss of all stimulation-evoked neurotransmission (Bacaj et al., 2013). These data implicate at least some form of syt in regulating asynchronous neurotransmission. In the calyx of Held, syt2 knockout shifted synchronous neurotransmission to asynchronous transmission (Sun et al., 2007). Furthermore, this asynchronous vesicle fusion was shown to have significantly different Ca^{2+} affinity and cooperativity than synchronous neurotransmission, implying an alternate Ca^{2+} sensor may control asynchronous neurotransmission in the calyx. Although no manipulation of syt has manifest as a selective augmentation of asynchronous transmission, manipulation of Doc2 has (Yao et al., 2011). Doc2, like syt1, is a Ca^{2+} , SNARE, and lipid binding protein and the Ca^{2+} binding kinetics are highly reminiscent of asynchronous vesicle fusion.

Optical studies using pH-sensitive GFP proteins showed that VAMP4 and syb2 do not traffic together during stimulations at a given synapse suggesting these vSNAREs are unequally distributed among the general population of synaptic vesicles (Raingo et al., 2012). Biochemically, VAMP4 was shown to form a SNARE complex with syntaxin 1 and SNAP-

25, however, this SNARE complex did not interact with complexin or syt1, distinguishing this SNARE complex from syb2-containing complexes. Moreover VAMP4 expression on syb2 deficient neurons could rescue some synchronous neurotransmission, but rescued cells were more susceptible to perturbations in Ca^{2+} influx (i.e. Ca^{2+} chelation) again hinting at a Ca^{2+} sensor that is not syt 1. Together synchronous and asynchronous neurotransmission comprise the Ca^{2+} -dependent forms of synaptic vesicle exocytosis, but a third form of spontaneous exocytosis persists at rest even when neuronal activity is pharmacologically inhibited.

Spontaneous fusion

Spontaneous neurotransmission was identified in 1952 and directly led to the recognition of the quantal nature of neurotransmission (Fatt and Katz, 1952; Del Castillo and Katz, 1954). Spontaneous vesicle fusion is the fusion of only a single synaptic vesicle and occurs at a relatively low frequency of 0.01-0.02 Hz (Geppert et al., 1994; Frerking et al., 1997; Murthy and Stevens, 1999). This low frequency release rate led to almost immediate debate as to whether spontaneous transmission could be a form of information transfer between neurons or if it represented accidental vesicle fusion and is thus “noise.” A mounting body of evidence now indicates that spontaneous neurotransmission does relay information (Kavalali et al., 2011) and that the synaptic vesicles that control spontaneous neurotransmission may be molecularly distinct from vesicles that undergo synchronous and asynchronous stimulation-evoked fusion (Ramirez and Kavalali, 2012; Smith et al., 2012).

Classically, spontaneous neurotransmission was assumed to be noise: the result of the spontaneous fusion of vesicles that would otherwise fuse during stimulation (Murthy and Stevens, 1999). This assumption was based on the low probability of spontaneous vesicle fusion (Del Castillo and Katz, 1954; Dodge and Rahamimoff, 1967), the relative Ca^{2+} -insensitivity of spontaneous neurotransmission compared to stimulated neurotransmission (Dittman and Regehr, 1996), and the similarity in postsynaptic response between spontaneous neurotransmission and unquantal stimulated neurotransmission (Cherki-Vakil et al., 1995 but see Van der Kloot, 1996 and Frerking et al., 1997). But more recent work has assigned spontaneous neurotransmission to roles in signaling, synapse maturation, and homeostatic synaptic plasticity (reviewed in Kavalali et al., 2011).

When spontaneous neurotransmission is blocked acutely (for 30 minutes) (Autry et al., 2011; Nosyreva et al., 2013) or for prolonged periods (hours to days), the postsynaptic cell responds by inserting receptors into the postsynaptic membrane (reviewed in Davis, 2006; Turrigiano, 2011). This homeostatic synaptic plasticity is fundamentally different from traditional Hebbian plasticity. Whereas Hebbian plasticity is associative in that synaptic strengths are modified together, homeostatic synaptic plasticity can allow synapses to alter their strengths autonomously to stabilize neuron circuits (Turrigiano, 2012). But how does spontaneous neurotransmission signal differently from stimulation-evoked neurotransmission such as fast synchronous and asynchronous neurotransmission?

Experiments utilizing the use-dependent NMDAR blocker, MK-801, showed that when action potential-driven neurotransmission was specifically inhibited, spontaneous transmission persisted. The reverse experiment also showed that inhibition of activity at rest

did not block receptors that were used during activity (Atasoy et al., 2008). This differential activation of postsynaptic receptors could be achieved by a variety of mechanisms (discussed below) but spatial segregation is highly likely. How then is spontaneous neurotransmission mechanistically different from synchronous or asynchronous neurotransmission at the presynaptic terminal?

Spontaneous synaptic vesicle fusion is sensitive to Ca^{2+} (albeit to a lower degree than activity-dependent neurotransmission) and can be triggered by either stochastic Ca^{2+} channel openings or by Ca^{2+} release from internal stores (Sharma and Vijayaraghavan, 2003). But how is this sensitivity to bulk Ca^{2+} achieved? Spontaneous vesicle fusion is paradoxically diminished by mutations in *syt1* that decrease Ca^{2+} affinity, but enhanced by *syt1* knockout. Additionally while double knockout of *syt1* and 7 severely affects synchronous and asynchronous neurotransmission, spontaneous transmission persists. The knockout of the alternate Doc2 family Ca^{2+} sensors (mentioned above) also attenuates spontaneous neurotransmission (Groffen et al., 2010). But even in the quadruple knockdown of Doc2 family proteins, ~30% of spontaneous neurotransmission persists (Pang et al., 2011). It may be that there is significant overlap of Ca^{2+} sensors instructing spontaneous transmission, but another alternative is, again, vSNARE composition.

Evidence for molecularly separate synaptic vesicles comes from observations that when spontaneously recycling vesicles are selectively labeled by incubating neurons in the styryl dye at rest—with action potentials pharmacologically blocked—these vesicles are reluctant to fuse when later challenged with stimulation (Sara et al., 2005). The reverse is also true: when vesicles are labeled during stimulation, the rate of destaining at rest is slower

than when also labeled at rest. Similarly, in an experiment where neurons expressed a biotinylated syb2 and two colors of fluorescent streptavidin were presented, one at rest, and the other just prior to stimulation, there was minimal overlap of labeling. Furthermore, vesicles that fused spontaneously seemed to preferentially belong to the resting pool of vesicles (Fredj and Burrone, 2009). Together, these studies imply that spontaneous synaptic vesicle fusion is maintained by a subpopulation of synaptic vesicles that are distinct from those that participate in activity-dependent neurotransmission. This conclusion is supported by a recent study in drosophila which used a genetically encoded Ca^{2+} sensor, GCaMP5, targeted to the postsynaptic terminal to monitor neurotransmission-dependent Ca^{2+} influx. Comparing Ca^{2+} influx at rest with influx during stimulation showed no correlation between spontaneous neurotransmission and fast synchronous neurotransmission suggesting these modes are regulated independently at a given synapse (Melom et al., 2013).

A molecular definition of spontaneous neurotransmission is more difficult to ascribe than evoked neurotransmission. This may be the result of multiple molecular pools of vesicles participating in spontaneous neurotransmission. For example, knockout of syb2 attenuates spontaneous transmission suggesting it may be involved (Schoch et al., 2001). A study using the pH-sensitive GFP, pHluorin, fused to the vSNARE VAMP7 (also known as tetanus insensitive- or TI-VAMP) found that while VAMP7 was targeted largely to the resting pool of vesicles and participated in spontaneous neurotransmission it also participated in stimulation-evoked neurotransmission (Hua et al., 2011). Similarly, another vSNARE, Vps10p-tail-interactor-1a (vti1a), tagged with pHluorin displayed comparable spontaneous trafficking with syb2-pHluorin, but was not easily mobilized during stimulation (Ramirez et

al., 2012). Interestingly, genetic deletion of *vtila* decreased a specific high-frequency component of spontaneous neurotransmission, but spontaneous neurotransmission as a whole was minimally altered. These studies (as well as work presented here; Bal et al., 2013) demonstrate that there are molecular determinants that assign subsets of synaptic vesicles to roles in spontaneous or stimulation-evoked neurotransmission. Whether these subsets of vesicles, or spontaneous neurotransmission as a whole, is responsible for the divergent signaling cascades initiated by spontaneous neurotransmission remains an open question.

Full-collapse and Kiss-and-Run fusion modes

Synaptic vesicles can fuse in a fast synchronous, asynchronous or spontaneous mode, but the actual mechanism of fusion can also differ. Currently, there are two models of synaptic vesicle exocytosis that occur at the synapse, but the forces and circumstances that determine which mode is used remains unclear. One model of vesicle fusion is the “full-collapse” mode where the synaptic vesicle completely joins with the presynaptic terminal; becoming ultrastructurally indistinct from the terminal membrane. The other model proposes that synaptic vesicles open a transient fusion pore where neurotransmitter can still exit the vesicle lumen, but the overall structure of the synaptic vesicle is maintained, this form is known as “Kiss-and-Run” (reviewed in Alabi and Tsien, 2013).

The differences between these two forms of transmission are significant. There is evidence that these two forms of fusion elicit distinct degrees postsynaptic signaling. For example, the amount of transmitter released may differ between kiss-and-run and full-collapse fusion events. In hippocampal neurons, experiments that simultaneously monitoring

styryl dye destaining and postsynaptic electrophysiological activity, show kiss-and-run fusion events elicit smaller postsynaptic signals (Richards, 2009). The fusion pore could also alter the kinetics of neurotransmitter release rather than the quantity. Intriguingly, while AMPARs and NMDARs both have desensitization periods after activation, the kinetics and onset of this desensitization differs between the two receptors. Studies using iontophoretic application of glutamate suggest that AMPARs open in response to large fast increases in glutamate, while NMDARs opened in response to slow prolonged application (Renger et al., 2001). Along these lines, another distinction between kiss-and-run and full-collapse fusion signaling depends on relative spatial distance from vesicle fusion sites to receptors. Evidence supporting this is found in experiments that monitor vesicle fusion location in three-dimensions using quantum dots (Park et al., 2012). These experiments show a preference of kiss-and-run fusion at the center of an active zone, while full-collapse fusion occurs predominantly at the periphery. It is important to note that these three possible signaling mechanisms—transmitter quantity, efflux kinetics, and release site location—are non-mutually exclusive within a synapse.

Besides postsynaptic signaling, a major difference between full-collapse fusion and kiss-and-run fusion lies in the rate of endocytosis of these vesicles. In the full-collapse fusion model, synaptic vesicle components are on the plasma membrane for ~15 s while during kiss-and-run fusion the lipid membranes of the vesicle and synaptic terminal are joined together for less than a second (reviewed in Alabi and Tsien, 2013). These different rates are important as they define the rate of synaptic vesicle reuse. Therefore, elucidating what factors control the mode of synaptic vesicle exocytosis and how these factors work has been

an area of intense focus. Significant progress has been made that shows the stimulation frequency, intracellular Ca^{2+} concentration, intrinsic vesicle fusion probability of a synapse, the vesicle's previous fusion history, the location of the vesicle, and vesicle pool identity are all deterministic of fusion mode. But one of the inherent difficulties in studying these modes of fusion is the small size of synaptic vesicles and the rapid rate at which kiss-and-run can proceed. Therefore attempts to dissociate these slow and fast modes of vesicle exo-endocytosis have generated a significant body of work.

Synaptic Vesicle Retrieval

Once synaptic vesicles fuse with the terminal membrane, the cell is presented with several problems including: physical enlargement of the synapse (e.g. $\sim 3,800 \text{ nm}^2$ for a single synaptic vesicle of 35 nm diameter) and depletion of synaptic vesicles. Neurons overcome these difficulties by locally recycling and reusing synaptic vesicles. This process of vesicle retrieval (endocytosis) and refilling (requiring reacidification) has been a focal point of research spanning several decades, and while there is general agreement on the molecular components involved the kinetics of endocytosis remain somewhat ambiguous. This ambiguity is bourn out of several factors: from the types of techniques applied to differences in cell types used. Understanding the molecular mechanisms that initiate and regulate endocytosis is not only a prerequisite for the complete understanding of synaptic neurotransmission but may yield insight into pathological conditions.

The quantal nature of neurotransmission supposed that neurons released fixed quantities of neurotransmitter during stimulation (Fatt and Katz, 1951; del Castillo and Katz

1952). Electron micrographs of frog neuromuscular junctions before and after nerve stimulation showed a clear disappearance of small clear organelles termed synaptic vesicles (Ceccarelli et al., 1972, 1973; Heuser and Reese, 1973, 1981). However, some time after stimulation, synaptic vesicles reappeared. These observations led to the hypothesis that, during stimulation, these synaptic vesicles undergo exocytosis, fusion with the cell membrane, and after stimulation, these synaptic vesicles were regenerated through local endocytosis at the nerve terminal. But how these vesicles were retrieved was debated. Heuser and Reese noticed the formation of large endosomal structures, coated pits (later shown to be clathrin), and membrane retrieval occurring away from release sites. The kinetics of this slow form of endocytosis was initially described by rapidly freezing cells at fixed time points after stimulation and found to be on the order of ~20s (Miller and Heuser, 1984). Ceccarelli, on the other hand proposed that recovery could occur quite fast by rapid reformation and closure of a fusion pore between the vesicle and the terminal membrane (Torri-Tarelli et al., 1985). The relative contributions of these two forms of vesicle endocytosis: slow clathrin-dependent endocytosis following full-collapse fusion and fast kiss-and-run exo-/endocytosis, are still debated to this day and their exact mechanics and kinetics remain enigmatic.

Calcium triggers endocytosis

The first implication of Ca^{2+} as a key component of the endocytic machinery came from electrophysiological experiments followed by post-stimulation fixation and electron microscopy (Hurlbut and Ceccarelli, 1974). Using black widow spider venom, they induced

Ca^{2+} -independent exocytosis and observed that in the absence of extracellular Ca^{2+} synaptic vesicle exocytosis caused a swelling of the frog neuromuscular junction, and ultimately a run down of neurotransmission. But when Ca^{2+} was included in the extracellular solution, neurotransmission could be maintained and cell swelling was reduced. This indicated that synaptic vesicles at the frog neuromuscular junction could only be recycled in the presence of Ca^{2+} (Ceccarelli et al., 1979). Similar experiments would later be performed in *Drosophila shibire* mutants (Ramaswami et al., 1994) and the lamprey reticulospinal neurons (Gad et al., 1998), and support the executive role of Ca^{2+} in endocytosis.

Electron microscopy, while unrivaled in its ability to visualize small structures, is difficult to apply towards understanding the kinetics of a given process. Doing so requires many preparations at different time points, and since each preparation must be fixed, it is impossible to perform before and after experiments within the same cell. Therefore, to understand the kinetics of endocytosis, methods that could be used on live cells that made real-time measurements would be better suited to characterize kinetics. So while Heuser, Reese, and Ceccarelli were characterizing the structural intermediates of endocytosis, electrophysiologists were working to refine the resolution of capacitance recordings that would be able to electrically monitor cellular surface area (capacitance) with high temporal resolution. In 1982, Neher and Marty succeeded in resolving membrane capacitance recordings to femptofarad capacitance changes in adrenal chromaffin cells (Neher and Marty, 1982). This allowed them to observe, in real time, single chromaffin granule exocytosis and endocytosis. Exocytosis was evoked an increase in cell capacitance and was often followed by an abrupt decrease back to baseline levels. This decrease could occur as fast as their

temporal resolution (30 ms) or on the order of seconds. Immediately, these experiments also showed Ca^{2+} as a requirement for endocytosis. Using the same technique in mast cells it was shown that the fusion and retrieval of small vesicles could be monitored in addition to large granule cells, and again, there was a clear Ca^{2+} dependence of endocytosis (Almers and Neher, 1987).

Throughout the nineties, evidence for Ca^{2+} as a trigger in endocytosis accumulated. Experiments in which whole-cell patch clamp or perforated patch clamp was used to dialyze cells with Ca^{2+} chelators or Ca^{2+} free solutions showed that Ca^{2+} was required to initiate endocytosis in melanotrophs (Thomas et al., 1990), saccular hair cells (Parsons et al., 1994) and chromaffin cells (Burgoyne, 1995). In experiments where Ca^{2+} was substituted by Ba^{2+} , Ba^{2+} could still trigger exocytosis but endocytosis was inhibited (Artalejo et al., 1995). Ba^{2+} was not itself inhibitory as endocytosis could proceed in the presence of barium so long as Ca^{2+} was also present (Artalejo et al., 1996). More recent evidence using the calyx of Held further supports these observations (Wu et al., 2009; Sun et al., 2010).

Despite the strength of electrophysiological measurements, a major limitation, of this technique is the requisite use of large synapses. Thus small glutamatergic and GABAergic synapses that make up the majority of central nervous system cannot be studied using capacitance recordings. To this end, optical approaches to studying endocytosis have dominated for these cell types. Styryl dyes, capable of being embedded in the outer lipid leaflet but also easily dissociated and washed away, were the favored technique to study exo/endocytosis in frog neuromuscular junction (Betz and Bewick, 1992) and later in hippocampal neurons (Ryan et al., 1993). Styryl dye experiments in both drosophila neurons

(Ramaswami et al., 1994) and in cortical synaptosomes (Marks and McMahon, 1998) confirmed Ca^{2+} as a trigger for endocytosis in small neurons of the central nervous system.

Calcium modulates the rate of endocytosis

In addition to triggering endocytosis, early capacitance recordings also suggested a second regulatory role for Ca^{2+} in governing the rate of endocytosis (Almers and Neher, 1987). A series of studies followed that directly manipulated internal Ca^{2+} by photo-uncaging in both melanotrophs (Thomas et al., 1993; Thomas et al., 1994) and chromaffin cells (Neher and Zucker, 1993; Heinemann et al., 1994). These studies found endocytosis proceeded with two kinetic components: a rapid component with time constant of less than 5 s when internal Ca^{2+} concentrations were greater than 10 μM and 50 μM in melanotrophs and chromaffin cells, respectively, and a slower component at low intracellular Ca^{2+} that was on the order of tens of seconds to minutes. Thus it would seem that increasing intracellular Ca^{2+} accelerated the rate of endocytosis. But the first study to systematically probe the rate of endocytosis at various Ca^{2+} concentrations found that endocytosis slowed as a function of increasing intracellular Ca^{2+} in goldfish retinal bipolar cells (von Gersdorff and Matthews, 1994). A slew of electrophysiological studies would follow, showing the opposite: that low Ca^{2+} inhibited endocytosis and increasing Ca^{2+} would shift endocytosis towards a faster rate in chromaffin cells (Burgoyne et al., 1995; Artalejo et al., 1995), in pancreatic b-cells (Eliasson et al., 1996). But, still other groups would produce data that corroborated the inhibitory effect of rising Ca^{2+} in both retinal bipolar cells (Neves and Lagnado, 1999) and in chromaffin cells (Smith and Neher, 1997; Engisch and Nowycky, 1998).

Again, membrane recycling in small synapses of neurons in the CNS cannot be monitored using electrophysiological techniques. In these neurons, optical experiments dominate. Initially, studies used styryl FM dyes staining to determine the rate and extent of synaptic vesicle endocytosis (Ryan et al., 1993). In these experiments, neurons were strongly stimulated in the absence of dye, once stimulation ceased, the extracellular solution was exchanged at varying time points with solution containing dye. The amount of dye uptake at different time points during endocytosis would be quantified, and used to determine the rate of endocytosis, which was found to proceed with a time till half-maximal fluorescence of 60 s (Ryan et al., 1993). When extracellular solution was changed to a Ca^{2+} -free solution, dye could still be taken up and to the same degree as uptake in Ca^{2+} -containing solution (Ryan et al., 1993; Ryan et al., 1996). These results were also extended to the frog neuromuscular junction (Wu and Betz, 1996). Together, these early imaging experiments generated the hypothesis that the rate of endocytosis was independent of Ca^{2+} but regulated by the number of synaptic vesicles that fused during stimulation. However, these early experiments suffered from a few technical flaws:

- The extracellular solution was changed after stimulation; therefore the Ca^{2+} signal that had initiated exocytosis (and thus endocytosis) was unaltered by these manipulations.
- The rate of extracellular solution change was rather slow: on the order of seconds, with the actual time till the solution in the chamber was fully replaced by the new solution not measured.

- Any vesicles participating in multiple rounds of exocytosis and endocytosis cannot be monitored.

Indeed, Ca^{2+} was shown to accelerate the rate of endocytosis using styrl dyes in combination with black widow spider venom in Ca^{2+} -lack and Ca^{2+} -containing solutions (Ramaswami et al., 1994). Regardless, the hypothesis that the number of vesicles that fuse controls the rate of endocytosis presented an alternate form of regulation.

A modicum of reconciliation followed in goldfish retinal bipolar cells when it was shown that in both very low and very high levels of Ca^{2+} no change in membrane capacitance was observed, while the rate of endocytosis rises and falls as Ca^{2+} increases (Rouze and Schwartz, 1998). This work went on to highlight the important point that capacitance measurements can only report a net change in membrane surface area. Therefore no change in capacitance could be the result of either no membrane added or removed, or of membrane being added at the same rate as being retrieved. Therefore the authors concluded that at low Ca^{2+} concentrations the relative rate of exocytosis was matched by the rate of endocytosis and as Ca^{2+} concentrations increased, exocytosis would initially dominate relative to endocytosis but eventually be overcome by endocytosis. Despite this work demonstrating both acceleration and deceleration of endocytosis relative to exocytosis, studies over the next decade were more partisan in their findings: attributing only an accelerating, decelerating, or independent role of Ca^{2+} in endocytic rate.

Evidence supporting an acceleration of endocytosis due by Ca^{2+} was obtained using multiple FM dyes with distinct washout kinetics. Increasing Ca^{2+} shifted vesicle retrieval

towards the faster form of endocytosis in hippocampal neurons (Klingauf et al., 1998) and chromaffin cells (Ales et al., 1999). Chelating bulk internal Ca^{2+} using EGTA in goldfish bipolar cells, found that brief low Ca^{2+} influx stimulation would result in slow endocytosis while strong stimulation would produce rapid endocytosis (Neves et al., 2001). Increasing Ca^{2+} shifted endocytosis towards a faster rate in snake motor terminals (Teng and Wilkinson, 2005). A variety of experiments in the calyx of held showed a Ca^{2+} -dependent acceleration of endocytosis (Wu et al., 2005; Hosoi et al., 2009; Wu et al., 2009; Sun et al., 2010).

Throughout this time, evidence accumulated that endocytosis was slowed by Ca^{2+} in goldfish bipolar cells (Neves and Lagnado, 1999), mouse bipolar cells (Wan et al., 2008; Wan et al., 2010) cortical synaptosomes (Cousin and Robinson, 2000) and recently in dissociated hippocampal neurons (Armbruster et al., 2013). Several studies also supported the notion that endocytosis Ca^{2+} -independent but regulated by the number of vesicles that fused. These studies were carried out in cortical synaptosomes (Marks and McMachon 1998), in the calyx of held (Sun et al., 2002).

All of these studies used a variety of cell types, and experimental procedures, but the one factor they had in common was the use of strong stimulation to elicit the fusion of many synaptic vesicles. This is a major complication because any rapid endocytosis that occurs during exocytosis and persisted through out stimulation would be occluded. For any given stimulation, the precise number of vesicles that underwent fusion was unknown. Membrane capacitance recordings can only report net changes in membrane surface area which during stimulation is dominated by exocytosis. Styrl FM dye staining can only label a vesicle once it ceases to participate in fusion. Therefore, neither of these techniques could accurately

monitor endocytosis during exocytosis. With the development of pHluorin, a pH-sensitive GFP (Miesenbock et al., 1998), synaptic vesicles could now be monitored individually by targeting pHluorin to the luminal domains of synaptic vesicle proteins. Now as vesicles fuse, fluorescence levels increase and as vesicles are retrieved and reacidified fluorescence decreases. Initially, pHluorin experiments varying the concentration of extracellular Ca^{2+} showed no effect of Ca^{2+} on endocytosis (Sankaranarayanan and Ryan, 2000). But in a follow up experiment using pHluorin and the vATPase-inhibitor bafilomycin it was shown that a significant amount of vesicle recycling occurred during stimulation and that endocytosis accelerated in higher extracellular Ca^{2+} concentrations (Sankaranarayanan and Ryan, 2001). But as is the case with FM dye, in experiments using pHluorin and bafilomycin, once vesicle reacidification is inhibited, a given synaptic vesicle is trapped in the fluorescent state regardless of how many rounds of fusion it participates in. So even in these pHluorin experiments, any rapid vesicle retrieval and reuse that occurs during stimulation is automatically occluded. How then, can endocytosis be investigated independent of exocytosis? One way to decouple these processes is to know the exact number of synaptic vesicles that participated in fusion during stimulation. To this end, several groups sought to monitor exocytosis and endocytosis at the level of a single synaptic vesicle.

Endocytosis at the single vesicle level

In search of resolving vesicle recycling at the single vesicle level, membrane capacitance recordings led the way in the calyx of held. Uniquantal spontaneous vesicle

fusion events were found to have a rapid endocytosis time course of 56 ms. When weak stimulation was given to elicit single vesicle fusion, these events were retrieved at a slower rate around 115 ms (Sun et al., 2002). This finding already hinted that Ca^{2+} influx decelerates synaptic vesicle endocytosis at the single vesicle level but these experiments did not probe the effect of varying Ca^{2+} at this level.

In hippocampal neurons, pHluorin measurements could not easily identify spontaneous vesicle fusion events. Therefore, single vesicle resolution relied on several corollary indicators during low frequency stimulation, such as vesicle fusion probability and fluorescence amplitude distributions. But each study produce different endocytic kinetics depending on which synaptic vesicle protein was tagged with pHluorin. First using synaptobrevin-pHluorin (SypH) found three distinct kinetic components of endocytosis: a fast mode consistent with “kiss-and-run” kinetics (with decay time of less than 3 seconds), a slower mode (with decay time in the tens of seconds) and a stranded mode where fluorescence did not decay. This latter case was probably due to probe leaking onto the surface during vesicle internalization (Gandhi and Stevens, 2003). Although the authors did not investigate directly the effect of Ca^{2+} on endocytosis, they did show that in higher Ca^{2+} the rapid component of decay was absent. This too suggests that as Ca^{2+} increases, the rapid component of endocytosis decreases and overall endocytosis slows. In these experiments single vesicle resolution was determined by a recapitulation vesicle fusion probability observed in classical literature, as well as quantal amplitude distribution analysis in elevated Ca^{2+} concentration. These results were supported by experiments monitoring FM dye destaining kinetics at the single vesicle level (Aravanis et al., 2003; Richards et al., 2005).

Together these findings suggest that kiss-and-run exo-/endocytosis predominates at low intracellular Ca^{2+} .

When pHluorin was fused to the luminal domain of synaptophysin (synaptopHluorin) only a single slow form of endocytosis was observed with decay time of ~ 14 s (on par with Heuser and Reese's estimates). When stimulation was increased and amplitudes normalized and compared to single vesicle events, decay times were nearly identical (Granseth et al., 2006). This was determined using only average traces of fluorescence steps due to single action potential stimulation, not actually single vesicle fusion. A year later pHluorin fused to the vesicular glutamate transporter 1 (vGlut-pHluorin) reported a similar single stochastic process with average time of ~ 14 s (Balaji and Ryan, 2007). Here the authors verified single-vesicle resolution based on quantal amplitude distributions of events. However, while vesicle fusion probability was not determined, example traces shown had a release probability of 1 in physiological Ca^{2+} , much higher than the known release probability of 0.2.

Using synaptopHluorin produced both fast and slow kinetic components to endocytosis (Zhu et al., 2009). Here the number of vesicles that fused altered only the slow component of endocytosis while the fast rate was fixed. This led the authors to propose a model where during synaptic vesicle fusion one vesicle fuses but two vesicles are retrieved. These experiments also failed to show synaptic vesicle fusion probability but instead relied on quantal amplitude distributions as validation of single vesicle resolution.

Each of these studies claimed to have visualized synaptic vesicle fusion at the single vesicle level, and each of these studies reported a different rate and kinetics of endocytosis. Moreover, none of these studies systematically varied Ca^{2+} concentrations nor did any study

report spontaneous synaptic vesicle fusion. The goal of the work presented here was two-fold: first to investigate the regulatory role of Ca^{2+} , if any, on endocytosis at the level of the single vesicle, and second to provide the first pHluorin-based visualization of spontaneous synaptic vesicle fusion. We found that during stimulation, synaptic vesicle retrieval and reacidification slow as a function of increasing extracellular Ca^{2+} , the number of vesicles that fuse, and we uncovered an inverse relationship between the rate of endocytosis and the intrinsic release probability of the synapse. We also found that this phenomenon persists during physiological stimulation. We went on to provide the first optical characterization of spontaneous synaptic vesicle fusion. Unlike in stimulation-evoked vesicle fusion, the rate reacidification of vesicles that fuse spontaneously is largely independent of Ca^{2+} . Furthermore there is little correlation between spontaneous fusion rate and stimulation-evoked vesicle fusion probability at a given synapse. Finally, we found that action potential-evoked neurotransmission and spontaneous neurotransmission could be regulated independently by mobilizing a molecular subset of synaptic vesicles. Together, these findings highlight major discrepancies in regulation between spontaneous and stimulation-evoked neurotransmission.

CHAPTER TWO

CALCIUM INFLUX SLOWS SINGLE SYNAPTIC VESICLE ENDOCYTOSIS

Background

Maintenance of synaptic transmission requires constant retrieval and reuse of synaptic vesicles (Murthy and De Camilli, 2003; Sudhof, 2004). Several mutants with deficiencies in synaptic vesicle endocytosis manifest rapid run-down of neurotransmitter release during activity, supporting a dynamic role of vesicle endocytosis and recycling in neurotransmission (Kavalali, 2007). The executive role of intrasynaptic Ca^{2+} transients in synaptic vesicle exocytosis is well-established (Bollmann et al., 2000; Schneggenburger and Neher, 2000; Sun et al., 2007). However, the impact of Ca^{2+} on synaptic vesicle endocytosis remains unclear. Ca^{2+} has been suggested as an essential trigger required to initiate synaptic vesicle retrieval (Marks and McMahon, 1998; Wu et al., 2009), but experiments manipulating Ca^{2+} concentrations directly or genetically have reported an inhibition of endocytosis (von Gersdorff and Matthews, 1994; Cousin and Robinson, 2000; Wan et al., 2010) as well as acceleration of endocytosis (Hosoi et al., 2009; Wu et al., 2009; Sun et al., 2010; Yamashita et al., 2010). A major drawback of these studies is their reliance on bulk measurements of synaptic vesicle endocytosis, which can be affected by a multitude of factors, such as the number of vesicles involved, the kinetics and duration of Ca^{2+} signals, as well as accumulation of released substances that may retrogradely alter release and retrieval processes. Indeed, there is evidence that the rate and pathway of synaptic vesicle retrieval can

be altered with increasing stimulus strength and endocytic load (i.e. the number of vesicles waiting to be retrieved (Kawasaki et al., 2000; Sankaranarayanan and Ryan, 2000, 2001; Sun et al., 2002; Wu and Wu, 2007; Clayton et al., 2008)).

Here, to investigate the role of action potential-evoked Ca^{2+} signals, in fusion and retrieval of individual synaptic vesicles, we took advantage of the improved optical signal-to-noise characteristics of pHluorin-tagged vesicular glutamate transporter (Vglut1-pHluorin) (Voglmaier et al., 2006; Balaji and Ryan, 2007; Santos et al., 2009). This setting circumvented the need for potentially toxic maneuvers, such as pre-photobleaching of surface membrane fluorescence, to improve signal-to-noise. Lentiviral expression of Vglut1-pHluorin in hippocampal neurons enabled us to visualize fusion and retrieval of single synaptic vesicles at individual release sites (boutons). We show that increasing extracellular Ca^{2+} increases release probability in the classical sense, but also recruits release-reluctant boutons to a more active state. We also detected a decrease in the rate of vesicle retrieval with increasing extracellular Ca^{2+} . Furthermore, we found that this decrease was dependent on intracellular Ca^{2+} and activation of calcineurin. Together, these findings indicate that Ca^{2+} entry into the nerve terminal acts to slow synaptic vesicle endocytosis of individual vesicles and antagonize the pace of synaptic vesicle reuse. We tested this premise during 1 Hz stimulation, which triggers aggregate fusion and retrieval of multiple vesicles. The relatively slow kinetics of vesicle retrieval after 1 Hz stimulation could be accounted for by a gradual decrease in the rate individual vesicle retrieval during the stimulation train. These results indicate a critical role for Ca^{2+} entry during single action potentials by setting the pace of subsequent vesicle retrieval and recycling.

Methods

Dissociated cultures.

Dissociated hippocampal cultures were prepared from postnatal day 1-3 Sprague Dawley rats of either sex, as described previously (Kavalali et al., 1999). The vGlut-pHluorin construct was a generous gift from Drs. Robert Edwards and Susan Voglmaier (University of California, San Francisco). At 5 days *in vitro* (DIV), cultures were infected with lentivirus expressing vGlut-pHluorin and experiments were conducted after 15 DIV when synapses reach maturity (Mozhayeva et al., 2002). In these experiments we relied on a lentiviral expression system. This is a rather robust and sustained gene expression system that enables protein expression in large fraction of neurons (thus presynaptic terminals) in dissociated cultures. This argument is supported by our previous observation that lentiviral expression of synaptobrevin-2 restores synaptic transmission to near wild type levels in synaptobrevin-2 knockout cultures (Deak et al., 2006). For all experiments, the extracellular solution was a modified Tyrode's solution containing (in mM): 150 NaCl, 4 KCl, 10 glucose, 10 HEPES, 2 MgCl and varying concentrations of CaCl₂ (1, 2, 4, and 8mM), pH 7.4 (310 Osm). To prevent network activity, postsynaptic ionotropic glutamate receptors antagonists 6-cyano-7-nitroquinoxaline-2,3-dione (CNQX; Sigma) and aminophosphonopentanoic acid (AP-5; Sigma) were added to the modified Tyrode solution at concentrations of 10 μ M and 50 μ M, respectively.

Ca²⁺ chelation and calcineurin inhibition.

In experiments where we introduced an exogenous internal Ca^{2+} buffer, cultures were incubated for 20 min with 10 μM EGTA-AM (Sigma) in the modified Tyrode's solution lacking extracellular Ca^{2+} . Similarly, to inhibit calcineurin we incubated neurons in modified Tyrode's solution containing 1 μM FK506 (Tocris) for 20 min and performed optical recordings in the continued presence of FK506.

Fluorescence imaging.

Experiments were performed from 17-22 DIV at room temperature. Experiments were performed using an Andor iXon+ back-illuminated EMCCD camera (Model no. DU-897E-CSO-#BV). Images were acquired at 5 Hz with an exposure time of 100 ms and binning of 4 to optimize the signal-to-noise ratio. Data was collected using MetaFluor and transferred to Excel for analysis.

Fluorescence analysis.

Amplitudes were determined as the difference between the average of 3 points after stimulus and the average of 8 points prior to stimulus. Successful events were those that had amplitudes greater than twice the standard deviation of 8 frames (~1.5 s) prior to the event. For the analysis of decay constants, single exponential Levenberg-Marquardt least sum of squares minimizations were used to fit data in Clampfit (Molecular Devices). Events were selected for decay analysis only if their decay stabilized, but did not assume events returned to pre-stimulus baseline. Dwell times, were calculated as the time between the initial fluorescence step, and the start of fluorescence decay predicted by the best fit decay in Clampfit.

Stimulation protocol.

Cultures were stimulated using parallel bipolar electrodes (FHC) delivering 15-20 mA pulses. Cultures stimulated at 0.025-0.2 Hz for 5-7 min, followed by a rest period prior to 10 APs delivered at 1 Hz. After the fluorescence returned to pre 1 Hz fluorescence, a 20 Hz stimulus for 20 s was delivered to help select active puncta.

Reconstructions of endocytic retrieval during 1 Hz stimulation.

Reconstructions of 1 Hz stimulus responses were performed using custom macros written in Microsoft Excel by summation of “ideal” single vesicle events derived from averages of amplitude, decay time, and dwell time. Therefore, each Ca^{2+} concentration had its own ideal event (i.e. the 8 mM Ca^{2+} 1 Hz reconstruction uses properties of 8 mM Ca^{2+} events). Least sum of squares error minimization was used to determine the best fitting sequential increase in decay time. Goodness of fit was determined by fitting fluorescence data with a single exponential decay, then fitting hypothetical decays with the same curve.

Results

Detection of synaptic vesicle fusion and retrieval during low frequency stimulation.

To investigate the properties of single synaptic vesicle exocytosis and endocytosis, we expressed the pHluorin-tagged version of the vesicular glutamate transporter (vGlut-pHluorin) in dissociated hippocampal cultures (Voglmaier et al., 2006) using a lentiviral expression system (Ertunc et al., 2007). Earlier work has shown that vGlut-pHluorin expression results in low levels of surface fluorescence, enabling reliable detection of single vesicle fusion events (Balaji and Ryan, 2007). Moreover, unlike pHluorin-tagged synaptobrevin and synaptotagmin based probes, vGlut-pHluorin shows limited lateral

diffusion upon vesicle fusion, thus providing a higher fidelity marker for synaptic vesicle exocytosis and endocytosis (Wienisch and Klingauf, 2006; Balaji and Ryan, 2007). These earlier findings also agree well with the detection of limited copy numbers of vGlut in purified synaptic vesicles (Takamori et al., 2006).

In mature neurons expressing vGlut-pHluorin, we assessed synaptic vesicle fusion and retrieval by applying low frequency stimulation (0.025-0.1 Hz) followed by 20 Hz high frequency burst stimulation to identify synaptic boutons (Figure. 2.1A). The low frequency stimulation protocol triggered positive fluorescence fluctuations with amplitudes two standard deviations above the mean baseline noise (Figure. 2.1B left) typically corresponding to 2.1 ± 0.2 fluorescence units (Figure. 2.1C top). Each positive fluorescence fluctuation was followed by swift decay back to baseline fluorescence consistent with rapid vesicle re-acidification and retrieval (Figure. 2.1D). Most importantly, this experimental strategy did not require measures, such as pre-photobleaching, to reduce background surface fluorescence levels, which may have adverse effects (Gandhi and Stevens, 2003; Atluri and Ryan, 2006; Balaji and Ryan, 2007).

To test whether the positive fluorescence fluctuations we detected were indeed due to synaptic vesicle fusion and retrieval, we performed similar experiments in the presence of the vacuolar ATPase inhibitor, folimycin. The decay phase of the vGlut-pHluorin signal reports the rate of synaptic vesicle re-acidification that follows vesicle retrieval. Therefore, in the presence of folimycin, fusion events take on a staircase-like fluorescence pattern (Figure. 2.1B bottom) as inhibition of re-acidification traps vesicles in an alkaline state. The amplitudes of fusion events we detected in these experiments were comparable to the

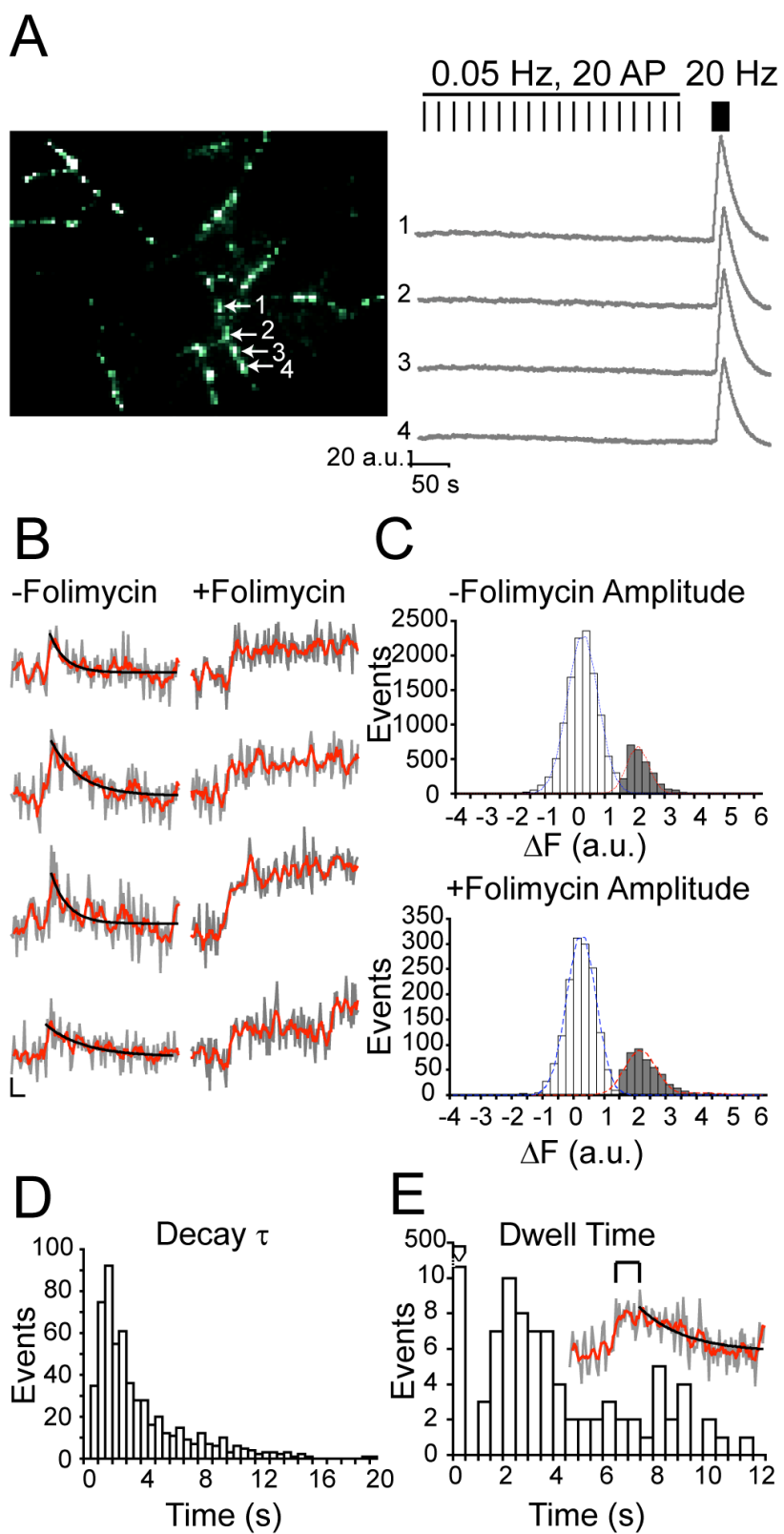


Figure 2.1. Single-vesicle fusion events are distinguishable from noise and decay rapidly. **A**, Example frame showing numerous punctate release sites, left, and corresponding vGlut1-pHluorin signal, right, evoked by low frequency single-AP stimulation (0.025-0.2Hz) in 2 mM CaCl₂ followed by 20 Hz stimulation. **B**, Raw fluorescence data (grey trace) can be fit with Levenberg-Marquardt single exponential decay (black trace). Red trace shows the moving average of five points (~1 s). Scale bar shows 1 arbitrary fluorescence unit (a.u.) amplitude over 2 s. **C**, Comparing the amplitude distribution of evoked events with and without folimycin shows no difference in distribution and mean, suggesting that the events observed in 2 mM extracellular Ca²⁺ are composed of single quanta. White bars show a normal distribution of noise (with Gaussian fit, blue trace, mean = 0.14 ± 0.52 a.u.). Grey bars depict successful events (with Gaussian fit, red trace, mean = 2.12 ± 0.23 a.u. without folimycin and 2.05 ± 0.48 a.u. with folimycin ($K_{S_{\text{test}}}=1$)). **D**, The distribution decay constants of 570 events from 355 boutons across 6 coverslips is exponential with (mean = 3.4 s and median = 2.2 s). **E**, In some cases events did not decay immediately but spent some dwell time on the surface (example inset). The frequency distribution of dwell times (from same population of events in D) shows a bimodal distribution with the vast majority of events decaying immediately (<200 ms).

distribution of events we analyzed above in the absence of folimycin (Figure. 2.1C bottom), indicating that our detection and analysis criteria can reliably uncover vesicle fusion and retrieval during low-frequency, sparse stimulation.

In 2 mM extracellular Ca^{2+} , the fluorescence decay time constants had a mean around 3 s ($\tau = 3.4 \pm 3.3$ s, Figure. 2.1D). The decay times followed an exponential distribution with ~72% of events decaying with time constants less than 4 s after fusion. At this near physiological Ca^{2+} concentration, fusion events were rarely followed by a plateau phase, suggesting that vGlut-pHluorin probes did not manifest a detectable period of residency at the surface membrane (Figure. 2.1E). This result implies that in these experiments, single synaptic vesicle endocytosis is initiated within our acquisition rate (200 ms) after vesicle exocytosis.

Ca^{2+} -dependent regulation of single synaptic vesicle fusion probability

During low frequency stimulation (<1 Hz), the behavior of most synapses is dictated by their baseline probability of synaptic vesicle fusion (Pr) as there is limited propensity for short-term synaptic plasticities seen at higher frequencies (Zucker and Regehr, 2002). Accordingly, in the presence of 2 mM extracellular Ca^{2+} , we detected only a small number of fusion events per synaptic bouton during sustained low frequency stimulation, suggesting a low Pr and preponderance of fusion failures. In the next set of experiments, we systematically investigated Ca^{2+} -dependence of Pr by tallying events at each stimulation as failures (events within two standard deviations of baseline noise) or successes (two standard deviations above the mean baseline noise as in Figure. 2.1) (Figure. 2.2A) and calculated the

Pr as the ratio of successful events to the total number of stimuli (i.e. trials) applied to a given bouton. At 1 mM and 2 mM extracellular Ca^{2+} concentration, this analysis yielded a distribution where 88% and 84% of synapses had a Pr of less than 0.2, respectively, with a median of 0.1 (Figure. 2.2B,C). This distribution is remarkably similar to earlier single synapse measurements conducted by measuring probability of FM1-43 uptake as a marker for Pr Murthy et al., 1997.

Next, we examined the distributions of Pr values measured per synaptic bouton at increasing extracellular Ca^{2+} concentrations. Interestingly, at 1 mM Ca^{2+} , ~35% of synaptic boutons were largely unresponsive to low frequency stimulation and therefore had an evoked release probability of near 0 ($\text{Pr} < 0.1$). At 2 mM extracellular Ca^{2+} , this fraction decreased to ~20% whereas at 4 and 8 mM Ca^{2+} , approximately 10% of synaptic boutons were unresponsive to low frequency stimulation. In addition to this decrease in the fraction of extremely low Pr synapses, we also detected an increase in overall release probability in the classical sense (Figure 2.2B-E). With increasing Ca^{2+} concentrations, Pr values showed a wide spread distribution with an increasing number of synaptic boutons reaching a Pr of 1. Cumulative data from all Ca^{2+} concentrations could be described with a Hill function ($\text{Pr} = 1/(1+(c/[\text{Ca}^{2+}]_e)^n)$) yielding a corresponding Hill coefficient (n) of 4.8, which suggests a degree of cooperativity consistent with previous electrophysiological estimates of Ca^{2+} -dependence of neurotransmitter release probability (Dodge and Rahamimoff, 1967; Mintz et al., 1995; Fernandez-Chacon et al., 2001). Furthermore, these results reinforce the premise that our optical measurements report single vesicle release from single release sites. Interestingly, increasing extracellular Ca^{2+} concentrations also caused a marked increase in

the amplitudes of fusion events suggesting multivesicular release (see below). However, P_r calculations we present here did not differentiate between single and multivesicular fusion events.

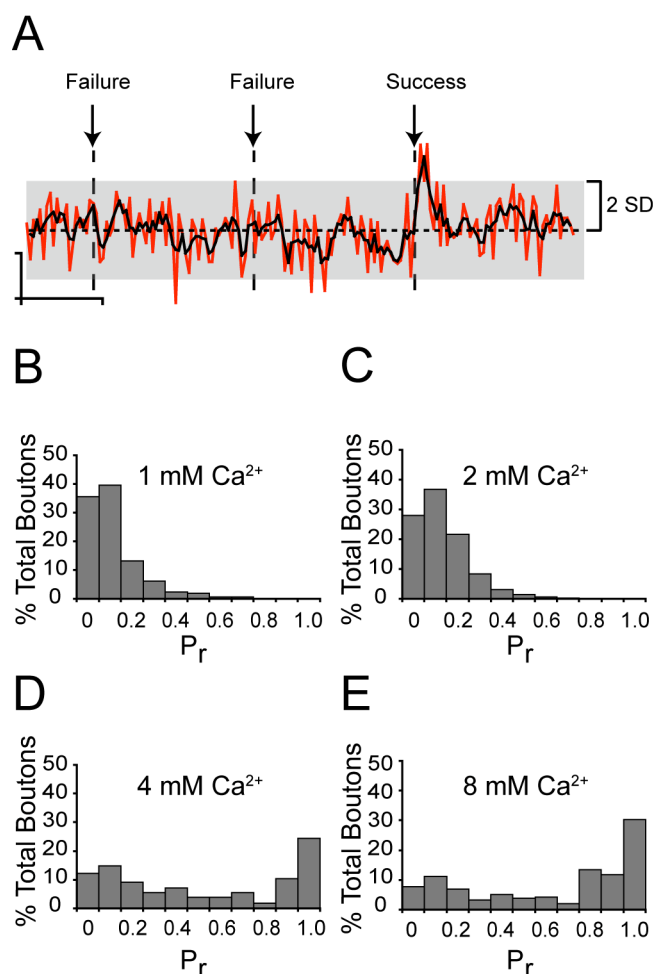


Figure 2.2 Increasing Ca^{2+} causes an increase in P_r . A, Example trace showing a successful event, the shaded area shows 2 standard deviations (S.D.) from the mean of the noise. Vertical scale bar represents 2 a.u. while horizontal scale bar is 5 s. B-E, Release probability, by bouton, shows classical Ca^{2+} sensitivity as extracellular Ca^{2+} increases. Overall increase in average P_r could be described with a Hill equation with a coefficient of 4.8. However, at high Ca^{2+} concentrations, a bimodal distribution of release probabilities reflects two populations of boutons: one reluctant-to-release and one release competent.

The effect of Ca^{2+} on multivesicular release.

During low frequency single action potential stimulation fluorescent responses showed an abrupt increase in fluorescence, consistent with fast exocytosis followed by a slower decay (Figure. 2.3A). As extracellular Ca^{2+} increased, the amplitudes of fluorescence changes also increased in a quantal fashion (Figure. 2.3B) consistent with an increase in multivesicular fusion events. At low extracellular Ca^{2+} (1 mM), fluorescence amplitude distributions could be represented with a single Gaussian curve (mean = 2.2 ± 0.5 a.u., reduced $\chi^2 = 0.97$). The amplitudes of events detected at near-physiological 2 mM extracellular Ca^{2+} were also fit well by a single Gaussian (mean = 2.1 ± 0.2 a.u., reduced $\chi^2 = 0.98$) suggesting that single vesicle fusion events predominate low-frequency evoked transmission at 1 and 2 mM extracellular Ca^{2+} . At 4 mM Ca^{2+} , the fluorescence amplitude distribution broadened and could be fit by the sum of two Gaussians (black traces) with means spaced at integer-multiples of one another, indicating quantal fluorescence steps (mean₁ = 2.2 ± 0.5 a.u.; mean₂ = 4.4 ± 1.1 a.u.; reduced $\chi^2 = 0.96$, red traces). At high 8 mM extracellular Ca^{2+} , the fluorescence amplitude distribution fit to the sum of three Gaussians (mean₁ = 2.2 ± 0.5 a.u.; mean₂ = 4.4 ± 1.1 a.u.; mean₃ = 6.6 ± 1.6 a.u., reduced $\chi^2 = 0.85$). Here, it is important to note that our acquisition rate (200 ms) was not fast enough to distinguish between synchronous multivesicular fusion events and fast asynchronous fusion events. Thus our reference to fluorescence changes greater than those observed in 1 and 2 mM Ca^{2+} as multivesicular fusion events includes asynchronous fusion events that occur in a single release site in tandem (Rudolph et al., 2011). These findings indicate that the increase in extracellular Ca^{2+} concentration does not only increase single vesicle fusion probability

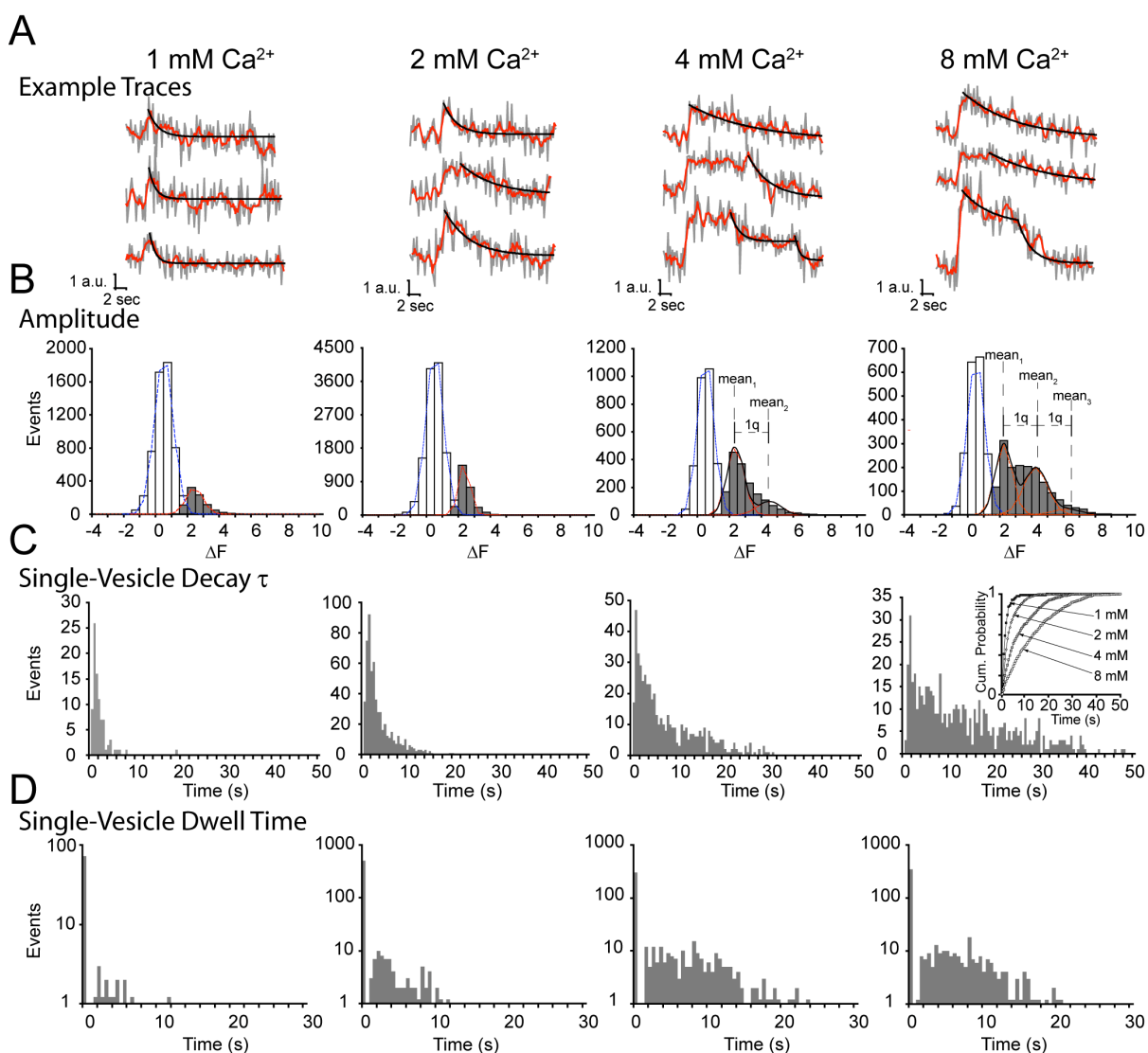


Figure 2.3. Increasing extracellular Ca^{2+} promotes multivesicular release, slows decay time, increases the propensity for a vesicle to dwell on the surface, and increases that dwell time. **A**, Sample traces of single vesicle events observed in extracellular 1 mM (left), 2 mM (center left), 4 mM (center right), and 8 mM (right) Ca^{2+} . The grey trace shows raw fluorescence data, the red trace is a moving average of five points (~ 1 s), the black trace is a single exponential decay fit using Levenberg-Marquardt least squares minimization to the grey trace. **B**, The amplitude distribution of fluorescence changes in response to single-AP stimuli delivered at low (0.025-0.2 Hz) frequency. Fluorescence intensity amplitudes increase with increasing Ca^{2+} . White bars show amplitude distribution during no stimulus and have a normal Gaussian distribution (blue dashed line). Grey bars are the change in fluorescence of successful release events (for calculation see methods) and can be fit with one (red dashed line) or multiple—quantally distributed—Gaussians (black line). **C**, Single vesicle decay time increases with increasing Ca^{2+} . Only events from **B** with amplitudes

within 1 S.D. of the mean in 2 mM Ca^{2+} (i.e. 2.1 ± 0.2 a.u.) were selected. At 1 mM extracellular Ca^{2+} , events decayed with an average τ of 1.9 ± 2.3 s (from 87 events from 55 puncta and 3 coverslips from 2 cultures). At 2 mM extracellular Ca^{2+} events decayed slower with an average τ to 3.4 ± 3.3 s (from 572 events from 233 puncta from 5 coverslips over 3 cultures). The decay increased to an average τ of 8.1 ± 7.3 s in 4 mM Ca^{2+} (from 511 events from 168 puncta over 6 coverslips from 3 sets of cultures). Finally, events in 8 mM extracellular Ca^{2+} had an average τ of 13.1 ± 10.5 s (from 542 events from 186 puncta from 6 coverslips from 4 cultures). The inset shows the cumulative probability histogram of decay times, all conditions are significantly different ($p < 0.001$) according to K-S test. **D**, The distribution of dwell times shows that increasing Ca^{2+} causes more vesicles to experience a delay prior to endocytosis. Additionally, increasing Ca^{2+} increases the length of that delay but appears to have some maximal effect after 4 mM Ca^{2+} .

but also increases the likelihood of multivesicular synchronous and/or asynchronous fusion events.

The effect of Ca^{2+} on single synaptic vesicle retrieval.

Next, we analyzed the fluorescence decay of single-vesicle events by only selecting fusion events with fluorescence amplitudes of univesicular fusion events within the first Gaussian distribution (i.e. mean = 2.2 ± 0.5 a.u.). We then determined the decay time (τ) and dwell time of those events. Surprisingly, increases in extracellular Ca^{2+} increased the τ of single-vesicle events (Figure 2.3C) skewing the distributions towards slower decay times. At 1 mM extracellular Ca^{2+} , events decayed with an average τ of 1.9 s and median τ of 1.3 s, which increased to 3.4 s and median τ of 2.2 s in 2 mM extracellular Ca^{2+} . In 4 mM extracellular Ca^{2+} , the average τ increased to 8.1 s, although half of those events decayed

within 5 s (median $\tau = 5.6$ s). Finally, events in 8 mM extracellular Ca^{2+} had an average τ of 13.1 s with median τ of 10.7 s.

In addition to the apparent slowing in the time course of fluorescence decay, increasing extracellular Ca^{2+} caused some vesicles to show a brief delay at the high fluorescence value before the onset of fluorescence decay (Figure. 2.3D). The majority of events in all extracellular Ca^{2+} conditions did not manifest a dwell time longer than 200 ms. However, in some cases, there were significant pauses prior to fluorescence decay and increasing extracellular Ca^{2+} caused more fusion events to dwell longer at elevated fluorescence values (Figure. 2.3D). In 1 and 2 mM extracellular Ca^{2+} , fusion events experienced dwell times of 3.8 ± 2.5 s and 4.2 ± 2.8 s, respectively. The dwell time distributions were not significantly different at low and near-physiological extracellular Ca^{2+} (Kolmogorov-Smirnov test $p = 1$). This dwell time increased to 8.3 ± 5.7 s and 7.3 ± 4.3 s in 4 and 8 mM extracellular Ca^{2+} , respectively. The distributions of dwell times were not significantly different between 4 and 8 mM extracellular Ca^{2+} (Kolmogorov-Smirnov test p value = 1) but there was a significant difference between high Ca^{2+} and low Ca^{2+} dwell times (Kolmogorov-Smirnov test $p < 0.005$), suggesting that a threshold level of intracellular Ca^{2+} delays vesicle retrieval for seconds.

The relation between probability of synaptic vesicle fusion and synaptic vesicle trafficking.

We next explored the relationship between the synaptic Pr (estimated as in Figure. 2.2) and the kinetic properties of individual fusion events (Figure. 2.4A-C). We found that synapses with a high Pr were indeed more likely to release multiple vesicles in response to a

single stimulation (Figure. 2.4A). This correlation was particularly striking in high Pr values detected in 8 mM Ca^{2+} (Figure. 2.4A). In this analysis, we observed a Ca^{2+} -dependent increase in single vesicle retrieval time, as documented in Figure 3C, which manifests as a vertical shift in decay times between 2 mM and 8 mM Ca^{2+} (Figure. 2.4B). However, we also found that synapses with a higher Pr were slower to retrieve vesicles (Figure. 2.4B) consistent with earlier observations (Gandhi and Stevens, 2003). Together these data suggest that intrinsic properties of synapses control the rate of endocytosis, but extrinsic factors, such as Ca^{2+} influx, also acts to slow vesicle retrieval. Dwell times, however, were relatively independent of release probability in high Ca^{2+} , but showed a slight increase with increasing Pr in 2 mM Ca^{2+} (Figure. 2.4C), suggesting the independence of processes underlying the initiation of the retrieval versus the actual retrieval. Finally, given that higher Pr synapses are more prone to multivesicular release, we probed how the decay times of multivesicular events compared to those of single vesicle events (Figure. 2.4D). In 8 mM Ca^{2+} , where we detect multivesicular events in high abundance, we found that the individual decay times comprising the retrieval of a multivesicular event (τ_{m1} , τ_{m2}) were slower than that of single-vesicle retrieval events (τ_s) (Figure. 2.4D) (multivesicular decay: mean τ_{m1} of 15.1 s with median τ_{m1} of 14.5 s vs. single-vesicle decay: mean τ_s of 13.1 s with median τ_s of 10.7 s; Kolmogorov-Smirnov test $p < 0.001$). Interestingly, within multivesicular events, the second decay time constant τ_{m2} was still slower than both the single-vesicle events τ_s and the first τ_{m1} , with average τ_{m2} of 17.8 s and median τ_{m2} of 17.0 s (Kolmogorov-Smirnov test $p < 0.001$). These findings suggest that multivesicular events are slower to recycle than single

vesicle events, which may point to a small but significant impact of exocytic load on the kinetics of vesicle retrieval.

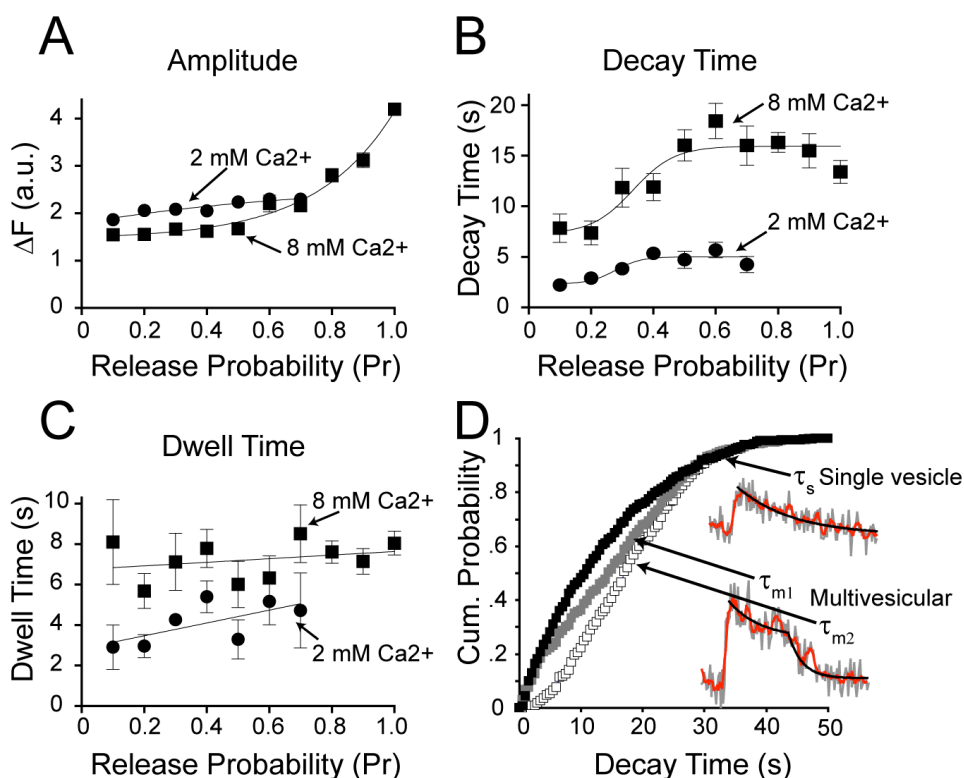


Figure 2.4. The probability of synaptic vesicle fusion correlates with the propensity of multivesicular fusion and a longer single-vesicle retrieval time. **A**, Synapses with a high release probability exhibit more multivesicular fusion events and **B**, slower single-vesicle retrieval times. **C**, Dwell times, however, are relatively unaffected by the Pr of the synapse. Error bars show S.E.M. **D**, The fluorescence decay time of multivesicular fusion events can be separated into two decay steps (τ_{m1} , τ_{m2}) (**D inset**). In 8 mM Ca^{2+} , the individual decay times comprising the retrieval of multivesicular events were slower than those of single-vesicle retrieval events (τ_s) (multivesicular decay: average τ_{m1} of 15.1 s with median τ_{m1} of 14.5 s vs. single-vesicle decay: average τ_s of 13.1 s with median τ_s of 10.7 s; Kolmogorov-Smirnov test $p < 0.001$). Within multivesicular events, the second decay time constant (τ_{m2}) was still slower than both the single-vesicle events τ_s and the first τ_{m1} , with average τ_{m2} of 17.8 s and median τ_{m2} of 17.0 s (Kolmogorov-Smirnov test $p < 0.001$).

Intrasynaptic Ca²⁺ acts to modulate vesicle endocytosis.

We sought to test the hypothesis that Ca²⁺ influx, rather than extracellular Ca²⁺ per se, acts to modulate the kinetics of endocytosis. To this end, we analyzed low-frequency evoked events in the presence of the internal Ca²⁺ chelator, EGTA-AM at near-physiological 2 mM extracellular Ca²⁺ (Figure. 2.5A) and high 8 mM extracellular Ca²⁺ (Figure. 2.5B). Low-frequency stimulation after incubation with 10 μM EGTA-AM (20 min. pre-treatment) decreased decay times in both 2 mM Ca²⁺ and 8 mM Ca²⁺ to an average τ of 1.3 s and 7.7 s, respectively (KS test p <0.001 for both 2 mM Ca²⁺ and 8 mM Ca²⁺) and median τ of 0.9 s and 5.7 s, respectively. At 2 mM Ca²⁺ as well as 8 mM Ca²⁺, EGTA-AM treatment resulted in a 3-fold decrease in Pr (2 mM Ca²⁺: without EGTA-AM average Pr~0.13, with EGTA-AM average Pr~0.04; at 8 mM Ca²⁺: without EGTA-AM average Pr~0.6, with EGTA-AM average Pr~0.18) and complete abrogation of multivesicular events. These results suggest that Ca²⁺ entry into the presynaptic terminal is required to mediate the negative action of increased extracellular Ca²⁺ on the rate of vesicle retrieval.

Intrasynaptic Ca²⁺ acts through calcineurin to modulate vesicle endocytosis.

Previous work has suggested that the Ca²⁺/calmodulin-dependent phosphatase, calcineurin, acts as a key regulator of synaptic vesicle endocytosis through dephosphorylation of endocytic proteins (Marks and McMahon, 1998; Wu et al., 2009; Sun et al., 2010). Next, we sought to test the hypothesis that Ca²⁺ influx acts through calcineurin to modulate the kinetics of endocytosis. We analyzed low-frequency evoked events in the presence of a specific calcineurin inhibitor, FK506, at near-physiological 2 mM extracellular

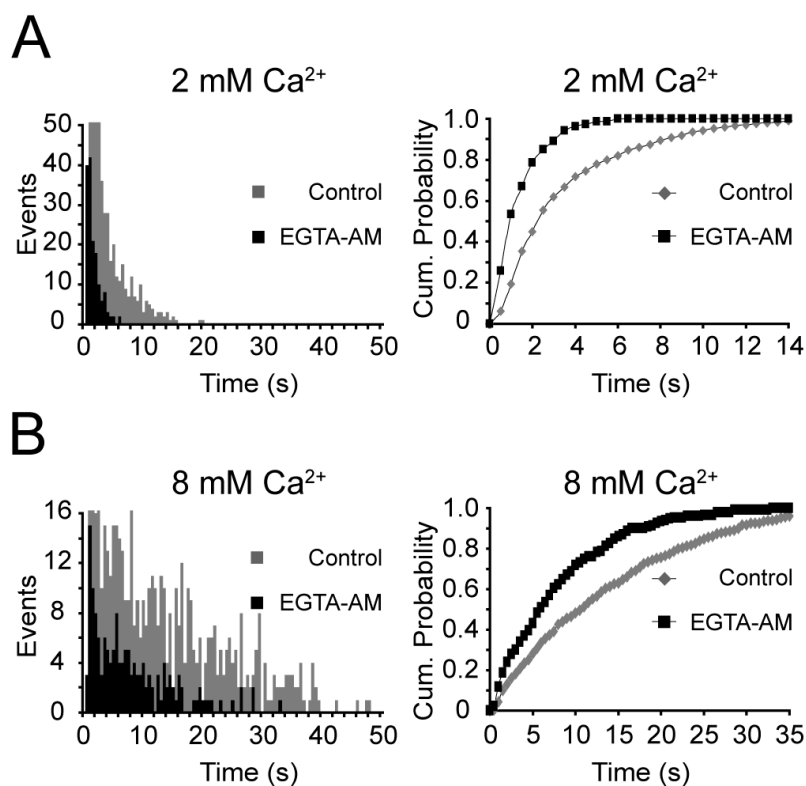


Figure 2.5. The rate of endocytosis is controlled by intracellular Ca²⁺ influx. **A, B,** The decay time of events, evoked by single action potential stimulation in 2 mM (**A**) or 8 mM (**B**) extracellular Ca²⁺, decrease with application of the slow intracellular Ca²⁺ chelator, EGTA-AM. Cumulative probability histograms show that incubation in EGTA-AM decreases the decay time of events in both 2 mM Ca²⁺ (KS test $p < 0.001$) and 8 mM Ca²⁺ (KS test $p < 0.001$).

Ca²⁺ (Figure. 2.6A) and high 8 mM extracellular Ca²⁺ (Figure. 2.6B). Under both conditions, as with internal Ca²⁺ chelation, inhibition of calcineurin using 1 μ M FK506 resulted in faster decay times. In 2 mM Ca²⁺, the mean τ decreased to 2.2 s, and in 8 mM Ca²⁺, the mean τ decay time decreased to 4.5 s (KS test $p < 0.001$ for both 2 and 8 mM Ca²⁺) with median τ of 1.5 s and 3.8 s for 2 and 8 mM Ca²⁺, respectively. Here, it is important to note that FK506 treatment induced only a small decrease in release probability at 8 mM Ca²⁺ from average Pr

of 0.6 without FK506 to 0.5 with FK506 supporting the premise that calcineurin inhibition directly facilitates vesicle retrieval rather than acting indirectly by regulation of release probability. Taken together, these results suggest that Ca^{2+} entry into the presynaptic terminal activates calcineurin to mediate the negative action of increased extracellular Ca^{2+} on the rate of vesicle retrieval.

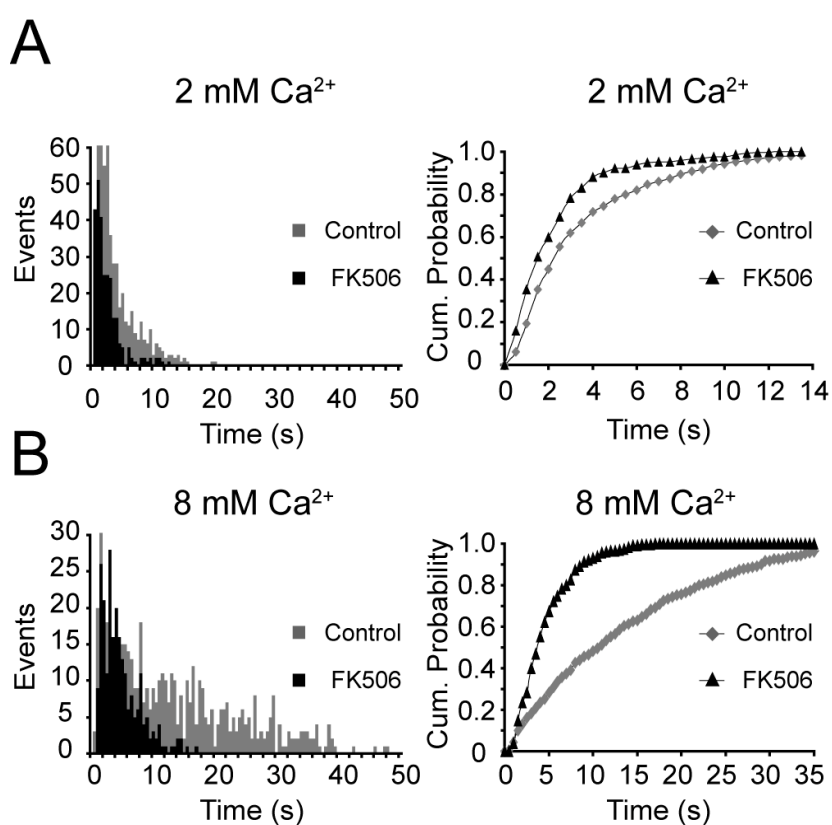


Figure 2.6. Intracellular Ca^{2+} activates calcineurin to control the rate of endocytosis.

A, B, The decay time of events evoked by single action potential stimulation in 2mM (**A**) and 8 mM (**B**) extracellular Ca^{2+} , decrease when calcineurin is inhibited with FK506.

Cumulative probability histograms show that incubation in FK506 decreases the decay time of events in both 2 mM Ca^{2+} (KS test $p < 0.001$) and 8 mM Ca^{2+} (KS test $p < 0.001$).

Estimating single vesicle retrieval during higher frequency stimulation.

Our results so far suggest that upon fusion synaptic vesicles are re-acidified and retrieved with a relatively rapid time course. However, this decay time is tightly controlled by intrasynaptic Ca^{2+} and calcineurin activation. Next, we tested this premise at 1 Hz stimulation where intrasynaptic Ca^{2+} accumulates (Zucker and Regehr, 2002) without inducing significant synaptic depression in this system (Ertunc et al., 2007). For this purpose, we compiled theoretical ideal single-vesicle events using mean decay times and dwell times for 2, 4 and 8 mM extracellular Ca^{2+} conditions (Figure. 2.7A). Neurons were stimulated with 10 APs delivered at 1 Hz and the resulting fluorescence traces were fit by the summation of ideal events using the probability of release estimate we obtained by fitting the rise time of each 1 Hz trace (Figure. 2.7B). Interestingly, predicted ideal 1 Hz traces obtained by cumulative summation of individual ideal events decayed faster than the observed experimental fluorescence decay and therefore were poor fits to the data (Figure. 2.7B, black traces). We hypothesized that this apparent slower decay could be the result of slowing individual retrieval events as intrasynaptic Ca^{2+} increases, because 1 Hz stimulation is faster than nerve terminal Ca^{2+} removal (Regehr et al., 1994). To seek a better fit to the observed 1 Hz decay phase, we serially increased vesicle decay time for each stimulus delivered. Increasing decay time as a function of stimuli mimics actual fluorescence data (Figure. 2.7B, blue traces). If endocytosis slows with each round of Ca^{2+} entry (i.e. stimulus) (Figure. 2.7C), then each stimulus slows vesicle retrieval by ~30%, in 2 mM extracellular Ca^{2+} . This scenario maximized the goodness of fit of idealized traces to the actual data ($R^2_{\text{per stim}} = 0.92$, compared to $R^2_{\text{no change}} = -1.5$). As extracellular Ca^{2+} increases, the serial

deceleration observed is occluded such that at high extracellular Ca^{2+} , succeeding vesicles show limited decrease in their rate of retrieval per stimulus (for 4 mM Ca^{2+} $R^2_{\text{per stim}} = 0.94$, compared to $R^2_{\text{no change}} = -0.2$) (Figure. 2.7B, middle). In fact, at 8 mM Ca^{2+} , decay times must increase only slightly, if at all, with each stimulus or fusion event to account for the actual data ($R^2_{\text{per stim}} = 0.99$, compared to $R^2_{\text{no change}} = 0.90$) (Figure. 2.7B, left). This finding suggests that single vesicle events at high Ca^{2+} concentrations are approaching a lower limit of vesicle retrieval rate.

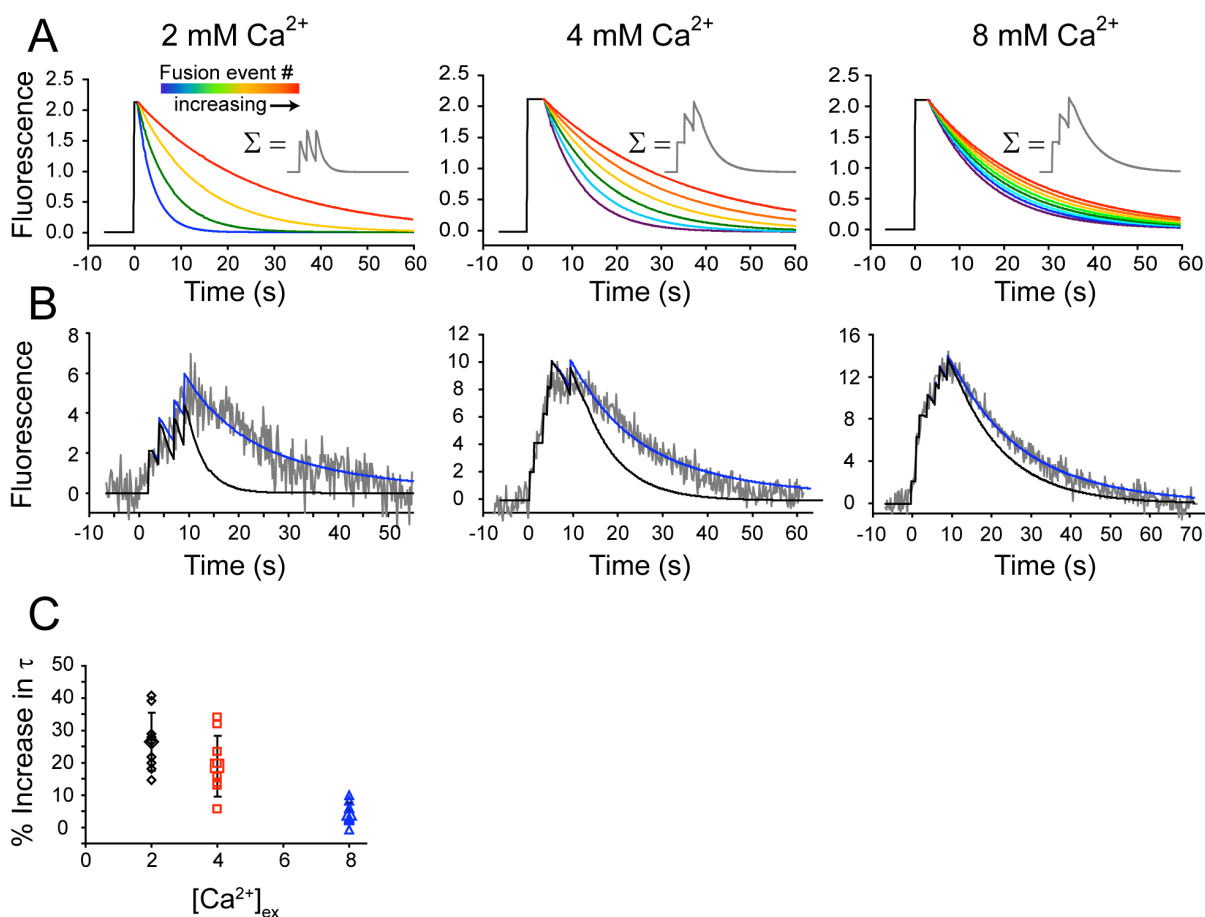


Figure 2.7. Modeling of 1 Hz stimulation requires a serial slowing in endocytic kinetics.

A, Ideal events generated by averaging all decay times and dwell times from single vesicle events during low frequency stimulation. Heat map colors show the effect of serial slowing on single vesicle events. Insets show examples of the summation of three events at stimulus number 1 ($t = 0$ s), 5 ($t = 4$ s) and 10 ($t = 9$ s). **B**, Ideal events can be used to fit higher frequency (1 Hz) stimulation data (grey trace). Two fits were generated where decay time is held constant (black trace) and where decay is increasing for each stimulus regardless of fusion event (blue trace). **C**, Increasing decay time per stimulus requires small adjustments to each vesicle fusion event as extracellular Ca^{2+} increases.

Discussion

Single vesicle endocytosis is rapid

Optical measurements of single synaptic vesicle endocytosis have resulted in a widespread disagreement of vesicle retrieval kinetics and time course (Gandhi and Stevens, 2003; Granseth et al., 2006; Balaji and Ryan, 2007; Zhu et al., 2009). In this study we use vGlut-pHluorin to optically monitor vesicle reacidification without prior photobleaching (Gandhi and Stevens, 2003) or event averaging (Granseth et al., 2006). Our results are consistent with earlier reports of fast single-vesicle endocytosis (Aravanis et al., 2003; Gandhi and Stevens, 2003; Bowser and Khakh, 2007; Zhang et al., 2009a, 2009b) that proceeds through a single process (Balaji and Ryan, 2007) during low frequency 0.025-0.1 Hz stimulation albeit with remarkably fast kinetics (Figure. 2.1). During low frequency stimulation, in physiological extracellular Ca^{2+} , small fluorescence steps occurred faster than our rate of acquisition (200 ms), consistent with fast vesicle fusion. To confirm that the observed events were the products of single vesicle fusion, we compared the fluorescence amplitude of events in the presence and absence of the vacuolar H^+ -ATPase inhibitor, folimycin (Figure. 2.1B,C). The similarity between the two fluorescence event amplitude distributions suggests that observed fluorescence steps were the result of single-vesicle fusion events. Additionally, our observed Pr distribution at 2 mM extracellular Ca^{2+} (Figure. 2.2B) was strikingly similar to previous estimates of probability of neurotransmitter release using FM dye uptake (Murthy et al., 1997) and electrophysiological methods (Fernandez-Chacon et al., 2001) in hippocampal neurons. This similarity in Pr estimates strongly

supports the premise that, in our experimental system, all recycling vesicles possess a comparable number of Vglut1-pHluorin molecules and a negligible population of untagged vesicles. Furthermore, these observations strongly support our assumption that the fluorescence changes we observe are due to single-vesicle fusion events originating from individual synaptic release sites.

The rise in fluorescence amplitude was followed by rapid fluorescence decay that could be fit with a single exponential (Figure. 2.1D). These decay times had a median τ of 2.2 s and average of 3.4 s, at near physiological extracellular Ca^{2+} , indicating rapid vesicle reacidification, and rapid vesicle retrieval (Gandhi and Stevens, 2003). The majority of events (~87%) began to decay in less than 0.5 s after vesicle fusion. But in some cases the fluorescence amplitude would pause prior to decay with an average dwell time of ~ 4.2 s (Figure. 2.1E). Although we cannot differentiate between a pause in vesicle reacidification and a period of vesicle residency on the synaptic surface, these measurements of single-vesicle endocytosis are significantly faster than the previous estimates of vesicle reacidification (Atluri and Ryan, 2006; Granseth et al., 2006) or endocytic time courses (Balaji and Ryan, 2007) at physiological Ca^{2+} levels.

Ca^{2+} increases vesicle fusion probability and slows retrieval

Given the sensitivity of our experimental system, we were able to examine single vesicle release probability (Figure. 2.2) as well as single vesicle retrieval as a function of extracellular Ca^{2+} concentration (Figure. 2.3). We found that increasing extracellular Ca^{2+} elevated vesicle fusion Pr, with a corresponding Hill coefficient of 4.8, similar to what is

observed using electrophysiological measures (Dodge and Rahamimoff, 1967; Mintz et al., 1995; Fernandez-Chacon et al., 2001). Interestingly, in addition to an increase in overall release probability as Ca^{2+} increased, the number of boutons with very low release probability ($\text{Pr} < 0.1$) decreased, suggesting that more boutons were recruited to an active state.

Higher extracellular Ca^{2+} concentrations produced larger steps in fluorescence amplitude increase, which could be described with quantal Gaussian distributions with equally spaced means. These results indicate that increasing extracellular Ca^{2+} raises the propensity for multivesicular and/or fast asynchronous release events (Figure. 2.3B). This observation also raises the possibility that dual discontinuous decay times detected in earlier work (Zhu et al., 2009) could in part reflect vesicle retrieval after multivesicular fusion events (e.g. Figure. 2.3A). When we selected events that had fluorescence amplitudes within one standard deviation of the first Gaussian mean (i.e. univesicular events), we found that increasing extracellular Ca^{2+} slowed vesicle retrieval (Figure. 2.3C), and encouraged vesicle residency at the synaptic surface membrane (Figure. 2.3C). Accordingly, buffering intracellular Ca^{2+} , by incubating neurons in EGTA-AM accelerated the rate of vesicle retrieval (Figure. 2.5), confirming previous results that show the rate of endocytosis is closely tied to Ca^{2+} influx into the synaptic terminal (Yao et al., 2009). However, our findings point to a negative regulation of synaptic vesicle retrieval by Ca^{2+} , which is consistent with earlier reports (von Gersdorff and Matthews, 1994; Wan et al., 2010). Previous work has suggested that Ca^{2+} /calmodulin-dependent phosphatase, calcineurin, acts as a key regulator of synaptic vesicle endocytosis through dephosphorylation of endocytic proteins (Marks and McMahon,

1998; Wu et al., 2009; Sun et al., 2010). Our results indicate that calcineurin may indeed play a key role in transducing the Ca^{2+} signal to the endocytic machinery thus slowing down single vesicle retrieval although its actual molecular target in this process remains to be determined (Figure. 2.6).

We found that synapses with higher release probability show an elevated propensity for multivesicular fusion and slower single-vesicle retrieval kinetics (Figure. 2.4A-C). In addition, we found that multivesicular fusion events were slower to be retrieved than single-vesicle events (Figure. 2.4D). This observation suggests that exocytic load (i.e. the number of vesicles fused with the plasma membrane) may exert a direct influence on the rate of retrieval. However, as Ca^{+2} appears to slow retrieval time regardless of Pr in low release probability boutons, this possibility does not preclude a strong direct impact of Ca^{+2} on vesicle retrieval kinetics (compare Figure. 2.4A and B).

Endocytosis progressively slows during higher frequency stimulation.

Is the observed slowing of vesicle retrieval at elevated Ca^{2+} concentrations significant in the context of physiological higher frequency stimulation? We recorded fluorescence waveforms during a 10 AP train delivered at 1 Hz and reproduced the observed waveform using the summation of theoretical ideal single-vesicle events (Figure. 2.7). We reasoned that because a 1 Hz stimulus is faster than presumed terminal Ca^{2+} clearance (~ 1.1 s; (Regehr et al., 1994)), endocytosis would slow with concomitant internal Ca^{2+} build up. Indeed, reconstructing experimental fluorescent traces obtained from 1 Hz stimulations required that each subsequent fusion event be retrieved slower than the previous one (Figure. 2.7B,C). At

near physiological extracellular Ca^{2+} , each successive retrieval time course had to be 15-40% slower than the previous, at physiological Ca^{2+} . At 4 mM extracellular Ca^{2+} , single-vesicle retrieval was already slower, than at physiological Ca^{2+} , therefore the gradual decrease in endocytosis rate was less significant, 13-33%. At 8 mM extracellular Ca^{2+} this progressive decrease in the rate of endocytosis (-0.5-9%) was near saturation, suggesting a lower limit to the rate of single synaptic vesicle retrieval.

Taken together, our findings show that the rate of single-vesicle endocytosis is tightly controlled by presynaptic Ca^{2+} influx and subsequent calcineurin activation. Surprisingly, during low levels of activity this Ca^{2+} dependent regulation acts in a negative manner, slowing the rate of vesicle retrieval. Accordingly, we find that during higher frequency repetitive stimulation, gradual presynaptic Ca^{2+} accumulation slows the rate of vesicle retrieval. These findings underscore the role of neuronal Ca^{2+} buffering as a key regulator of endocytic synaptic vesicle retrieval rate, which may constitute a global, neuron-wide means to set the pace of synaptic vesicle recycling and neurotransmitter release (Armbruster and Ryan, 2011). Therefore, these results go beyond the proposal that synaptic vesicle retrieval is indeed fast, and they provide a basis where earlier seemingly contradictory results can be reconciled in a single coherent scheme.

CHAPTER THREE

FAST RETRIEVAL AND AUTONOMOUS REGULATION OF SINGLE SPONTANEOUSLY RECYCLING SYNAPTIC VESICLES

Background

Synaptic terminals release neurotransmitters either spontaneously or in response to presynaptic action potentials (APs) (Fatt and Katz, 1952). In addition to the well-established role of AP-evoked neurotransmitter release in information transfer and processing, a growing number of studies assign a key role for spontaneous release in synaptic homeostasis and plasticity (Sutton and Schuman, 2005; Kavalali et al., 2011; Hawkins, 2013). Recent work indicates that these two modes of neurotransmission are largely independent in terms of their presynaptic regulation as well as postsynaptic signaling consequences (Lou et al., 2005; Sara et al., 2005; Sutton et al., 2006; Sutton et al., 2007; Atasoy et al., 2008; Melom et al., 2013; Nosyreva et al., 2013; Wierda and Sorensen, 2014). However, the molecular mechanisms that underlie the segregation of the two forms of release are only beginning to be elucidated (Hua et al., 2011; Pang et al., 2011; Ramirez et al., 2012; Bal et al., 2013; Zhou et al., 2013; Wang et al., 2014). There is strong evidence that synaptic vesicles recycle at rest in the absence of presynaptic APs and take up exogenous probes such as FM dyes, antibodies or horseradish peroxidase (Ryan et al., 1993; Murthy and Stevens, 1998; Sara et al., 2005; Peng et al., 2012; Kavalali and Jorgensen, 2014). Studies also suggest that endocytic mechanisms mediating synaptic vesicle retrieval after spontaneous fusion diverge from those that trigger

endocytosis after AP-evoked exocytosis (Chung et al., 2010; Peng et al., 2012; Meng et al., 2013). However, visualizing single spontaneous vesicle fusion and retrieval events has been technically difficult as the stochastic nature and low probability of spontaneous fusion requires long-term imaging with high temporal resolution, which typically gives rise to significant photobleaching and potential photodamage. Earlier attempts at detecting spontaneous synaptic vesicle exo-endocytosis using capacitance measurements heavily relied on signal averaging and was confounded by susceptibility to contamination by fusion events unrelated to synaptic vesicle exocytosis (Sun et al., 2002; Yamashita et al., 2005).

The current lack of insight into single synaptic vesicle retrieval leaves open the question of whether spontaneous synaptic vesicle exocytosis is tightly and temporally coupled to vesicle retrieval. In this study, we used the vesicular glutamate transporter or the vesicle protein synaptophysin as carriers for luminal pH-sensitive fluorescent probes and optimized imaging conditions to minimize photobleaching without compromising our ability to detect a majority of spontaneous synaptic vesicle fusion events. Our optical recording conditions were similar to our earlier work where we characterized single AP-evoked fusion events with a median probability of 0.2 (Leitz and Kavalali, 2011) indicating that these settings enable visualization of release from single boutons (Murthy et al., 1997). Under these conditions, we found that single synaptic vesicles are retrieved extremely rapidly (< 370 ms) after spontaneous fusion indicating the fluorescence decay of individual events was dominated by vesicle re-acidification. These spontaneous fusion events were coupled to postsynaptic N-methyl-D-aspartate (NMDA) receptor-driven Ca^{2+} signals as supported by their temporal and spatial juxtaposition to D(-)-2-Amino-5-phosphonopentanoic acid (AP-5)-

sensitive fluorescence signals originating from a Ca^{2+} indicator targeted to postsynaptic densities. Surprisingly, we uncovered a significant fraction of multiquantal events that increased in prevalence at elevated Ca^{2+} concentrations. Furthermore, we could not detect significant correlation between the propensities of evoked and spontaneous fusion events at increasing Ca^{2+} concentrations. These experiments demonstrated that spontaneous fusion propensity in a given synapse is regulated autonomously and independently of evoked release probability. Taken together, these results expand classical quantal analysis (Del Castillo and Katz, 1954; Boyd and Martin, 1956) to incorporate exocytic and endocytic phases of single fusion events and provide insight into the properties and regulation of single spontaneous fusion events in relation to their AP-evoked counterparts that originate from the same synaptic bouton.

Methods

Cell culture

Dissociated hippocampal neurons were cultured from postnatal day 0-3 Sprague Dawley rats of either sex as described previously (Kavalali et al., 1999). At 4 days *in vitro* (DIV), cultures were infected with lentivirus expressing vGlut-pHluorin or with SypHTomato and PSD-95-GCaMP, and experiments were conducted between 15-20 DIV when synapses reach maturity (Mozhayeva et al., 2002).

Lentiviral preparations

In these experiments we relied on a lentiviral expression system. The vGlut-pHluorin construct was a generous gift from Drs. Robert Edwards and Susan Voglmaier (University of

California, San Francisco). A modified, synaptophysin pHTomato was a generous gift from Dr. Richard Tsien (New York University Medical Center and Stanford University). The primers:

ATATggatccggtggttctggtgtgagcaagggcgaggagaataacatggccatcatcaaggagttcatgcgcttcaag

(pHTomato.FIX.F) and atataccggtaccagaaccacccttgtagcagctcgccatgccgccggtggagtgccggccc

(pHTomato.FIX.R) were used to return pHTomato to the published version and attach small

flexible linkers. All lentiviruses were prepared by transfection of human embryonic kidney

(HEK) 293-T cells with the plasmid of interest together with viral coat and packaging protein

constructs (pVSVG, pRsv-Rev, and pPRE) using FuGENE 6 (Promega). Three days after

transfection, virus was harvested from HEK 293-T cell-conditioned media and added to

neuronal media at 4 DIV.

vGlut1-pHluorin imaging and analysis

Single-wavelength experiments were performed using an Andor iXon Ultra 897 back-

illuminated EMCCD camera (Model no. DU-897U-CSO-#BV) collected on a Nikon Eclipse

TE2000-U microscope. For illumination we used a Lambda-DG4 (Sutter instruments) with

FITC filter. Images were acquired at ~8 Hz with an exposure time of 100 ms and binning 4

(Using Nikon Elements Ar software). For analysis, square regions of interest (ROIs) with

length and width of 2.5 mm were generated and the resulting fluorescence values were

exported to Microsoft Excel for analysis. Successful fusion events were those where the

average of 3 points was greater than twice the standard deviation of 17 points (~2.1 sec)

prior. Additionally, at least one point after the initial fluorescence increase had to be greater

than twice the standard deviation of the 17 points prior; this excluded large single point

increases in fluorescence from which decay times could not be determined. Decay times were analyzed in Clampfit (Molecular Devices) by fitting raw data with a single exponential decay using Levenberg-Marquardt least sum of squares minimizations. For all control experiments, the extracellular solution was a modified Tyrode's solution containing (in mM): 150 NaCl, 4 KCl, 10 glucose, 10 HEPES, 2 MgCl and varying concentrations of CaCl₂ (2, 4, and 8mM), pH 7.4 (310 Osm). In experiments with folimycin (Concanamycin A, Sigma), a final concentration of 80 nM was used. For Tris-buffered experiments, solutions contained (in mM): 108 NaCl, 4 KCl, 2 MgCl₂, 10 glucose and 50 Tris-HCl and 2 or 8 CaCl₂. All solutions were adjusted to pH 7.4 with NaOH and 310 Osm prior to use. To prevent network activity, postsynaptic ionotropic glutamate receptor antagonists 6-cyano-7-nitroquinoxaline-2,3-dione (CNQX 10 μM; Sigma) and D(-)-2-Amino-5-phosphonopentanoic acid (AP-5 50 μM; Sigma) were added to the experimental solutions. To prevent spontaneous action potential generation, we incubated neurons in 1 μM tetrodotoxin (TTX). For simultaneous spontaneous activity and evoked stimulation experiments, TTX was omitted from the extracellular solution and neurons were stimulated using parallel bipolar electrodes (FHC) delivering 15-20 mA pulses with pulse width of 1 ms. At the end of each experiment, Tyrode containing 20 mM NH₄Cl was added to help identify putative synaptic boutons.

SypHTomato/PSD-95-GCaMP imaging and analysis

For dual color experiments, FITC and TRITC filters (Chroma Technology) were inserted into the Lambda-DG. Images were collected on the same hardware as above but with increased acquisition interval of 180 ms (using 40 ms FITC and 140 ms TRITC excitation intervals). The extracellular solution was the same as above, however 2,3-dihydroxy-6-nitro-

7-sulfamoyl-benzo[f]quinoxaline-2,3-dione (NBQX 10 μ M; Tocris) was used instead of CNQX as it is a more specific AMPAR antagonist. AP-5 and Mg^{2+} were omitted from all experiments to allow Ca^{2+} entry through NMDARs. Full waveforms of sypHTomato and GCaMP5K fluorescence were fit with a double exponential decay time and linearized to correct for photobleaching. Corrected fluorescence waveforms were analyzed as above for fluorescence increases. Once events were determined to be successful, the raw data at that time was linearly corrected according to the baseline slope from 15 s before the event. This method proved successful as in the absence of folimycin events would decay back to baseline but in the presence of folimycin the events had a staircase fluorescence waveform. All sypHTomato and GCaMP5K events were then aligned and averaged for each experiment.

Multivesicular delay analysis

Hypothetical single-vesicle fusion events were generated in Microsoft Excel with amplitudes of 623 ± 122 a.u and decaying as a single exponential with decay time of 371 ms (as determined by the non-geometric average decay time of events in 2 mM Ca^{2+} fit using a Beta-function). 4,000 hypothetical fusion events were then generated with varying amplitudes using the random number generator in Microsoft Excel with constraints of a Gaussian distribution according the first Gaussian curve ($1q = 623 \pm 122$ a.u) in 2 mM Ca^{2+} . Random pairs of these amplitudes were then summed together with varying temporal offsets (delays between the first and second hypothetical events) to generate 2,000 hypothetical 2-vesicle fusion events. The amplitudes of the 3 point moving averages were then calculated— analogous to the amplitude calculations of raw data—and the distribution of these hypothetical multivesicular events was compared to the multivesicular only component of the

amplitude distribution in 8 mM extracellular Ca^{2+} . The most similar distribution had a temporal offset of 118 ms, which we interpret as an approximate interval between two vesicles fusing spontaneously during multivesicular fusion.

Results

Synaptic vesicles that fuse spontaneously recycle rapidly.

To identify spontaneous fusion events, we first imaged synapses expressing vGlut-pHluorin at 8 Hz to minimize photobleaching and identified small, rapid increases in fluorescence (Figure 3.1A-D) in the presence of the voltage-gated Na^+ channel blocker, tetrodotoxin (TTX). These increases in fluorescence were distinguishable from noise with a maximum amplitude of 623 ± 122 a.u (Figure 3.1B and C) and average $\Delta F/F$ of $3.8 \pm 0.93\%$. These events decayed rapidly with an average decay time of 0.37s and median decay time of 0.28s (Figure 3.1 D). To confirm that these rapidly decaying increases in fluorescence were due to genuine spontaneous vesicle fusion, we sought to manipulate the rate of decay by addition of 50 mM Tris-HCl in the extracellular solution. It has been shown that incubation in Tris can buffer, and thus slow, vesicle reacidification (Gandhi and Stevens, 2003; Zhang et al., 2009). Indeed, equiosmolar substitution of extracellular NaCl with 50 mM Tris-HCl slowed vesicle reacidification to an average decay time of 0.55 s with median decay time 0.32 s (Figure 3.1E and F) indicating that the decay phase of these events was dominated by vesicle re-acidification. We then compared these spontaneous fluorescence increases to those evoked by single action potential stimulation in the absence of TTX (Figure 3.1G-I). We found that fusion events evoked by stimulation had mean fluorescence amplitude of $641 \pm$

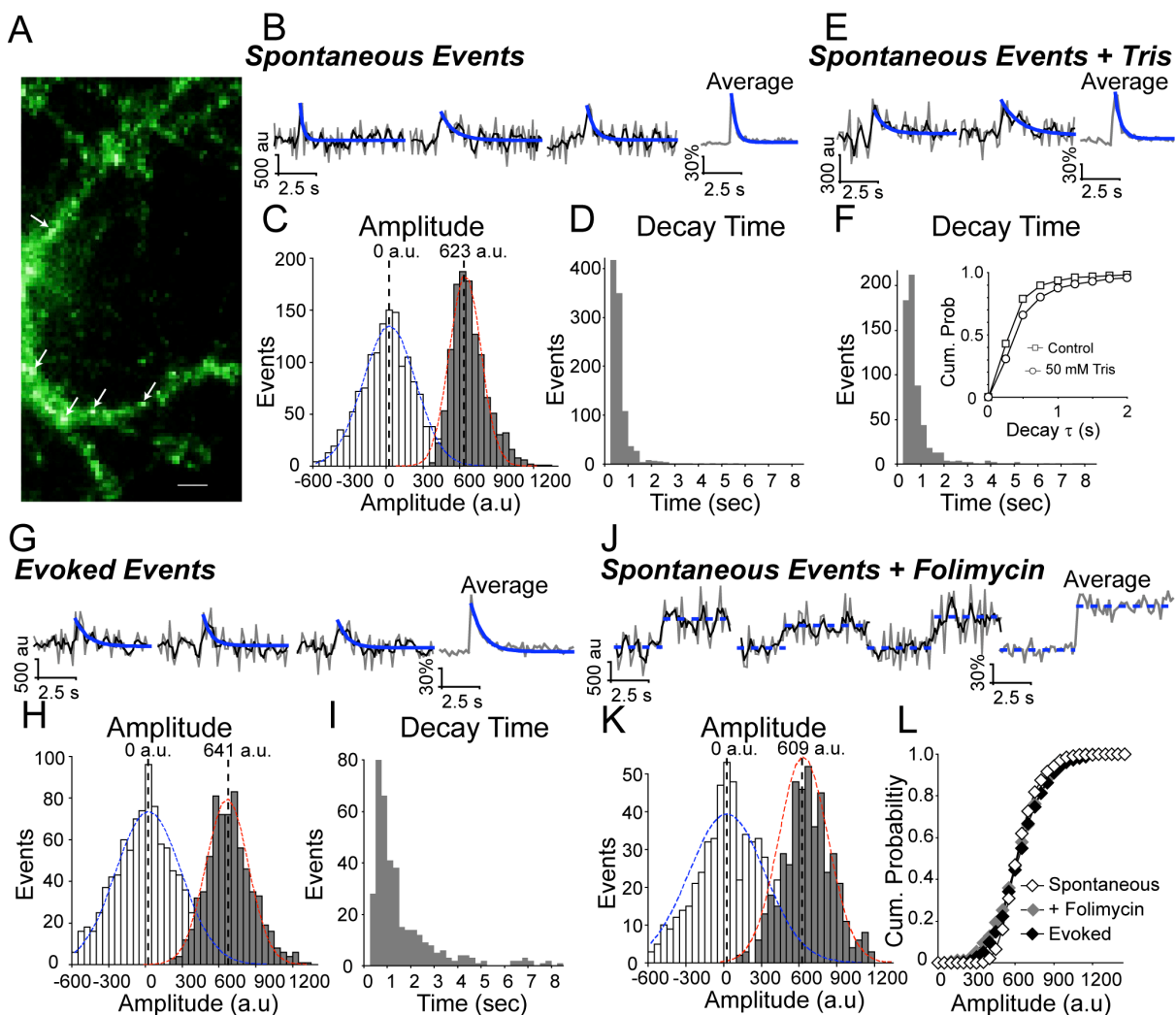


Figure 3.1. Spontaneous increases in vGlut1-pHluorin fluorescence decay rapidly. vGlut1-pHluorin was expressed via lentiviral infection in dissociated hippocampal cultures and neurons were imaged at 16-19 days in vitro. **A**, Example image of vGlut1-pHluorin expression in NH_4Cl (20 mM). Arrows indicate putative synapses. Scale bar is $5 \mu\text{m}$. **B**, Example traces of spontaneous increases in fluorescence (3 left traces) and the average of all events in this experiment (right trace). Raw data is in grey, black trace is the moving average of 3 points, and the blue trace is a fit to a first order decay. **C**, The amplitudes of spontaneous increases in fluorescence are distinguishable from noise. White bars are the amplitude change of a random section of the fluorescence recording, successful events are in grey (for detection criteria see methods). Blue dashed line is a Gaussian fit centered at 0 a.u. and standard deviation of 212 a.u. ($\chi^2 = 0.9$). Red dashed line is a Gaussian distribution fit to the data with mean of 623 ± 122 a.u. ($n = 1178$ events from 4 coverslips prepared from 2 cultures). **D**, Distribution of decay times of spontaneous increases in fluorescence have a non-geometric (Beta-function) average of 0.37 s with upper bound = 7 and lower bound = 2

(n = same as above). **E**, Example traces of spontaneous increases in fluorescence in the presence of high (50 mM) Tris-buffered extracellular solution. **F**, The resulting spontaneous increases in fluorescence were slower to decay with average decay time of 0.55 s with upper bound = 3.8 and lower bound = 2.1 (n = 1212 events from 3 coverslips generated from 2 cultures.) Inset shows cumulative probability distribution of decay time in cells with extracellular solution containing HEPES (Control; squares) and 50 mM Tris-HCl (circles) (KS-test $p < 0.001$ with $d_{max} = 0.13$ at 0.5 s). **G**, Example traces of increases in fluorescence in response to single action-potential stimulation delivered at 0.05 Hz. **H**, Amplitudes of stimulated increases in fluorescence are distinguishable from noise (white bars and blue Gaussian distribution) and could be fit with a Gaussian distribution centered at 641 ± 117 a.u. (red dashed line; $X^2 = 0.94$) **I**, Increases in fluorescence due to single-action potential stimulation delivered at 0.05 Hz were much slower to decay with a non-geometric average of 0.83 s with upper bound = 4.4 and lower bound 3.6 and median decay time of 0.83 s (n = 694 events from 4 coverslips generated from 2 cultures). **J**, Example traces of spontaneous increases in fluorescence in the presence of folimycin (80 nM). With inhibition of the vATPase, vesicles cannot be reacidified and therefore increases in fluorescence do not decay. **K**, Amplitude distribution of spontaneous increases in fluorescence in the presence of folimycin are also distinguishable from noise and can be fit with a Gaussian curve with mean amplitude of 609 ± 195 a.u. ($X^2 = 0.87$). **L**, Cumulative probability histogram of amplitudes of spontaneous increases in fluorescence in the absence (open diamond) and presence of folimycin (grey diamond), and amplitudes of fluorescence increases evoked by stimulation (black diamonds). There was only a significant difference between spontaneous increases in fluorescence with and without folimycin (KS-test $p < 0.05$ $maxD = 0.08$ at bin 450 a.u.).

171 a.u. (Figure 3.1H), similar to spontaneous fluorescence increases. However, these events decayed more slowly with average decay time of 0.83s and median decay time of 0.83s (Figure 3.1I). Finally, to evaluate whether we were able to visualize the entirety of the fluorescent signal originating from spontaneous vesicle fusion events, we incubated neurons with the vacuolar ATPase inhibitor, folimycin (80 nM), and measured spontaneous increases in fluorescence (Figure 3.1J and K). In the presence of folimycin, increases in fluorescence take on a staircase-like waveform with mean amplitude of 609 ± 195 a.u. (Figure 3.1K), similar to that of spontaneous fusion events observed in the absence of folimycin. There were no significant differences in the mean amplitude between spontaneous increases in

fluorescence with or without folimycin and those that were evoked by stimulation (ANOVA p value >0.5). However, when comparing amplitude distributions there was a significant difference between spontaneous events in the absence of folimycin and both spontaneous events in the presence of folimycin and action-potential evoked single vesicle fusion events (KStest < 0.05 maxD = 0.08 at bin 450 a.u.) (Figure 3.1L). This result suggests that while we were able to acquire the entire fluorescence waveform of the majority of spontaneous fusion events, there remains a small population of low amplitude events that we were unable to detect due to the rapid decay of fluorescence signals. Regardless, our results still indicate a clear divergence in the reacidification rate between vesicles that recycle at rest and those that fuse in response to action potentials.

Dual color imaging shows that spontaneously fusing vesicles elicit postsynaptic Ca^{2+} signals.

To investigate the relationship between these fast spontaneous increases in presynaptic fluorescence to postsynaptic receptor activation, we moved to a dual-color system utilizing the red-shifted pHluorin variant, pHTomato, fused to the presynaptic vesicle protein synaptophysin (SypHTomato) (Li and Tsien, 2012) and the green fluorescent Ca^{2+} indicator, GCaMP5K, fused to the post-synaptic density protein 95 (PSD-95-GCaMP5K) (Akerboom et al., 2012). In this system, in the absence of extracellular Mg^{2+} , we are able to visualize presynaptic vesicle fusion events in the red channel and use the resulting Ca^{2+} influx visualized in the green channel as a coincidence detector of a successful presynaptic fusion event (Figure 3.2). However, this system is not without caveats: first, because we are now monitoring two wavelengths our temporal resolution decreased from >8 Hz to ~4 Hz;

second, SypHTomato results in an elevated surface expression level compared to vGlut-pHluorin that required a post-hoc decay correction to compensate for photobleaching (see Experimental Procedures). Despite these issues, spontaneous increases in SypHTomato fluorescence were still detected and were distinguishable from noise with mean amplitude of 303 ± 92 a.u. (Figure 3.2 C) and $\Delta F/F$ of $1.9 \pm 0.67\%$. Spontaneous increases in fluorescence that were correlated (within ± 1 s) with Ca^{2+} signals were also distinguishable from noise with mean amplitude of 170 ± 50 a.u. (Figure 3.2D) and $\Delta F/F$ of $2.2 \pm 1.3\%$. We next compared the amplitudes of these spontaneous fusion events with increases in fluorescence elicited by single action potential stimulation (Figure 3.2E and F). Stimulation resulted in events that were distinguishable from noise with mean amplitude of 345 ± 95 a.u. (Figure 3.2F). Although both spontaneous and AP-evoked fluorescence increases were distinguishable from noise, the small amplitude of these events combined with the rapid decay times made precise measurements of individual decay times difficult. Therefore we averaged all events within an experiment together and compared the decay times of averages (Figure 3.2G). We found that, as with vGlut-pHluorin, spontaneous fluorescence increases in SypHTomato decayed faster than those evoked by stimulation with average decay times of 0.5 ± 0.2 s and 1.0 ± 1.5 s, respectively. To confirm that we were able to observe the full fluorescence increase of spontaneous fusion events with our reduced temporal resolution, we incubated neurons in folimycin and observed stepwise increases in SypHTomato fluorescence. In the same experiments to verify that the increases in the GCaMP5K fluorescence were due to Ca^{2+} influx through NMDA receptors, we perfused an extracellular solution containing the NMDA receptor blocker AP-5 (Figure 3.2H-S). We were able to

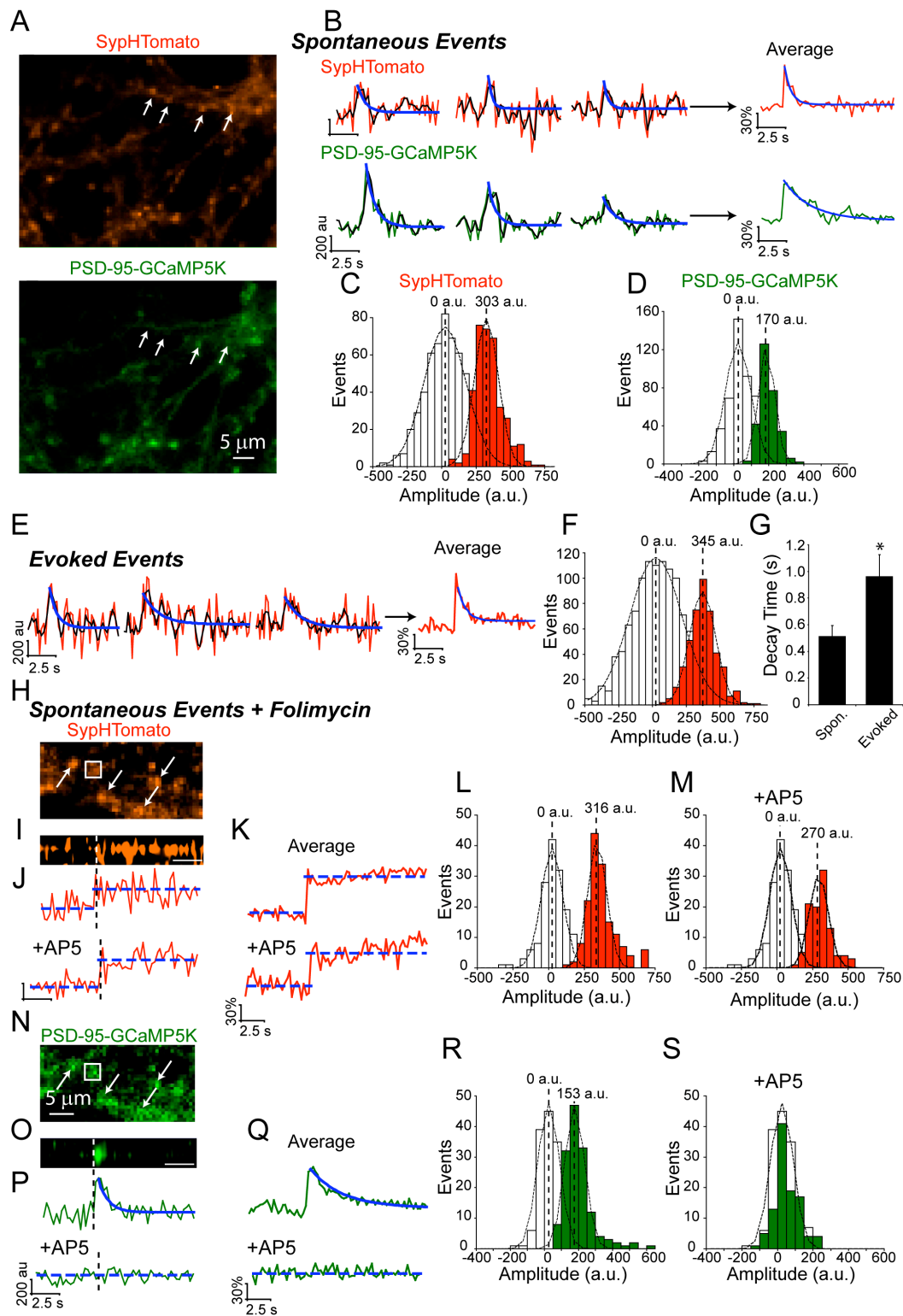


Figure 3.2. Dual color imaging of cells expressing SypHTomato and PSD-95-GCaMP5K show spontaneous increases in fluorescence that are analogous to those observed in vGlut-pHluorin. **A**, Example images of SypHTomato and PSD-95-GCaMP5K expression. Arrows indicate putative synapses. Scale bar is 5 μm . **B**, Example traces of SypHTomato (raw data in red, a moving average of 3 points in black and a fit of the decay time t in blue) and PSD-95-GCaMP5K (raw data in green, a moving average of 3 points in black and a fit of the decay time in blue). Because spontaneous increases in fluorescence were very small, we averaged events for each experiment representative average traces are shown at right. **C**, The amplitude distribution of SypHTomato could be well fit with a Gaussian curve centered at 303 ± 92 a.u. ($X^2 = 0.86$). **D**, Amplitudes of PSD-95-GCaMP were distinguishable from noise and could be fit with a Gaussian curve with mean amplitude of 170 ± 50 ($X^2 = 0.98$). **E**, Example traces of SypHTomato fluorescence in response to single action potentials delivered at 0.05 Hz. Again, raw data is in red, a moving average of 3 points is in black and the decay time fit is in blue. **F**, Amplitudes of fluorescence increases evoked by action-potential stimulation could be well fit by a Gaussian curve with mean of ($X^2 = 0.99$). **G**, Averaged traces of spontaneous increases in fluorescence decayed back to baseline with decay time = 0.51 ± 0.08 s ($n = 4$), while events that responded to stimulation ($n = 3$) decayed much slower $t = 0.96 \pm 0.06$ (Student's t-test p value < 0.05). **H**, Example image of SypHTomato expression in the presence of folimycin. Arrows indicate putative synapses. The box is the region from which a line scan was taken (shown in panel **I**). **I**, Line scan of SypHTomato fluorescence. White dashed line indicate where on the corresponding trace the fluorescence step occurred, scale bar = 2.6 s. **J**, Example traces of events in the presence and absence of AP-5 from the same synapses. **K**, Average of traces from the experiment of step-wise increase in fluorescence in the presence and absence of AP-5. **L**, Increases in fluorescence in the presence of folimycin were separable from noise and could be fit with a Gaussian with mean amplitude of 316 ± 65 a.u. ($X^2 = 0.49$). **M**, The same synapses in the presence of AP-5 showed spontaneous increases in fluorescence that were still distinguishable from noise albeit with a slightly smaller amplitude distribution 270 ± 65 a.u. ($X^2 = 0.48$) that was not significantly different from amplitudes in the presence of folimycin (not shown; KS-test $p < 0.01$). **N**, Example image of corresponding PSD-95-GCaMP5K fluorescence. White arrows indicate putative synapses. The box is the region from which a line scan was taken. **O**, Line scan of PSD-95-GCaMP5K fluorescence signal that occurred at the same time as the above SypHTomato signal. **P**, Example traces of events in the presence and absence of AP-5. **Q**, Average of traces in the presence and absence of AP-5. In the presence of AP-5, entry of Ca^{2+} into the postsynaptic terminal is prevented and thus there is no GCaMP5K signal. **R**, PSD-95-GCaMP5K signals were separable from noise and could be fit with a Gaussian curve with mean amplitude of 153 ± 58 a.u. ($X^2 = 0.80$). **S**, In the presence of AP-5, Ca^{2+} is prevented from entering the postsynaptic terminal and results in no detectable GCaMP5K events.

identify spontaneous fusion events according to stepwise increases in SypHTomato fluorescence alone without relying on the coincidence with GCaMP5K mediated Ca^{2+} signals (Figure 3.2H-S). Under these conditions, we observed spontaneous fusion events with mean amplitude of 316 ± 64.9 a.u (Figure 3.2L) similar to both those in the absence of folimycin and those due to stimulation. Events in the same synapses in the presence of AP-5 were also similar with mean amplitude of 270 ± 65 a.u. (Figure 3.2M). The GCaMP5K signal in the absence of AP-5 had mean amplitude of 153 ± 57.6 a.u. (Figure 3.2R), similar to without folimycin, but in the presence of AP-5, the GCaMP signal amplitude decreased to within noise, 13.2 ± 56.0 a.u. (Figure 3.2S). Together these data complement our observations using vGlut1-pHluorin and show that spontaneous vesicle fusion events are coupled to postsynaptic NMDA receptor-driven Ca^{2+} signals and, following exocytosis, these vesicles are retrieved and re-acidified on a much faster time course than their AP-evoked counterparts.

Increasing extracellular Ca^{2+} triggers multiple successive spontaneous fusion events.

Using presynaptic imaging similar to that used in this study, we have previously shown that increasing extracellular Ca^{2+} increased synaptic vesicle fusion probability and increased the likelihood of multivesicular fusion events, which is observed as an increase in fluorescence amplitude (Leitz and Kavalali, 2011). To assess if this scenario also applied to vesicles that fuse spontaneously, we measured the amplitude of spontaneous increases in vGlut-pHluorin fluorescence in 2, 4 and 8 mM extracellular Ca^{2+} (Figure 3.3 A-C). Surprisingly, we found that fluorescence amplitude distributions even in 2 mM extracellular

Ca^{2+} did not fit well to a single Gaussian curve, nor could the sum of two Gaussian curves with means at integer multiples (i.e. a quantal distribution of amplitudes indicative of two or more vesicles undergoing fusion simultaneously) account for the distribution of amplitudes (Figure 3.1B red lines). Instead, amplitude distributions in 2 and 4 mM extracellular Ca^{2+} (Figure 3.3D and E, respectively) were best fit by the sum of two Gaussian curves at 1 quantal mean ($1q = 623 \pm 91$ a.u.) and 1.3 times the first mean ($1.3q = 834 \pm 111$ a.u.) (Figure 3.3D and E black lines). Fluorescence amplitudes in 8 mM Ca^{2+} were best fit by the sum of three Gaussian curves distributed at 1 quantal mean ($1q = 623 \pm 91$ a.u.), 1.3 times the first quantal mean ($1.3q = 834 \pm 111$ a.u.) and 2 times the first quantal mean (1246 ± 182 a.u.) (Figure 3.3F). Given our sampling rate and the rapid fluorescence decay time of these spontaneous events, we hypothesized that 1.3q events might be two spontaneous events occurring close together in time but with a slight delay such that at our acquisition rate of >8 Hz, two near simultaneous events might appear to be a single event with a normalized amplitude of 1.3q (Figure 3.3G). To determine the delay between two events that would be required for such a fluorescence signal, we modeled the fluorescence decay of two hypothetical spontaneous fusion events with randomly generated amplitudes within the observed first Gaussian distribution ($1q$) and fixed decay times of 371 ms (the average decay time of spontaneous events in 2 mM Ca^{2+}). We used this model to generate 2,000 hypothetical decay times and found that a fusion delay of 118 ms would result in an amplitude ~ 1.3 times greater than the single quantal amplitude. We then estimated the percent of fusion events that were multivesicular (Figure 3.3H) and found that at 2 mM Ca^{2+}

17% of events were multivesicular, increasing to $\sim 30\%$ in 4 mM Ca^{2+} and up to 70% of events were multivesicular in 8 mM Ca^{2+} .

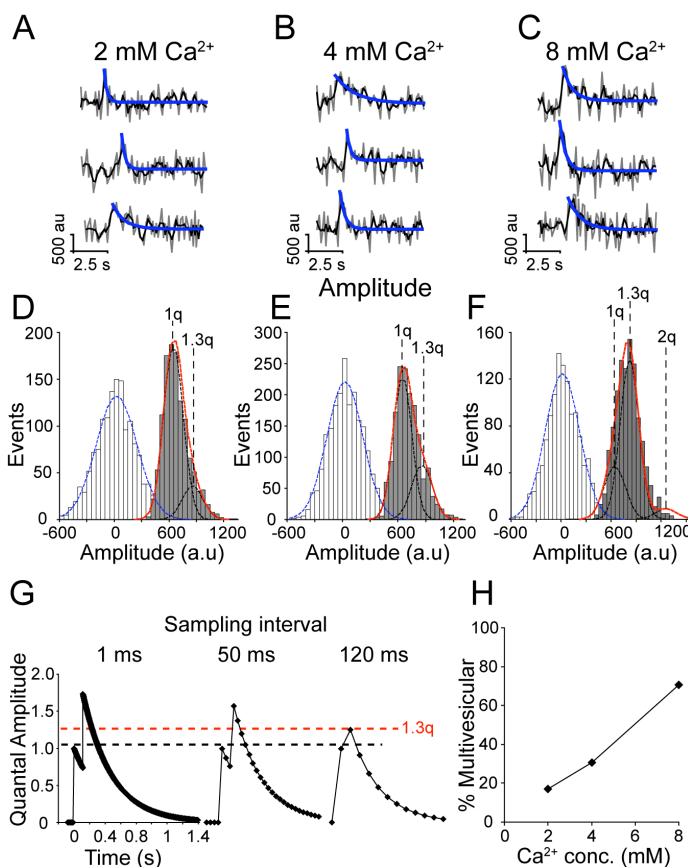


Figure 3.3. Increasing extracellular Ca^{2+} increases multivesicular release. **A-C**, Example traces of events in 2 mM (**A**), 4 mM (**B**) and 8 mM (**C**) extracellular Ca^{2+} . Raw data are shown in grey, a moving average of 3 points is shown in black and the blue line indicates a fit of the decay. **D-F**, Fluorescence amplitude distributions. White bars are noise fit by blue Gaussian distribution centered at 0 a.u., grey bars are successful fusion events fit by multiple Gaussian curves (black lines) and a sum of Gaussian curves (in red). **D**, Fluorescence amplitudes in 2 mM extracellular Ca^{2+} were best fit by the sum of two Gaussian curves with mean amplitudes 623 ± 122 a.u. (1q) and 834 ± 111 a.u. (1.3q) ($X^2 = 0.88$). **E**, Fluorescence amplitudes in 4 mM extracellular Ca^{2+} were well fit with two similar Gaussian curves 623 ± 98 a.u. (1q) and 834 ± 111 a.u. (1.3q) ($X^2 = 0.70$). **F**, Fluorescence amplitudes of 8 mM Ca^{2+} were best fit with the sum of three Gaussian curves with mean amplitudes 623 ± 91 a.u. (1q), 834 ± 111 a.u. (1.3q) and 1246 ± 182 a.u. (2q) ($X^2 = 1$). **G**, Model of two hypothetical events with normalized amplitudes of 1, decay times of 371 ms, and delay of onset of 118 ms, the same two events sampled at 120 ms results in a fluorescence amplitude of 1.3 times a single event (1.3q). **H**, The percent of events in 2, 4 and 8 mM extracellular Ca^{2+} that have

amplitudes greater than a single Gaussian distribution were defined as multivesicular. This suggests that there are more multivesicular events at increasing extracellular Ca^{2+} concentrations.

We also detected a similar Ca^{2+} -dependent increase in the amplitude of spontaneous events detected in SypHTomato/PSD-95-GCaMP5K expressing cultures (Figure 3.4A). In these cultures, there was an increase in GCaMP5K event amplitudes as a function of increasing extracellular Ca^{2+} indicative of the increased driving force of Ca^{2+} influx. Taken together, these data suggest that increasing extracellular Ca^{2+} increases the probability of two spontaneous fusion events occurring in close temporal proximity within a single synapse.

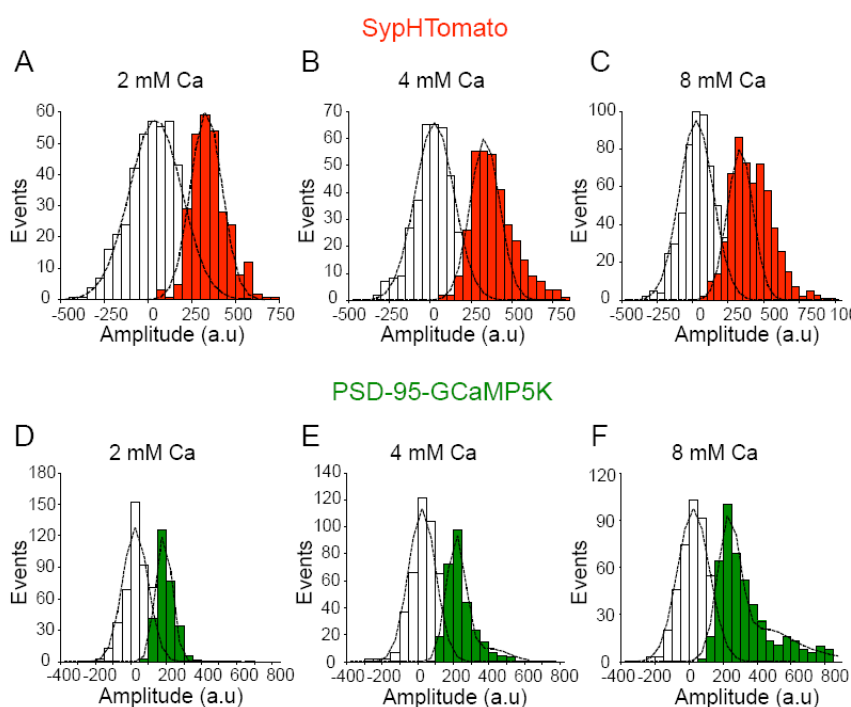


Figure 3.4. Increasing extracellular Ca^{2+} increases amplitude of spontaneous events in both SypHTomato and PSD-95-GCaMP5K. A-C, Fluorescence amplitude distributions of spontaneous increases in sypHTomato (red) were separable from noise (white). Black lines are Gaussian distribution fits. D-F, Fluorescence amplitudes of PSD-95-GCaMP5K (green) signals that corresponded with increases in sypHTomato were also separable from noise

(white). Black lines are Gaussian distribution fits. **A**, Fluorescence amplitudes of spontaneous increases in sypHTomato fluorescence in 2 mM extracellular Ca^{2+} . Events could be fit with a single Gaussian distribution (black line) with mean amplitude of 303 ± 92 a.u. ($X^2 = 0.86$; $n = 361$ events from 4 experiments). **B**, Fluorescence amplitudes of spontaneous increase in sypHTomato fluorescence in 4 mM extracellular Ca^{2+} . The amplitude of SypHTomato events increased in a non-quantal fashion as in the case of vGlut-pHluorin signals. Black line is the Gaussian curve due to single vesicle fusion as predicted from 2 mM Ca^{2+} experiments. ($n = 335$ events from 4 experiments). **C**, Fluorescence amplitudes of spontaneous increases in sypHTomato fluorescence increase further in 8 mM extracellular Ca^{2+} ($n = 573$ events from 5 experiments). **D**, Amplitude distribution of PSD-95-GCaMP5K signals that correlated with SypHTomato signals in 2 mM extracellular Ca^{2+} . PSD-95-GCaMP5K signals had a mean amplitude of 170 ± 50 a.u. ($n = 361$ events from 4 experiments) **E**, Amplitude distribution of PSD-95-GCaMP5K signals that correlated with SypHTomato signals in 4 mM extracellular Ca^{2+} . PSD-95-GCaMP5K signals could be well fit by the sum of two Gaussian distributions (black dashed line) with mean amplitudes of 191 ± 53 a.u. and 382 ± 106 a.u. ($n = 292$ events from 4 experiments) **F**, Amplitude distribution of PSD-95-GCaMP5K signals that correlated with SypHTomato signals in 8 mM extracellular Ca^{2+} . PSD-95-GCaMP5K signals could be well fit by the sum of three Gaussian distributions (black dashed line) with mean amplitudes of 208 ± 66 a.u., 416 ± 132 a.u. and 624 ± 198 a.u. ($n = 472$ events from 5 experiments)

Ca^{2+} does not alter the kinetics of fluorescence transients originating from spontaneous fusion events.

We have previously shown that increasing extracellular Ca^{2+} increases the fluorescence decay times of vGlut1-pHluorin containing vesicles that fuse in response to stimulation (Leitz and Kavalali, 2011). Here, we wanted to determine if this property was applicable to vesicles that undergo fusion in the absence of stimulation. We increased extracellular Ca^{2+} to 4 mM and found that fluorescence signals decay with an average decay time of 0.44 s (with upper bound = 4.8 and lower bound = 2.1) and median decay time of 0.29 s (Figure 3.5A). In 8 mM extracellular Ca^{2+} , the average decay time was identical (0.44 s with upper bound = 4.8 and lower bound = 2.1), and the median decay time did not

appreciably change from 0.29 s to 0.28 s (Figure 3.5B). When compared to 2 mM extracellular Ca^{2+} there was no significant difference in either 4 or 8 mM extracellular Ca^{2+} . Compared to the decay times of evoked-fusion events, decay times of spontaneous fusion events—regardless of extracellular Ca^{2+} concentration—were much faster (Figure 3.5C). These data suggest that there is a fundamental difference in the kinetics of endocytosis and reacidification between vesicles that fuse spontaneously and those that fuse in response to stimulation.

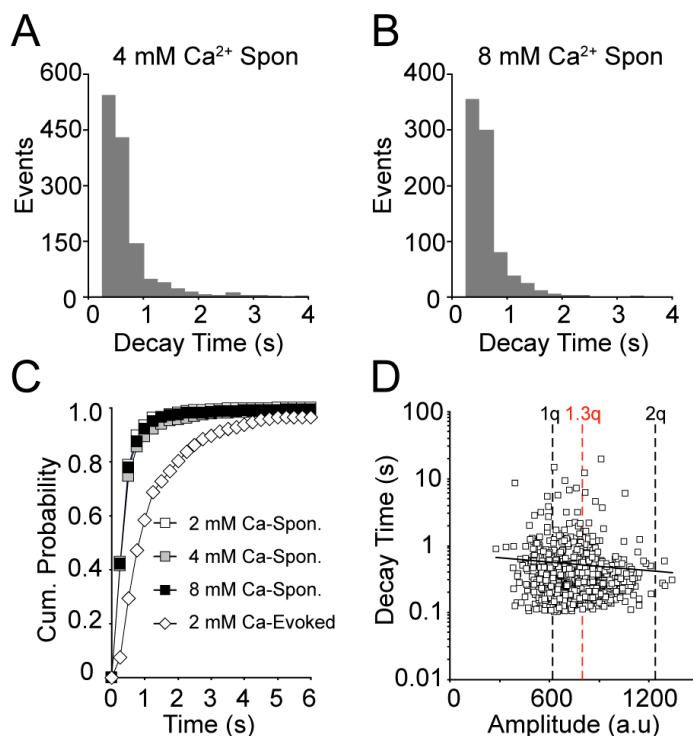


Figure 3.5. Increasing extracellular Ca^{2+} does not alter fluorescence decay time.

A, Distribution of fluorescence decay times in 4 mM extracellular Ca^{2+} can be fit with a beta-distribution with mean of 0.44 s with upper bound = 4.8 and lower bound = 2.1 ($X^2 = 0.9$; $n = 1308$ events from 6 coverslips over 3 cultures). **B**, Distribution of fluorescence decay times in 8 mM extracellular Ca^{2+} were fit with a beta-distribution with mean of 0.44 s with upper bound = 4.8 and lower bound = 2.1 ($X^2 = 1$; $n = 844$ events from 3 coverslips from 2 cultures). **C**, Cumulative probability histogram of decay times of spontaneous fluorescence

events in 2, 4, and 8 mM extracellular Ca^{2+} showed no significant difference in decay time distribution (KS-test most significant difference between 2 and 8 mM spontaneous $p > 0.3$ with $D_{\text{max}} = 0.04$ at 0.5 s). However, the decay times of all spontaneous events were significantly different from the decay times of evoked-fusion events (for all comparisons KS-test $p < 0.01$ with $D_{\text{max}} = 0.5$ sec). **D**, Decay time did not correlate with amplitude of spontaneous events in 8mM Ca^{2+} ($R^2 = 0.0014$). $1q$ is the Gaussian mean of 1 event while $2q$ is the Gaussian mean of 2 simultaneous events, $1.3q$ is the amplitude calculated in Figure 3.

Our earlier work showed that an increase in the number of vesicles that fuse slows the fluorescence decay time of fusion events (Leitz and Kavalali, 2011). Therefore, here, we analyzed the decay times of events in 8 mM Ca^{2+} as a function of amplitude and found that there was no correlation in event size and fluorescence decay times (Figure 3.5D). Furthermore, we also found a similar trend of Ca^{2+} -independence in neurons expressing SypHTomato/PSD-95-GCaMP5K (Figure 3.6A and B). All of these decay times, regardless of extracellular Ca^{2+} levels, were faster than those observed during stimulation-evoked fusion (Figure 3.6C). It is important to note that the rate of decay is approaching the limit of our temporal resolution, which is lowered in an attempt to reduce photobleaching during long imaging episodes required to identify spontaneous fusion events. Thus, it is possible that we either cannot detect a significant change in decay times, or we are missing a subset of ultra fast decay times. Regardless, these data not only suggest that the mechanisms controlling the rate of synaptic vesicle reacidification are not the same for spontaneous and stimulation-evoked vesicle fusion but that endocytosis of synaptic vesicles released at rest is rapid even during multivesicular fusion events, unlike retrieval of vesicles released in response to stimulation.

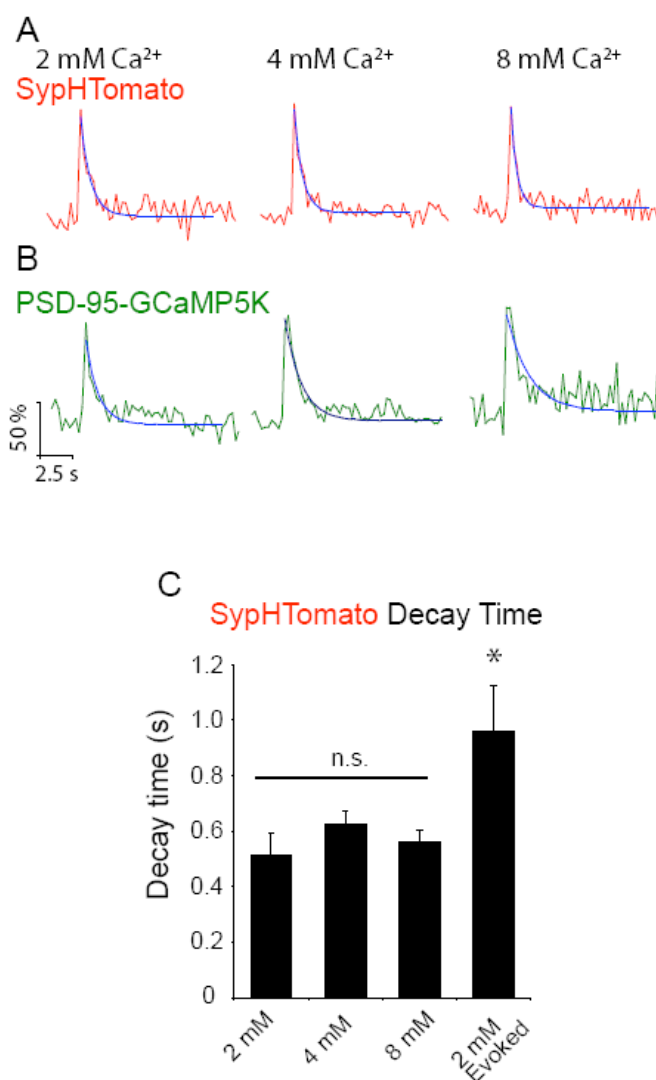


Figure 3.6. Increasing extracellular Ca²⁺ does not alter decay time of spontaneous increases in sypHTomato fluorescence. **A**, Example average traces of spontaneous increases in sypHTomato fluorescence (red) single experiments in 2 mM (left), 4 mM (middle), and 8 mM (right) extracellular Ca²⁺ with decay time fit in blue. **B**, Example average traces from the same experiments as **A** of PSD-95-GCaMP5K events (green) that correspond with sypHTomato spontaneous increases in fluorescence in 2 mM (left), 4 mM (middle), and 8 mM (right) extracellular Ca²⁺ with decay time fit in blue. **C**, Decay time does not change as a function of extracellular Ca²⁺, however increases in fluorescence due to stimulation are slower to decay than spontaneous increases in fluorescence ($p < 0.05$ One-way ANOVA with Bonferroni post hoc analysis).

Increasing extracellular Ca^{2+} concentration increases the frequency of fast spontaneous vesicle fusion and retrieval

It is well established that increasing the concentration of extracellular Ca^{2+} increases spontaneous vesicle fusion rate at rest (Lou et al., 2005; Sun et al., 2007; Xu et al., 2009). We wanted to know if we see the same increase in our system. We counted all events with amplitudes within the first quantal mean as a single event, and events with larger amplitudes as two events. Surprisingly we found that there was only a small change in vesicle fusion frequency between 2 mM and 8 mM extracellular Ca^{2+} beyond the increase in multivesicular events we reported earlier (Leitz and Kavalali, 2011), (Figure 3.7A). However, when vesicle reacidification was buffered using 50 mM Tris-HCl (Figure 3.7B) we were able to detect a slight shift in vesicle fusion rate in 8 mM extracellular Ca^{2+} compared to 2 mM Ca^{2+} . Addition of folimycin further exacerbated this effect and clearly showed an increase in spontaneous fusion rate as a function of extracellular Ca^{2+} (Figure 3.7C). Taken together, these data indicate that increasing extracellular Ca^{2+} increases the vesicle fusion rate in our system in a manner that is detectable in the presence of folimycin. However, this increase in spontaneous fusion rate cannot be detected without increasing extracellular pH buffering or inhibiting vesicle re-acidification, indicating that elevated extracellular Ca^{2+} specifically increases fusion of synaptic vesicles that are retrieved and re-acidified rapidly, below the temporal resolution of our imaging protocol. This finding suggests that although elevated Ca^{2+} levels do not alter the kinetics of slower events detectable without the aid of altered re-acidification, Ca^{2+} elevation generates a new population of events that are faster in their kinetics. This observation is consistent with earlier work, which demonstrated that increasing

extracellular Ca^{2+} facilitates the propensity of vesicle retrieval events with fast kinetics (Ales et al., 1999; Wu et al., 2009).

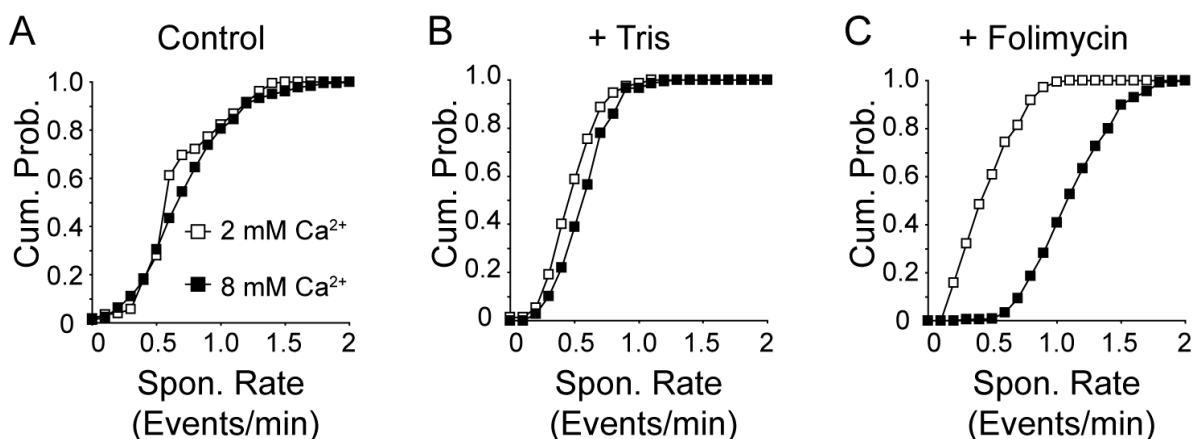


Figure 3.7. Increasing extracellular Ca^{2+} increases spontaneous release rate.

A, Cumulative probability histogram of spontaneous event rate per synapse per minute in 2 mM and 8 mM extracellular Ca^{2+} ($n = 175$ synapses from 4 coverslips for both conditions, KS-test $p < 0.05$ with $D_{\text{max}} = 0.6$ fusion events per minute per synapse, Student's t-test $p > 0.1$ with averages of 0.70 and 0.76 events per minute per synapse for 2 and 8 mM Ca^{2+} , respectively). **B**, Cumulative probability histogram of spontaneous event rate per synapse per minute in Tris-buffered (50 mM) 2 mM and 8 mM extracellular Ca^{2+} solutions ($n = 150$ synapses from 3 coverslips for both conditions, KS test $p < 0.05$ with $D_{\text{max}} = 0.5$ fusion events per minute per synapse, Student's t-test $p < 0.05$ with average 0.4 and 0.5 fusion events per minute per synapse for 2 and 8 mM Ca^{2+} , respectively). **C**, Cumulative probability histogram of spontaneous event rate per synapse per minute in 2 and 8 mM extracellular Ca^{2+} extracellular solution containing folimycin ($n = 175$ synapses from 4 coverslips for 2 mM Ca^{2+} and 216 synapses from 4 coverslips for 8 mM Ca^{2+} ; KS-test $p < 0.05$ $D_{\text{max}} = 0.8$ fusion events per synapse per minute, Student's t-test $p < 0.05$ with average rates of 0.4 and 1.1 fusion events per minute per synapse for 2 and 8 mM Ca^{2+} respectively)

The rate of spontaneous synaptic vesicle fusion and the probability of stimulation-evoked fusion do not correlate within a given synapse

Next, to evaluate the relationship between the rate of spontaneous synaptic vesicle fusion and the probability evoked vesicle fusion in a synapse. For this purpose, we incubated neurons in folimycin in order to visualize all events and delivered single action potential stimulations with long inter-stimulus intervals (30 s). Increases in fluorescence that occurred within 1s of a stimulation were considered to be due to evoked release (note that we cannot then differentiate between synchronous vesicle fusion and fast asynchronous fusion) while increases in fluorescence that did not match with a stimulation time were labeled as spontaneous vesicle fusion events (Figure 3.8A). We found that at increasing Ca^{2+} concentrations the spontaneous vesicle fusion rate and evoked fusion probability estimates obtained from individual release sites did not show appreciable correlation (at 2 mM Ca^{2+} : slope = 1.0, $R^2 = 0.08$; at 4 mM Ca^{2+} : slope = -0.14, $R^2 = 0.006$; at 8 mM Ca^{2+} : slope = 0.47, $R^2 = 0.02$) (Figure 3.8B-D). Although, a large fraction of the nerve terminals (> 70%) were capable of maintaining both evoked and spontaneous neurotransmission across all Ca^{2+} concentrations, the rate of spontaneous transmission and the probability of successful AP-stimulated transmission are not correlated within a given release site. Furthermore, these data imply that the processes that control the kinetics of trafficking vesicles released at rest and those released in response to stimulation are distinct not only between synaptic terminals, but within a single synaptic terminal.

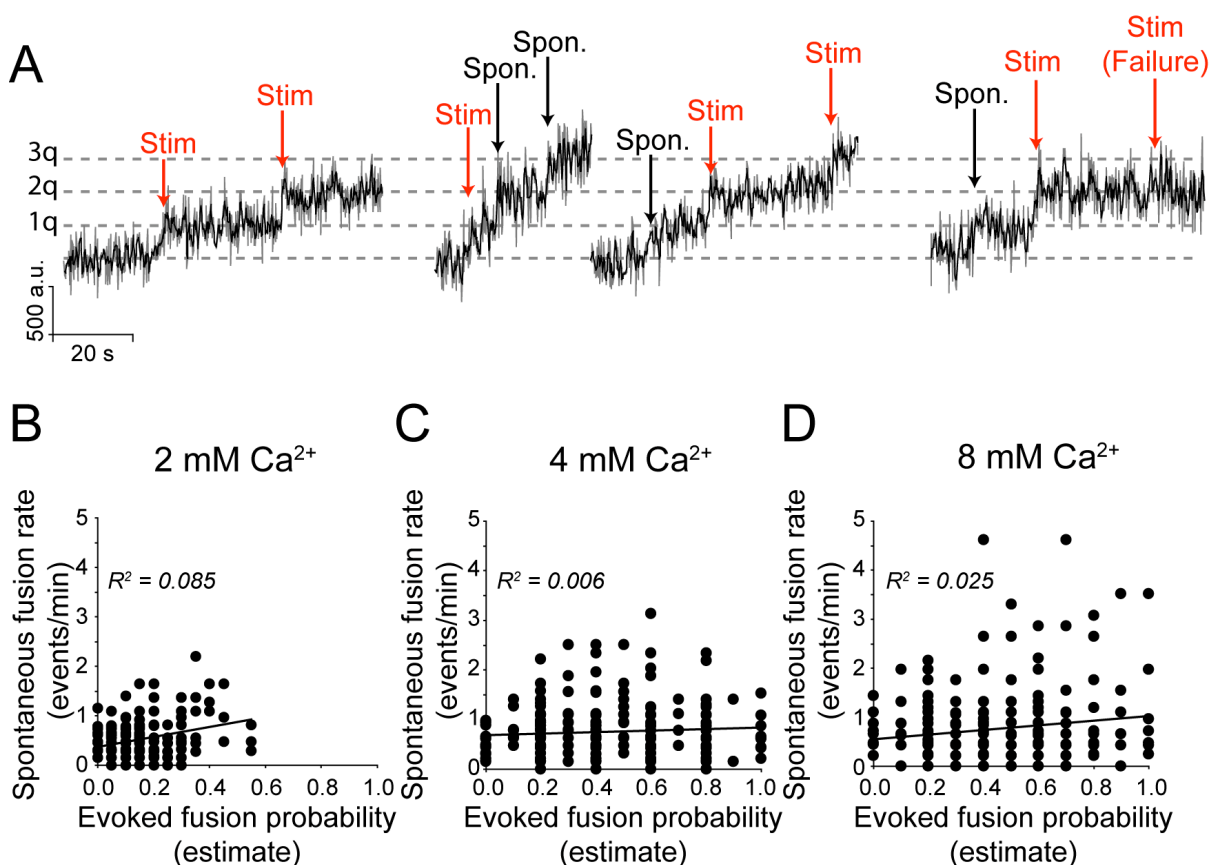


Figure 3.8. Spontaneous vesicle fusion rate and stimulation-evoked fusion probability do not correlate at a given synapse. **A**, Example traces of fusion events in the presence of folimycin. Neurons in 2 mM Ca²⁺ extracellular solution were stimulated with 1 AP delivered at 0.1 Hz while neurons in 4 and 8 mM Ca²⁺ were stimulated with 1 AP delivered at 0.033 (30 sec inter-stimulus interval) due to the higher probability of release. Fusion events were categorized as spontaneous or evoked by their temporal distance from the stimulation time, with events within ± 1 sec of stimulation selected as evoked fusion events. Note that spontaneous and evoked events are both quantal, indicated by the dashed grey line. **B**, There is very little correlation between spontaneous fusion rate and evoked fusion probability in 2 mM Ca²⁺. Distributions were best fit with a linear trend line with slope = 1.0 ($R^2 = 0.08$; $n = 200$ synapses from 4 coverslips). **C**, The correlation between spontaneous and evoked transmission decreases further as extracellular Ca²⁺ increases to 4 mM best fit line with slope = 0.2 ($R^2 = 0.01$; $n = 311$ synapses from 6 coverslips). **D**, The correlation remains low between spontaneous and evoked transmission in 8 mM extracellular Ca²⁺ with best fit line with slope = 0.5 ($R^2 = 0.02$; $n = 240$ synapses from 4 coverslips)

Discussion

To visualize spontaneous exocytosis and endocytosis of single synaptic vesicles, we used a lentiviral system to express the pH-sensitive GFP (pHluorin) fused to the luminal domain of the vesicular glutamate transporter (vGlut1) in hippocampal neurons. In an earlier study, we employed the same approach to investigate trafficking of single synaptic vesicles that fuse in response to AP stimulation where the time of stimulation can be used to identify a successful fusion event (Leitz and Kavalali, 2011). For spontaneous vesicle fusion, however, such a time stamp does not exist; therefore, to confirm our findings using vGlut1-pHluorin, we also used dual color imaging with a red-shifted pHluorin variant (pHTomato) fused to the luminal domain of the synaptic vesicle protein synaptophysin (SypHTomato) and a green Ca^{2+} -sensitive probe (GCaMP5K) fused to the post-synaptic density protein 95 (PSD-95-GCaMP5K). In this setting, we could monitor presynaptic vesicle fusion and postsynaptic Ca^{2+} entry upon NMDA receptor activation. We found that in both systems, synaptic vesicles that fuse spontaneously are retrieved and re-acidified much faster than their counterparts that fuse in response to stimulation. The rapid decay was not due to lateral diffusion of the probe because in the presence of folimycin, these events remained stable without decay and fluorescence accumulated in a stepwise fashion. Taken together, these results indicate that spontaneous synaptic vesicle exocytosis and endocytosis are tightly coupled processes and that the decay phase of these transients was mainly due to vesicle re-acidification upon endocytosis (Alabi and Tsien, 2013). Although we see extremely fast endocytosis of spontaneous recycling vesicles, large probes such as antibodies against the luminal domain of synaptotagmin1 or horseradish peroxidase are known to label

spontaneously endocytosing vesicles (Sara et al., 2005; Fredj and Burrone, 2009). Therefore, spontaneously endocytosing vesicles may still form a fairly large fusion pore or may even fully collapse onto the plasma membrane —albeit without lateral dispersion of their protein components — despite being retrieved quickly. However, we cannot fully exclude the possibility that some spontaneous fusion events may form narrow fusion pores where uptake of large probes can be curtailed as seen after spontaneous fusion of peptidergic vesicles (Vardjan et al., 2007).

Why is synaptic vesicle re-acidification after spontaneous fusion faster than vesicle re-acidification after evoked fusion? We propose three non-mutually exclusive scenarios that can explain this difference. First, the pH buffering capacity of vesicles that endocytose after AP stimulation could be higher. Second, the function of the v-ATPase on vesicles that endocytose after AP stimulation may be slowed down since this complex is known to incorporate Ca^{2+} sensor proteins (Zhang et al., 2008) and was recently shown to be differentially regulated during evoked versus spontaneous fusion (Wang et al., 2014). Finally, vesicles endocytosed during activity may rapidly trigger formation of larger vesicular structures that are expected to be slower to re-acidify due to their larger volume, consistent with findings from capacitance measurements in salamander photoreceptors (Van Hook and Thoreson, 2012) as well as recent electronmicrographic analysis of endocytosis in hippocampal synapses after rapid high-pressure freeze fixation (Watanabe et al., 2014).

In this study, we also investigated the Ca^{2+} -dependent regulation of spontaneous synaptic vesicle fusion events. At elevated Ca^{2+} concentrations we detected an increase in the

amplitudes of fusion events consistent with exocytosis of multiple synaptic vesicles. Interestingly, this result is similar to bursting activity that has been observed previously using single-synapse recordings in hippocampal neurons (Abenavoli et al., 2002). Importantly, fluorescence signals originating from these multivesicular events were not slower in their rate of decay, which contrasts our earlier observations on evoked multivesicular fusion events (Leitz and Kavalali, 2011), indicating that spontaneous exocytic load (i.e. the number of spontaneously fused vesicles on the plasma membrane) does not significantly impact retrieval kinetics. In contrast to our earlier findings with vesicles that fuse in response to APs (Leitz and Kavalali, 2011), we found that the kinetics of endocytosis of spontaneous fusion events were not slowed in response to elevated extracellular Ca^{2+} concentrations. In all likelihood, at 8 mM Ca^{2+} the average kinetics of fluorescence decay became faster due to emergence of events that could only be detected following inhibition of re-acidification. Therefore, with increasing extracellular Ca^{2+} there was a clear increase in the rate of spontaneous fusion and the number of vesicles that undergo fusion. The relative insensitivity of vesicle retrieval kinetics to Ca^{2+} suggests that synaptic vesicle retrieval after spontaneous and evoked fusion is regulated via diverse mechanisms consistent with differential dependence of the two forms of endocytosis on distinct dynamin isoforms (Chung et al., 2010; Raimondi et al., 2011; Meng et al., 2013) and distinct postendocytic transport machineries (Peng et al., 2012).

Finally, in our system we were able to directly compare the rate of spontaneous fusion and evoked-fusion probability within a single synapse. This analysis did not reveal a

significant correlation between spontaneous fusion rate and evoked fusion probability estimates from individual release sites, further supporting the notion that these two modes of neurotransmission are controlled and maintained independently (Sara et al., 2005; Atasoy et al., 2008; Fredj and Burrone, 2009; Melom et al., 2013; Peled et al., 2014; Wang et al., 2014). Importantly, at elevated Ca^{2+} concentrations the propensity to fuse of each of the two forms of vesicle fusion were increased, although their lack of correlation persisted suggesting a divergence in the mechanisms that regulate Ca^{2+} sensitivity of evoked and spontaneous fusion events (Xu et al., 2009; Groffen et al., 2010; Pang et al., 2011; Vyleta and Smith, 2011; Ermolyuk et al., 2013). This difference in Ca^{2+} regulation of spontaneous and evoked fusion probability may underlie differential sensitivity of the two forms of neurotransmission of certain neuromodulators and Ca^{2+} signaling pathways (Peters et al., 2010; Ramirez and Kavalali, 2011; Bal et al., 2013). Recent studies in the *Drosophila* neuromuscular junction have shown that a substantial fraction of release sites carry out exclusively spontaneous or evoked neurotransmitter release (Peled et al., 2014; Walter et al., 2014) also see (Melom et al., 2013). In our measurements, we detected a substantial overlap of release sites that are capable of both forms of neurotransmission, in agreement with our earlier estimates from lower temporal resolution experiments (Atasoy et al., 2008). This discrepancy may be consistent with the premise that in immature presynaptic release sites, spontaneous neurotransmission dominates and release gradually shifts towards evoked transmission during synapse maturation (Polo-Parada et al., 2001; Mozhayeva et al., 2002; Andreae et al., 2012 also Walter et al., 2014). Taken together, the findings we present here provide insight into the segregation of spontaneous and evoked neurotransmitter release mechanisms at the

level of single synaptic vesicle fusion events. The differential regulation of spontaneous vesicle fusion suggests it has a role in neuronal signaling distinct from information transfer patterns mediated by evoked release, even within a single synapse.

CHAPTER FOUR

REELIN MOBILIZES A VAMP7-DEPENDENT SYNAPTIC VESICLE POOL AND SELECTIVELY AUGMENTS SPONTANEOUS NEUROTRANSMISSION

Background

Synaptic vesicles (SVs) within individual presynaptic nerve terminals are divided into distinct pools with respect to their relative propensities for fusion (Alabi and Tsien, 2012). Putative segregation of SV populations giving rise to action potential (AP) evoked versus spontaneous neurotransmitter release is a key functional outcome of this vesicle heterogeneity (Sara et al., 2005; Fredj and Burrone, 2009; Chung et al., 2010). Recent studies have demonstrated that the heterogeneous distribution of SV associated SNARE (soluble N-ethylmaleimide-sensitive factor attachment protein receptors) proteins underlies this functional diversity among SVs (Hua et al., 2011; Raingo et al., 2012; Ramirez et al., 2012). In central synapses, synaptobrevin2 (syb2, also called VAMP2) is the predominant SV SNARE protein that interacts with the plasma membrane SNAREs SNAP-25 and syntaxin1 to execute exocytosis (Sudhof and Rothman, 2009). However, while neurons lacking syb2 have a nearly complete absence of evoked neurotransmission they still maintain significant levels of spontaneous neurotransmitter release (Schoch et al., 2001). SVs in central synapses contain lower levels of alternative vesicular SNARE proteins such as VAMP4, VAMP7 (also called tetanus-insensitive or TI-VAMP) and Vps10p tail interactor 1 a (Vti1a), with structures similar to that of syb2 (Takamori et al., 2006). Recent evidence

suggests that these alternative vesicular SNAREs maintain neurotransmission independently of syb2 (Raingo et al., 2012; Ramirez et al., 2012). Moreover, they also constitute molecular tags for independently functioning SV populations and provide a potential molecular basis for selective regulation of distinct forms of neurotransmitter release (Ramirez and Kavalali, 2012). Earlier work has provided several examples where spontaneous or evoked neurotransmission is differentially sensitive to neuromodulatory signaling cascades (Phillips et al., 2008; Pratt et al., 2011; Ramirez and Kavalali, 2011; Vyleta and Smith, 2011), however, the SV-associated substrates that link this differential regulation to vesicle pool heterogeneity have not yet been identified. Despite the accumulating functional and molecular evidence in support of this SNARE-dependent vesicle pool diversity, the physiological role of this functional specialization, in particular the biological significance of the residual syb2-independent forms of neurotransmitter release remains poorly understood.

Here, we examined the presynaptic effects of Reelin, a glycoprotein critical for proper layering of neocortex as well as dynamic regulation of glutamatergic postsynaptic signaling in mature synapses (D'Arcangelo et al., 1995; Herz and Chen, 2006). During development, Reelin is secreted by Cajal-Retzius cells in the marginal zone of embryonic brain where it guides the migration of newly generated neurons from the ventricular zone to the marginal zone, thus forming a properly layered structure in the adult brain (Trommsdorff et al., 1999; Kubo et al., 2002; Soriano and Del Rio, 2005; Knuesel, 2010). Reelin is a ligand for both apolipoprotein receptor 2 (ApoER2) and very low density lipoprotein receptor (VLDLR), which are required for its developmental role (Hiesberger et al., 1999; Trommsdorff et al., 1999). After development, the production of Reelin is dramatically decreased but remains

prominent in GABAergic interneurons (Alcantara et al., 1998) of the cortex and hippocampus (Pesold et al., 1998). In mature neuronal circuitry, Reelin modulates AMPA and NMDA receptor activity by postsynaptic activation of ApoER2 and VLDLR (Beffert et al., 2005; Qiu et al., 2006). The interaction between Reelin and its receptors leads to a signaling cascade initiated by phosphorylation of disabled-1 (Dab-1) which in turn leads to activation of Src, Fyn or PI-3 kinases (Trommsdorff et al., 1999; Kuo et al., 2005). Here, we demonstrate that Reelin also acts presynaptically in mature neurons to rapidly enhance spontaneous neurotransmitter release without detectable alterations in the properties of evoked neurotransmission. This action of Reelin depended on the function of the vesicular SNARE protein VAMP7 but not syb2, VAMP4 or vti1a. This finding demonstrates a novel example where an endogenous neuromodulator relies on the diversity of SV pool associated SNAREs and selectively mobilizes a subset of vesicles independent of electrical activity.

Methods

Cell culture and mouse lines

Dissociated hippocampal cultures were prepared from postnatal day 0-3 Sprague Dawley rats of either sex as described previously (Kavalali et al., 1999). For syb2 KO and SNAP-25 KO experiments, dissociated hippocampal cultures were prepared from embryonic day 18 mice constitutively deficient in syb2 (syb2 *-/-*) or SNAP-25 (SNAP-25 *-/-*) as well as their littermate controls (Schoch et al., 2001; Washbourne et al., 2002). ApoER2 KO and VLDLR KO cultures were prepared from mice generated by constitutive deletion of *Apoer2* (Trommsdorff et al., 1999) and *vldlr* genes (Frykman et al., 1995). To generate neurons deficient in p110 α and p110 β isoforms of PI3K (gift of Drs. Joel Elmquist, UTSW and Jean

Zhao, Dana-Farber Cancer Institute), hippocampal cultures from mice expressing conditionals alleles of *p110 α* and *p110 β* genes were infected with lentivirus expressing Cre. Lentiviral expression system shows high infection efficacy (>90%) as previously demonstrated by full rescue of synaptic transmission in *syb2*^{-/-} cultures by lentiviral expression of *syb2* (Deak et al., 2006). All experiments were performed on 14-21 *days in vitro* (DIV) cultures. All experiments were performed in accordance with protocols approved by the UT Southwestern Institutional Animal Care and Use Committee.

Lentiviral preparations

The short hairpin sequences used to knockdown the vesicular SNARE proteins are as follows: for *Vt1a*, sense 5'-tgtacagcaacagaatgagtcaagagactcattctgtgtgtaca-3', VAMP4, sense 5'-tcgaggagaatattaccaaggaattcaagagattaccttggaatattcttta-3'. For VAMP7 knockdown, two constructs were used: VAMP7 KD3 5'-ctgaagcatcactccgagattcaagagatctcggagtgtgcttcag -3' and VAMP7 KD4 5'-ctgaaagcatcatggctcattcaagagatgaccatgatgcctttcag-3'. In all cases, shRNA sequences were inserted into XhoI through XbaI cloning sites in the L307 lentiviral transfer vector, downstream of the human H1 promoter.

Lentiviruses encoding pHluorin-tagged *syb2*, VAMP4, *vt1a*, VAMP7, mOrange-tagged *syb2*, and all shRNA constructs were prepared by transfection of human embryonic kidney (HEK) 293-T cells with FUGENE 6 and necessary viral coat and packaging protein constructs (pVSVG, pRsv-Rev, and pPRE). Three days after transfection, virus was harvested from HEK 293-T cell-conditioned media and added to neuronal media at 4 DIV. Lentiviral constructs to decrease expression of all four isoforms of the Doc2 protein family

(Doc2A, Doc2B, Doc2G, and rabphilin) were a gift of Dr. Thomas C. Südhof (Stanford Univ.) (Pang et al., 2011).

Electrophysiology

Cultured neurons from hippocampus were used between 12 to 18 DIV for the study. Whole cell recordings were made at -70 mV holding potential. The extracellular solution contained the following ingredients (in mM): 150 NaCl, 10 Glucose, 10 HEPES, 4 KCl, 2 MgCl₂ and 2 CaCl₂. The pH and osmolarity of the solution was adjusted to 7.4 and 310 mOsm, respectively. To isolate AMPA currents (EPSCs), extracellular solution contained AP-5 (50 μM) and picrotoxin (50 μM). When recording spontaneous miniature excitatory activity (mEPSCs), 1 μM tetrodotoxin TTX was added to the extracellular solution. For the isolation of GABA mIPSCs, AP-5 (50 μM), CNQX (10 μM) and TTX (1 μM) was added to the extracellular solution. Finally, to isolate NMDA EPSCs the extracellular solution contained picrotoxin (50 μM), Glycine (15 μM), Strychnine (1 μM), CNQX (10 μM) and extracellular Mg²⁺ was reduced to 100 μM. The pipette internal solution was composed of the following (in mM): 115 Cesium-methanesulphonate, 10 Cesium Chloride, 5 Sodium Chloride, 10 HEPES, 0.6 EGTA, 20 Tertaethylamonium chloride, 4 Magnesium adenosine triphosphate, 0.3 Guanosine triphosphate *sodium* and 10 *N*-ethyl bromide 2(triethylamino)-*N*-(2,6-dimethylphenyl) acetamine. The final solution was adjusted to pH 7.3 and 300 mOsm. Final resistance of the electrode tips were ~ 3-6 mega ohms. The current recordings were performed with the assistance of Axopatch 200B and Pclamp 9.0 software (Molecular Devices). The cells were visualized by using Zeiss Axiovert S100 microscope. The evoked

EPSCs were recorded at different time intervals by the aid of constant current unit (WPI A385) set at 25 mA.

Reelin and pharmacology

Reelin-conditioned media from HEK 293 cells was subjected to centrifugation at 3000 rpm for 30 min using Centricon Plus 70 filters (Millipore). The resulting supernatant was then dialyzed at 4 °C overnight in 20 mM Tris, 2 mM CaCl₂, and 10 mM NaCl with pH adjusted to 8. After dialysis, the Reelin solution was passed through an ion exchange column (HiTrap Q 5ml from Amersham #171154-01) for 60 min and fractions were collected every 1 min. Every other fraction from fraction 29-45 was analyzed by western blot for the concentration of Reelin and BSA, fractions containing the highest Reelin:BSA ratio were then consolidated. The consolidated Reelin solution was then subjected to an additional round of centrifugation using Amicon centrifugal filters (Millipore) followed by dialysis at 4 °C overnight in solution containing 124 mM NaCl, 5 mM KCl, 1.2 mM NaH₂PO₄, 26 mM NaHCO₃, 10 mM D-Glucose, 2 mM CaCl₂ and 1 mM MgSO₄. Preparation of the Vehicle was identical but used media from HEK 293 cells not expressing Reelin. Reelin was added to the extracellular solution with a final concentration of ~5 nM in all experiments. It is important to note that the efficacy of Reelin is quite variable among different batches. Therefore, in each round of experiments, we verified the validity of a negative result (i.e. no effect of Reelin) by conducting parallel positive controls.

RAP-GST, a high-affinity non-receptor subtype specific ligand for the LRPs was perfused at a final concentration of 20 μM. For all pharmacological experiments, neurons were preincubated in drug for 45 min prior to whole-cell patch-clamp recordings. Drugs

were added to the extracellular solution, with the following final concentrations (in μM): 10 PP1 (Tocris), 10 Ryanodine (Tocris), 10 Dantrolene (Sigma), 10 EGTA-AM (Sigma), 20 BAPTA-AM (Invitrogen) 200 CdCl_2 (Sigma-Aldrich), 10 Wortmannin (Tocris), 10 LY294002 (Tocris).

Single color imaging

For AP-evoked synaptophysin-pHluorin trafficking experiments, neurons were stimulated using parallel bipolar electrodes (FHC) delivering 15-20 mA pulses at 20 Hz for 10 s and puncta were selected based on their subsequent response to 20 mM NH_4Cl . For 20 Hz stimulation experiments, synaptophysin-pHluorin images were acquired at ~ 3 Hz with an exposure time of 100 ms. For spontaneous synaptophysin-pHluorin experiments, images were acquired at 0.2 Hz with an exposure time of 100 ms. For experiments using synaptobrevin-pHluorin, VAMP4-pHluorin, vti1a-pHluorin and VAMP7-pHluorin images were acquired at 0.2 Hz with an exposure time of 150 ms. To prevent network activity, TTX (1 μM) CNQX (10 μM), and AP-5 (50 μM) were added to the modified Tyrode solution. Reelin was added by quickly exchanging the bath solution with an identical Tyrode's solution containing 20 μL of Reelin per 1 mL of solution (5 nM final Reelin concentration).

In calcium imaging experiments dissociated cultures at 5 DIV were infected with lentivirus carrying syb2-mOrange and imaged on 14-18 DIV. Immediately before imaging, cells were loaded with Ca^{2+} indicators by incubating in conditioned media containing 3.8 μM of either Fluo-4 AM (Ca^{2+} $K_D \sim 335$ nM, Invitrogen) or Calcium Green-1 AM (Ca^{2+} $K_D \sim 190$ nM, Invitrogen) for 20 min at 37°C . Neuronal activity and postsynaptic signaling was suppressed by 2 minute-long perfusion in Tyrode's solution containing 1 μM TTX, 5 μM

NBQX and 50 μ M AP-5 prior to the start of the experiment. Cells were kept under constant perfusion of this solution, first imaged for 2 minutes at baseline, before switching to Tyrode's solution containing Reelin or Vehicle for two minutes. 50 mM NH_4Cl was used to alkalinize synaptic vesicles and maximize fluorescence of syb2-mOrange puncta for post-hoc synapse identification. Imaging was performed at room temperature using a Nikon TE2000-U inverted microscope and 40X objective. Images were captured at 2 Hz using an Andor iXon Ultra EMCCD camera with an 80 ms exposure time. Traces were obtained in Nikon NIS-elements 4.10 software, placing $2 \times 2 \mu\text{m}$ square ROIs over syb2 positive puncta. 70-80 puncta were chosen per experiment.

Dual color imaging

For vti1a-pHluorin/syb2-mOrange experiments, images were collected at 0.1 Hz with images size of 512×512 and every 2 images averaged. An argon laser was used at 6% transmission to excite pHluorin at 488 nm. A HeNe laser was used at 15% transmission to excite mOrange at 543 nm. For VAMP7-pHluorin/syb2-mOrange imaging the image size was decreased to 256×256 and the number of averaged images increased to 4. The green excitation was increased to 25% transmission and the red excitation remained at 15%. Specific filters (500-550 bandpass for the green channel and 543 longpass for the red channel) were used to minimize bleed-through. Solutions were identical to those used in single color imaging described above.

Statistical analysis

For statistical comparisons between electrophysiological experiments, Student's t-test was used (2-tailed, paired) as experiments were performed within the same cell, before and

after Reelin treatment. In pHluorin imaging experiments, n refers to the number of synapses pooled from multiple experiments performed, with each experiment containing up to 100 regions of interest. Student's t-test (2-tailed, unpaired) was used to analyze all pHluorin imaging experiments. The Kolmogorov-Smirnov test was used to determine differences in Ca^{2+} $\Delta\text{F}/\text{F}$ slope change distributions. For analysis of the 20 Hz synaptophysin-pHluorin fluorescence responses, a two-way repeated measures ANOVA was used.

ApoER2 and synapsin immunocytochemistry

Neurons were plated on poly-D-lysine and cultured as described above. Briefly, after 14DIV, neurons were fixed in 4% paraformaldehyde for 15 minutes at room temperature and processed for immunostaining as described (Ramirez et al., 2012) using an anti-ApoER2 rabbit polyclonal antibody (1:100; #2561, gift of Dr. Joachim Herz) and an anti-synapsin mouse monoclonal antibody (1:500; clone 46.1, Synaptic Systems). Imaging was performed on a Zeiss LSM 510 laser scanning confocal microscope and LSM software was used to collect synaptic intensity profiles.

Results

Reelin causes an increase in spontaneous neurotransmitter release.

To assess the effect of Reelin on neurotransmitter release, we applied Reelin (5 nM) to hippocampal neurons and recorded spontaneous miniature postsynaptic currents in the presence of TTX to block APs. Using whole-cell voltage clamp recordings, we monitored pharmacologically isolated excitatory postsynaptic currents (mEPSCs) generated by activation of AMPA or NMDA receptors as well as GABAergic miniature inhibitory

postsynaptic currents (mIPSCs) for 5 minutes in normal Tyrode's solution. Reelin was then perfused into the chamber and mPSCs were measured for at least 5 minutes followed by washout of Reelin (Figure 4.1). Reelin robustly increased the frequency of spontaneous AMPA mEPSCs (Figure 4.1B) from 0.8 ± 0.1 Hz up to 4.8 ± 0.2 Hz during Reelin (~ 6 -fold increase with $t_{1/2} = 67.6 \pm 14.4$ s). This effect was dependent on acute Reelin application as upon Reelin removal, spontaneous event frequency returned to baseline levels (0.9 ± 0.2 Hz with $t_{1/2} = 75.1 \pm 23.3$ s). Similarly, Reelin increased the frequency of both NMDA-derived mEPSCs (from 0.7 ± 0.1 Hz before Reelin to 3.2 ± 0.3 Hz during Reelin and 0.7 ± 0.1 Hz after Reelin washout, ~ 4.5 -fold increase with a rise time of: $t_{1/2} = 43.1 \pm 21.0$ s and a decay time of: $t_{1/2} = 26.1 \pm 7.5$ s) and GABA-mediated mIPSCs (from 0.4 ± 0.04 Hz before Reelin to 1.7 ± 0.1 Hz during Reelin and 0.4 ± 0.1 Hz after Reelin washout, a ~ 4 -fold increase with a rise time of: $t_{1/2} = 17.0 \pm 4.8$ s and decay time of: $t_{1/2} = 37.1 \pm 15.1$ s) (Figure 4.1C, D). In all cases the elevated spontaneous release frequency was sustained for longer than 5 minutes in the presence of Reelin (Figure 4.1E). Furthermore, the Reelin-dependent increase in spontaneous mEPSC frequency was present as early as 6 days *in vitro* (DIV) (bal et al 2013) at a developmental time point when synapses are not capable of robust evoked release (Mozhayeva et al., 2002). This finding suggests an early developmental significance for the Reelin effect. Previous studies have shown that Reelin can augment the amplitude of AP-evoked NMDA receptor mediated currents (Chen et al., 2005). We found a modest, but significant, increase in NMDA mEPSC amplitudes from 13.3 ± 1.8 pA at baseline to 16.9 ± 1.6 pA after Reelin application (Figure 4.1F and see Bal et al., 2013 for additional details). This observation could account for the previously reported increase in evoked

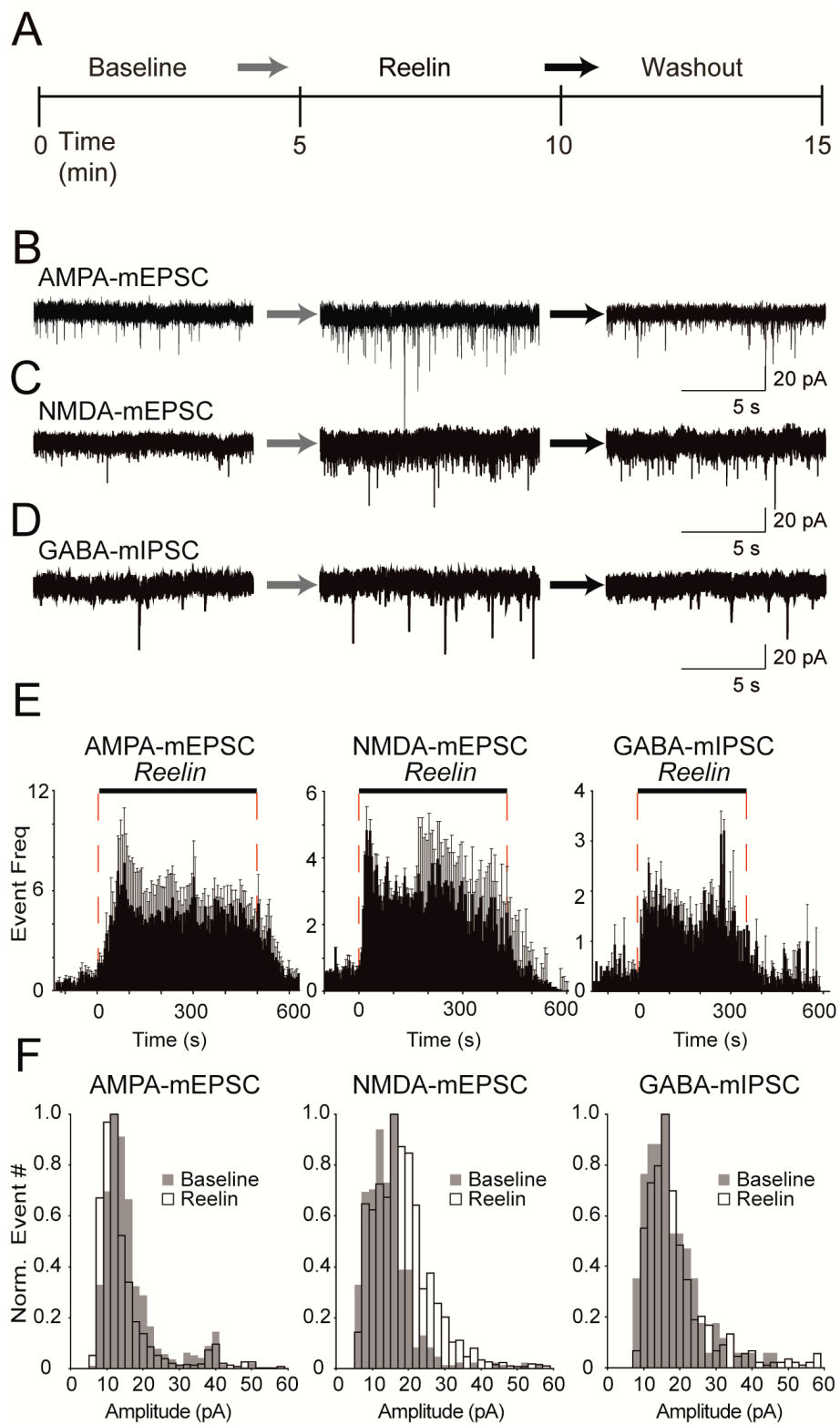


Figure 4.1. Reelin increases the frequency of spontaneous neurotransmission.

A, Whole-cell voltage clamp recordings of AMPA-mEPSCs, NMDA-mEPSCs as well as GABA- mIPSCs were performed for 5 minutes in normal Tyrode's solution (baseline), followed by at least 5 minute-long Reelin application and subsequent 5 minutes during washout of Reelin. **B-D**, Example traces of spontaneous neurotransmission derived from recordings of AMPA-mEPSC (**B**), NMDA-mEPSC (**C**) and GABA-mIPSCs (**D**) before Reelin application (left), during 5 minutes of Reelin application (middle), after Reelin washout (Right). **E**, The mEPSC and mIPSC frequency for AMPA-, NMDA- and GABA-mediated spontaneous events increases in response to Reelin (AMPA n = 6; NMDA n = 8; GABA n = 5). AMPA mEPSC frequency increased from 0.8 ± 0.1 Hz before Reelin to 4.8 ± 0.2 Hz during Reelin and decreased to 0.9 ± 0.2 Hz after Reelin washout. Reelin similarly affected both NMDA- mEPSCs (from 0.7 ± 0.1 Hz before Reelin to 3.2 ± 0.3 Hz during Reelin and 0.7 ± 0.1 Hz after Reelin washout) as well as GABA-mediated mIPSCs (from 0.4 ± 0.04 Hz before Reelin to 1.7 ± 0.1 Hz during Reelin and 0.4 ± 0.1 Hz after Reelin washout). **F**, Distribution of AMPA-mEPSC, NMDA-mEPSC and GABA-mIPSC amplitudes before Reelin (Baseline, grey bars) and during Reelin (white bars) application. Overall averages of AMPA mEPSC amplitude showed a slight decrease during Reelin treatment ($p < 0.05$ paired student's T-test, n = 7) while NMDA mEPSC amplitude increased ($P < 0.01$ paired student's T-test, n = 10). GABA mIPSC amplitudes did not reveal a marked change after Reelin application ($p > 0.3$, n = 4). All error bars represent standard errors of the mean. (Courtesy Dr. Manjot Bal)

NMDA receptor mediated synaptic responses (Chen et al., 2005). Under the same conditions, the amplitude of AMPA mEPSCs showed a slight decrease from 16.2 ± 1.3 pA before Reelin to 14.5 ± 1.3 pA in the presence of Reelin, while GABA mEPSC amplitude was relatively unchanged (Figure 4.1F). Although Reelin action on spontaneous release may have a transient component, within the time frame of our experiments, our data did not reveal a statistically significant difference between the initial and later phases of Reelin action. Moreover, it is important to note that as Reelin is a large protein delivered at nM concentrations, it is difficult to ensure the consistency of Reelin concentrations during application.

Reelin selectively augments spontaneous transmission.

To assess the effect of Reelin on evoked SV fusion probability, we measured paired-pulse facilitation of evoked AMPA receptor mediated synaptic responses in hippocampal neurons in the presence of Reelin (within ~5 minutes of treatment). Neurons were stimulated using single APs with increasing inter-stimulus intervals of 50 ms, 100 ms, 500 ms and 1000 ms (Figure 4.2A). These experiments did not reveal a significant difference in the ratio of synaptic responses to paired-pulse stimulation in the presence or absence of Reelin, suggesting that Reelin does not alter AP-dependent release probability (Figure 4.2B), in agreement with earlier observations (Qiu et al., 2006). In addition, absolute amplitudes of evoked AMPA-EPSCs were stable and did not show a significant difference before or during Reelin application (Figure 4.2C; before Reelin: 1223.3 ± 130.7 pA; after Reelin: 1292.2 ± 88.0 pA; $p > 0.7$).

To directly examine the effect of Reelin on presynaptic SV trafficking, we turned to optical monitoring of a SV associated protein, synaptophysin, tagged with pH-sensitive GFP within the vesicle lumen (synaptophysin-pHluorin, syp-pH). Exogenous expression of syp-pH typically leads to its wide distribution across SV pools (Kwon and Chapman, 2011). Neurons were stimulated using a bipolar electrode delivering 200 APs at 20 Hz, before, 5 minutes after, and 10 minutes after Reelin application (Figure 4.2D). In this setting, we did not detect a significant change in peak fluorescence amplitude (Figure 4.2E), fluorescence decay kinetics (Figure 4.2F) or fluorescence rise time (Figure 4.2G), indicating that under these conditions Reelin did not significantly alter activity-evoked SV trafficking.

In the presence of the vacuolar ATPase inhibitor folimycin, SVs cannot be re-acidified after endocytosis, thus trapping the pHluorin molecules present in vesicles that have undergone fusion in a fluorescent state (Sara et al., 2005). Therefore, in the presence of folimycin, the AMPAR antagonist CNQX, the NMDA antagonist AP-5, and TTX to prevent AP firing, spontaneous transmission can be directly monitored as an accumulation of fluorescence at rest (Atasoy et al., 2008; Hua et al., 2011; Ramirez et al., 2012). Under these conditions, Reelin application increased spontaneous trafficking of syp-pH more than two-fold from 2.11 ± 0.05 a.u. after 10 minutes in Vehicle to 5.06 ± 0.24 a.u. after 10 minutes in Reelin (Figure 4.2H, I). Together these data indicate that Reelin selectively facilitates

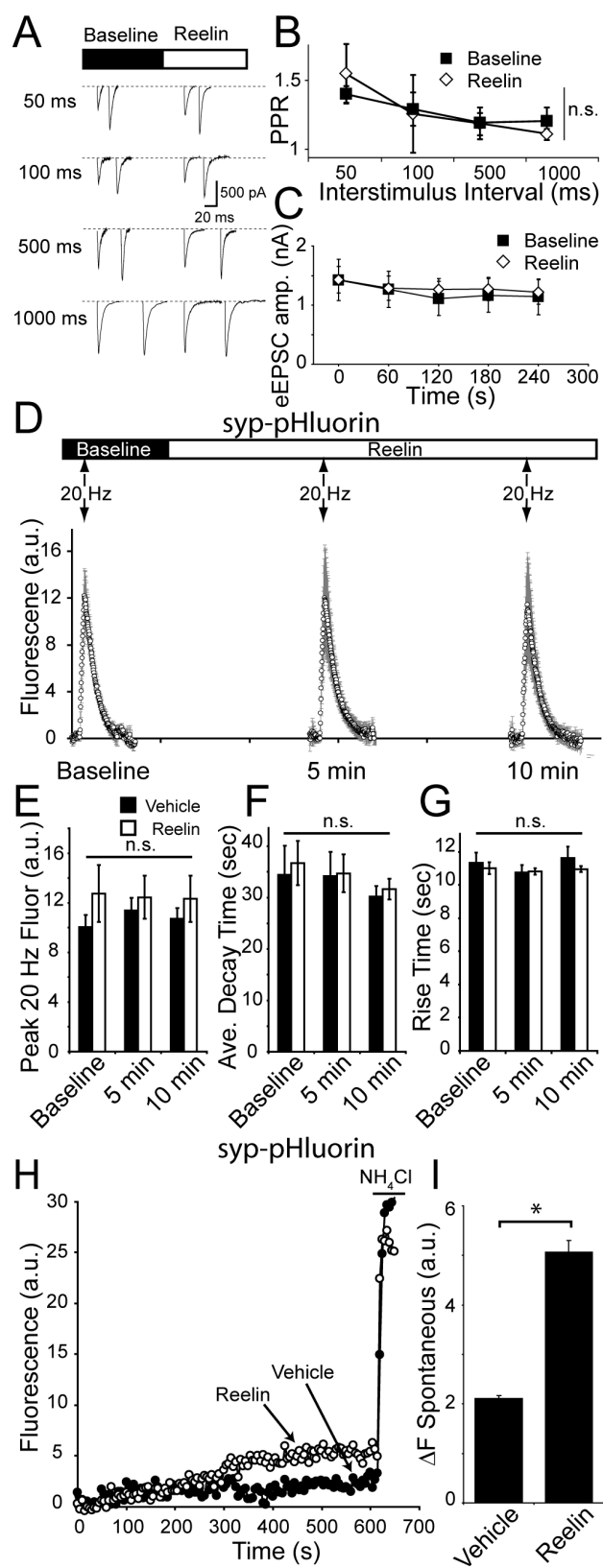


Figure 4.2. Reelin selectively augments spontaneous synaptic vesicle trafficking without altering the properties of evoked neurotransmission.

A, Example of paired-pulse ratio traces for AMPA receptor mediated events before Reelin and after Reelin application. **B**, Paired-pulse ratio before and after Reelin application was unaltered compared to Vehicle control (Vehicle $n = 5$; Reelin $n = 5$). **C**, Single AP stimulation delivered at 60 s intervals did not alter AMPA-EPSC amplitude in the absence (closed squares) or presence (open diamonds) of Reelin (No Reelin $n = 7$, Reelin = 13). **D**, Optical measurements of cells infected with synaptophysin-pHluorin. Cells were electrically stimulated with 200 APs delivered at 20 Hz before, 5 minutes after, and 10 minutes after Reelin application. **E-G**, Reelin did not affect 20 Hz stimulation driven fluorescence peak amplitude, decay time or rise time (Vehicle $n = 5$; Reelin $n = 6$). **E**, Peak fluorescence amplitudes before Vehicle 10.1 ± 0.9 a.u., after 5 minutes in Vehicle 11.4 ± 1.0 a.u., and after 10 minutes in Vehicle 10.7 ± 0.9 a.u., compared to 12.7 ± 2.3 a.u. before Reelin, 12.4 ± 1.7 a.u. after 5 minutes of Reelin application, and 12.3 ± 1.9 a.u. 10 minutes after Reelin application. **F**, Fluorescence decay kinetics were not different with 34.5 ± 5.7 s before Vehicle, 34.2 ± 4.8 s 5 minutes after Vehicle, and 30.2 ± 2.1 s after 10 minutes in Vehicle compared to 35.7 ± 3.5 s before Reelin application, 34.6 ± 3.0 s after 5 minutes in Reelin and 32.1 ± 1.8 s after 10 minutes in Reelin. Finally, fluorescence rise time **G**, in Reelin was not significantly different from Vehicle (11.3 ± 0.6 s before Vehicle, 10.8 ± 0.4 s after 5 minutes in Vehicle, and 11.6 ± 0.7 10 minutes after Vehicle compared to 11.0 ± 0.4 s before Reelin application, 10.8 ± 0.2 s after 5 minutes in Reelin and 11.0 ± 0.2 s after 10 minutes in Reelin). There were no significant differences between any of the groups, analyzed by ANOVA ($p > 0.2$ between all groups). **H**, Example traces of fluorescence increase in Vehicle (closed circles) and Reelin (open circles) followed by NH_4Cl application to visualize the total syp-pHluorin pool. **I**, In the presence of Reelin, spontaneous syp-pHluorin fluorescence increased to 5.06 ± 0.24 a.u. after 10 minutes compared to 2.11 ± 0.05 a.u. after 10 minutes in Vehicle (Vehicle, $n = 701$ synapses from 6 experiments; Reelin, $n = 917$ synapses from 6 experiments; p -value < 0.001).

spontaneous neurotransmission while leaving evoked neurotransmission and SV trafficking relatively unaffected.

Reelin-dependent facilitation of spontaneous neurotransmission requires SNAP-25 but not syb2.

Our results so far suggest that Reelin acting via its canonical receptors ApoER2 and VLDLR causes a modest but significant increase in presynaptic Ca^{2+} which in turn augments resting neurotransmitter release rate without significantly altering the properties of evoked neurotransmitter release. At synaptic terminals, SNARE protein interactions are largely responsible for vesicle fusion and neurotransmitter release. The canonical synaptic SNARE complex composed of syb2 on the SV and syntaxin 1 and SNAP-25, both on the target plasma membrane, mediates rapid exocytosis. Syb2 is the most abundant vesicle associated SNARE and is essential for fast synchronous neurotransmission (Schoch et al., 2001; Takamori et al., 2006). Therefore, in order to examine the presynaptic fusion machinery that underlies this effect, we tested the effect of Reelin on neurons deficient in the canonical synaptic SNARE proteins SNAP-25 and syb2 (Figure 4.4A). Although neurons from their wild type littermates showed swift responses to Reelin application (Figure 4.4B), neurons lacking SNAP-25 (SNAP25 $-/-$) showed no response to Reelin and had an overall lower mEPSC frequency (Figure 4.4C) (Bronk et al., 2007). Here, it is important to note that SNAP-25 deficient synapses respond to other secretagogues such as hypertonic sucrose, ionomycin or α -latrotoxin (Bronk et al., 2007; Deak et al., 2009). These data indicate that

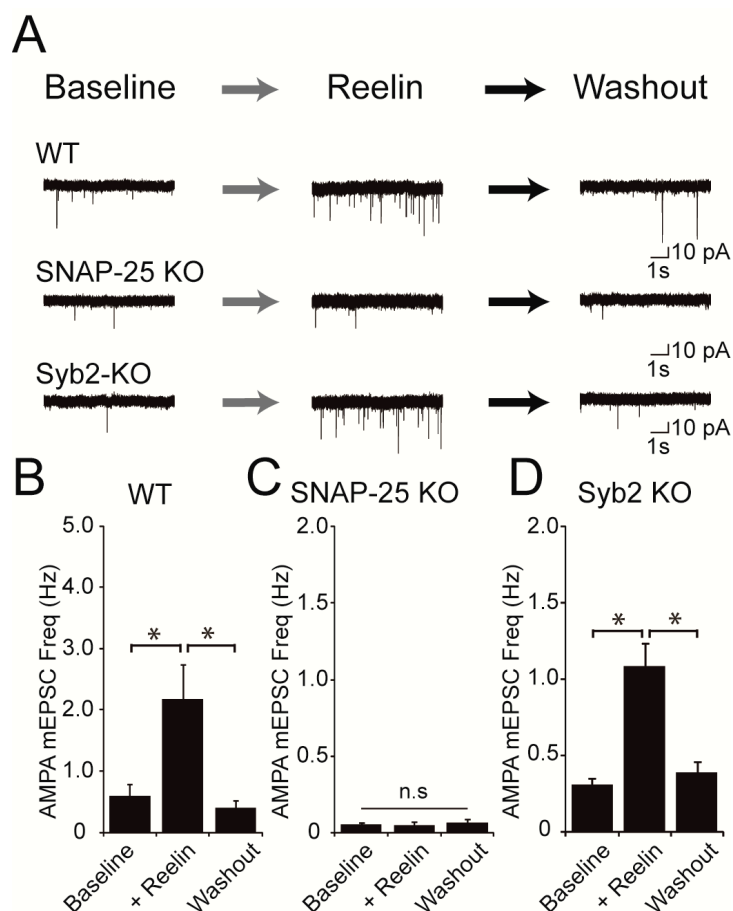


Figure 4.3. Reelin-induced increase in spontaneous release requires SNAP-25 but not syb2. **A**, Example traces of AMPAR mEPSCs from WT, SNAP-25 KO and Syb2 KO neurons. **B**, Reelin increases mEPSC frequency in WT cells (0.6 ± 0.2 Hz before Reelin, 2.2 ± 0.6 Hz during Reelin and 0.4 ± 0.1 Hz after Reelin washout in WT cells; asterisks $p < 0.005$). **C**, SNAP-25 KO cells do not respond to Reelin (0.06 ± 0.01 Hz before Reelin, 0.05 ± 0.02 Hz during Reelin and 0.06 ± 0.00 Hz after Reelin washout; $p > 0.5$). **D**, However, Reelin still caused an increase in mEPSC frequency in syb2 KO cells (0.31 ± 0.04 Hz before Reelin compared to 1.1 ± 0.1 Hz after Reelin application and 0.4 ± 0.1 Hz after washout; $p < 0.005$). All p-values were calculated by paired Student's T-test. All error bars represent standard errors of the mean. (Courtesy Dr. Manjot Bal)

reelin causes an increase in SV fusion frequency that requires the function of the plasma membrane associated SNARE, SNAP-25, in agreement with an earlier study suggesting a SNAP-25 dependent role for Reelin in presynaptic function (Hellwig et al., 2011). To test if the SV SNARE syb2 is also required for the Reelin dependent augmentation in transmission, we added Reelin to neurons deficient in syb2 (syb2 $-/-$) (Figure 4.3A, D). Surprisingly, neurons lacking syb2 still responded to Reelin despite their low basal mEPSC frequency (Figure 4.3D). Taken together, these results suggest that the Reelin-dependent increase in spontaneous transmission requires a SNARE complex that contains SNAP-25 but does not require the vesicle associated protein syb2.

Reelin facilitates trafficking of VAMP7 expressing synaptic vesicles.

The ability of Reelin to increase spontaneous release in the absence of syb2 but not SNAP-25 suggests that the presynaptic Reelin effect requires an alternative vesicular SNARE. This observation is rather surprising as we detected a modest Reelin-dependent increase in presynaptic Ca^{2+} levels in presynaptic terminals identified via co-expression of syb2-mOrange in our Ca^{2+} imaging experiments. These findings suggest that Reelin can signal to presynaptic terminals expressing syb2 but its effect on neurotransmitter release does not require syb2 function. To identify the alternative vesicular SNARE that mediates the observed Reelin-elicited exocytosis, we monitored the fluorescence of wild type neurons expressing one of four vesicular SNAREs (syb2, VAMP4, vti1a, or VAMP7) tagged with pHluorin at their C-terminal ends in the SV lumen. Using the same setting as in Figure 4.2G, we took advantage of the vacuolar ATPase inhibitor, folimycin, to prevent SV

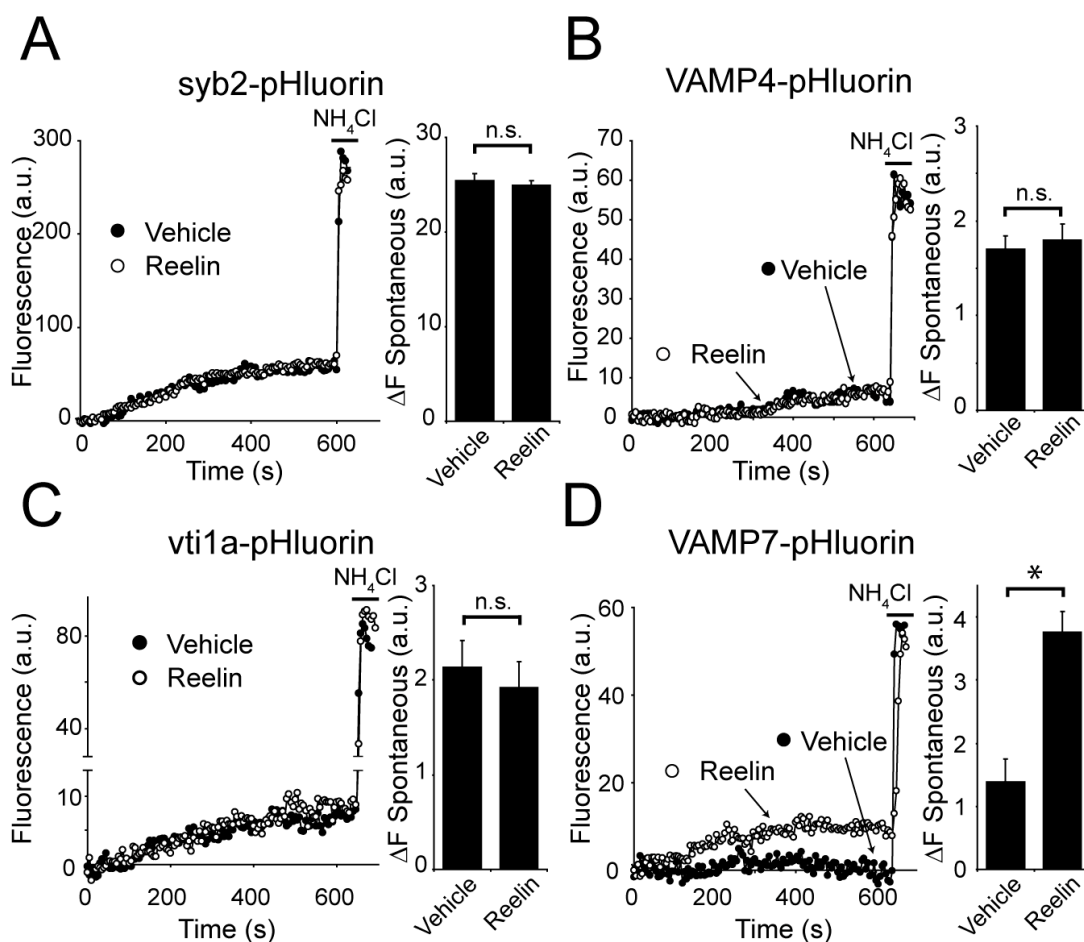


Figure 4.4. Reelin selectively mobilizes a pool of vesicles tagged with VAMP7.

A-D, Example traces of spontaneous pHluorin-tagged SV trafficking in 2 mM Ca^{2+} followed by application of NH_4Cl is shown on left, and quantification of fluorescence change after 10 minutes in Vehicle or Reelin is shown on right. **A**, Reelin does not alter syb2-pHluorin trafficking (25.4 ± 0.7 a.u. after 10 minutes for Vehicle compared to 24.9 ± 0.5 a.u. in Reelin; Vehicle: $n = 576$ synapses, 5 experiments; Reelin: $n = 689$ synapses, 5 experiments; $p > 0.5$). **B**, Reelin does not alter VAMP4-pHluorin trafficking (1.7 ± 0.1 a.u. over 10 minutes in Vehicle compared to 1.8 ± 0.2 a.u. in Reelin; Vehicle: $n = 350$ synapses, 4 experiments; Reelin: $n = 466$ synapses, 5 experiments; $p > 0.5$). **C**, Reelin does not affect vti1a-pHluorin spontaneous trafficking (2.1 ± 0.3 a.u. after 10 minutes in Vehicle compared to 1.9 ± 0.3 a.u. in Reelin; Vehicle: $n = 340$ synapses, 4 experiments; Reelin: $n = 512$ synapses, 5 experiments; $p > 0.5$). **D**, VAMP7-pHluorin trafficking is increased more than 2-fold in the presence of Reelin compared to Vehicle (1.4 ± 0.4 a.u. after 10 minutes in vehicle to 3.8 ± 0.3 a.u. in Reelin; Vehicle: $n = 209$ synapses, 7 experiments; Reelin: $n = 263$ synapses, 7 experiments; $p < 0.001$). The p-values reported were calculated by unpaired Student's T-test. All error bars represent standard errors of the mean.

re-acidification at rest, and monitored spontaneous fusion of vesicles tagged with the four vesicular SNAREs. In this setting, we measured the increase in fluorescence after 10 minutes of Reelin application. Under these conditions, syb2-pHluorin (Figure 4.4A), VAMP4-pHluorin (Figure 4.4B) or vti1a-pHluorin (Figure 4.4C) trafficking did not respond to Reelin when compared to vehicle. Reelin did, however, robustly increase the cumulative rate of spontaneous fusion of vesicles labeled with VAMP7-pHluorin from 0.14 ± 0.04 a.u. per min. (in vehicle) to 0.38 ± 0.03 a.u. per min. (in Reelin) (Figure 4.4D). The rise in VAMP7-pHluorin fluorescence was in striking contrast to the very limited trafficking of VAMP7 under normal conditions compared to other vesicular SNAREs (Figure 4.4D). This finding is consistent with our earlier observations (Ramirez et al., 2012) as well as the earlier proposal that VAMP7 primarily resides within the resting SV pool (Hua et al., 2011). These results suggest that Reelin facilitates spontaneous neurotransmitter release specifically through mobilization of VAMP7-containing SVs.

Reelin selectively acts on VAMP7 expressing SVs within an individual synaptic terminal.

To evaluate the premise that in a single presynaptic terminal, VAMP7-containing SVs are selectively mobilized over those containing other vesicular SNAREs in response to Reelin, we utilized dual color imaging to compare relative vesicular SNARE trafficking within individual nerve terminals (Raingo et al., 2012; Ramirez et al., 2012). We co-infected cells with syb2-mOrange and either vti1a- or VAMP7-pHluorin. Synaptic boutons were then selected based on syb2-mOrange fluorescence and fluorescence changes in both channels were measured. Under these conditions, we detected significant fluorescent co-localization

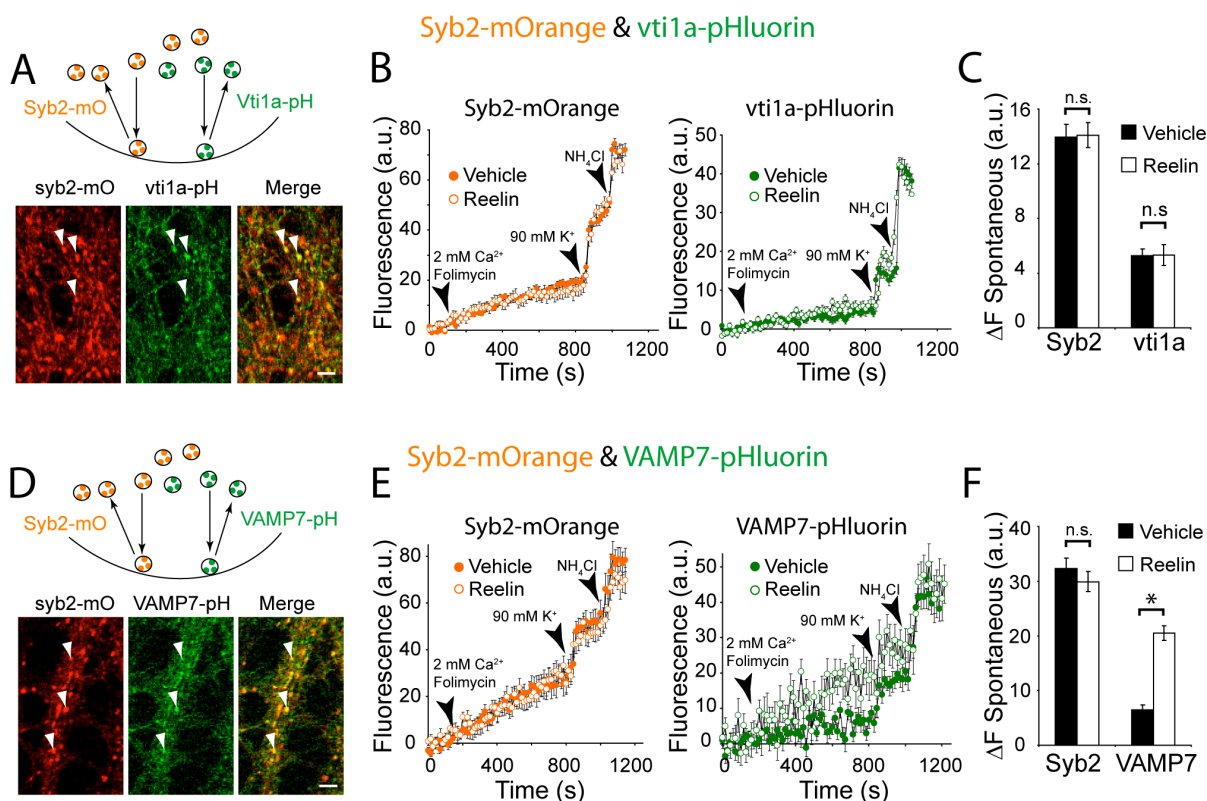


Figure 4.5. Dual color analysis of vesicular SNARE trafficking reveals that VAMP7 specifically responds to Reelin application. **A**, Neurons were co-infected with syb2-mOrange and vti1a-pHluorin. (Top) Cartoon depicting the segregation of these fluorescent signals to distinct SV pools. (Bottom) Co-localization of syb2-mOrange and vti1a-pHluorin fluorescence within individual synaptic boutons. Arrows indicate representative regions of interest selected for analysis. Scale bars indicate 5 μ m. **B**, In synapses co-labeled with syb2-mOrange and vti1a-pHluorin, application of Reelin did not alter the trafficking of either vesicular SNARE compared to Vehicle application. **C**, In Vehicle syb2-mOrange fluorescence increased to 13.9 ± 0.9 a.u. after 10 minutes in Vehicle compared to 14.1 ± 0.9 a.u. after Reelin application ($p > 0.5$). In the case of vti1a-pHluorin, during Vehicle application fluorescence reached to 5.3 ± 0.5 a.u. after 10 minutes, whereas in Reelin vti1a-pHluorin fluorescence was leveled at 5.3 ± 0.8 a.u. (Vehicle: $n = 382$ synapses, 5 experiments vs. Reelin: $n = 351$ synapses, 5 experiments; $p > 0.5$). **D**, Neurons were co-infected with syb2-mOrange and VAMP7-pHluorin. (Top) Cartoon depicting the segregation of these fluorescent signals to distinct SV pools. (Bottom) Co-localization of syb2-mOrange and VAMP7-pHluorin fluorescence within individual synaptic boutons. Arrows indicate representative regions of interest selected for analysis. **E**, Reelin selectively enhances VAMP7 trafficking in synapses that co-express syb2-mOrange and VAMP7-pHluorin. **F**, During application of Vehicle, syb2-mOrange fluorescence reached to 32.3 ± 1.9 a.u. in 10 minutes. Under the same condition, VAMP7-pHluorin fluorescence reached to 6.4 ± 0.9 a.u. after 10 minutes. In the presence of Reelin, however, syb2-mOrange fluorescence was relatively unaffected (29.9 ± 1.9 a.u. in 10 minutes; $p > 0.2$), whereas VAMP7-pHluorin

fluorescence reached 20.5 ± 1.3 a.u. in 10 minutes (Vehicle: $n = 108$ synapses, 8 experiments; Reelin $n = 77$ synapses, 6 experiments; $p < 0.001$). All error bars represent standard errors of the mean.

of syb2-mOrange and vti1a-pHluorin as well as syb2-mOrange and VAMP7-pHluorin (Figure 4.5A and D) (also see Ramirez et al., 2012). However, addition of Reelin did not alter syb2-mOrange or vti1a-pHluorin trafficking (Figure 4.5B and C). In contrast, Reelin could selectively increase the rate of trafficking of VAMP7-pHluorin-containing vesicles, while syb2-mOrange labeled vesicles in the same boutons were unaffected (Figure 4.5E and F). Collectively, these data demonstrate that within a given presynaptic terminal, Reelin selectively mobilizes a subset of VAMP7-containing SVs and leaves vesicles harboring other vesicular SNAREs relatively unaffected.

VAMP7 knockdown abolishes the effect of Reelin.

To further examine whether VAMP7 expression is indeed required for the effect of Reelin on spontaneous neurotransmitter release, we infected neurons with shRNA constructs directed against VAMP7, VAMP4 or vti1a (Bal et al., 2013). In addition to the constructs against VAMP4 (Raingo et al., 2011) and vti1a (Ramirez et al., 2012) we reported earlier, we developed two VAMP7-knock down (KD) constructs (VAMP7-KD3 and VAMP7-KD4), which effectively reduced endogenous VAMP7 protein levels as detected by western blot. Uninfected control neurons and neurons infected with the vti1a- and VAMP4-KD constructs still responded to Reelin, while knockdown of VAMP7 using either the VAMP7-KD3 or

VAMP7-KD4 construct abolished the effect of Reelin (Bal et al., 2013). Moreover, insufficient knockdown of VAMP4 or *vtila* did not attenuate the effect of Reelin on AMPA mEPSC frequency whereas cells with substantial amounts of VAMP7 expression remaining still exhibited increased AMPA-mEPSC frequency in the presence of Reelin (Bal et al., 2013). Taken together, these results provide further support that Reelin mobilizes a specific subset of SVs containing VAMP7 to facilitate spontaneous neurotransmission.

Discussion

In this study, we examined the presynaptic effect of the secreted glycoprotein Reelin and found that Reelin increases spontaneous neurotransmitter release from excitatory as well as inhibitory synaptic terminals without significantly altering the properties of evoked neurotransmission. This effect of Reelin is initiated by the ApoER2 and VLDLR signaling pathway(s) leading to activation of PI3 kinase and an increase in presynaptic Ca^{2+} , via Ca^{2+} -induced Ca^{2+} release. The Reelin-induced Ca^{2+} signal and the subsequent increase in SV fusion was widely distributed across synaptic boutons indicating that the presynaptic action of Reelin was not restricted to a small subpopulation of synapses. Although our results from synaptophysin-pHluorin trafficking (Figure 4.2G, H) and presynaptic Ca^{2+} imaging (data not shown) experiments indicate a robust effect of Reelin on the majority of synaptic boutons in our hippocampal cultures, the degree to which presynaptic Ca^{2+} levels increased after Reelin application varied across synapses examined. This variability may suggest a heterogeneous ability to respond to Reelin across synaptic boutons. Such heterogeneity may also agree with the earlier work showing relative enrichment of VAMP7 expression in the mossy fiber terminals that originate from dentate granule cells (Scheuber et al., 2006).

The selective increase in spontaneous neurotransmitter release was dependent on the plasma membrane associated SNARE protein SNAP-25, consistent with an earlier study that proposed a SNAP-25 dependent role for Reelin in presynaptic function (Hellwig et al., 2011). Surprisingly, however, the effect of Reelin persisted in neurons deficient in *syb2*, which is the most abundant vesicular SNARE protein in the central nervous system (Schoch et al., 2001; Takamori et al., 2006). A functional survey of alternative SV associated SNAREs VAMP4, *vtila* and VAMP7 (Takamori et al., 2006; Hua et al., 2011; Raingo et al., 2012; Ramirez et al., 2012) revealed that Reelin mediated signaling selectively targeted VAMP7 to augment spontaneous release. Dual color imaging at individual synaptic boutons showed that Reelin application could selectively mobilize vesicles tagged with VAMP7-pHluorin but spare vesicles tagged with *syb2*- or *vtila*-pHluorin. Importantly, loss-of-function experiments showed that the Reelin mediated increase in spontaneous release was absent after shRNA mediated knockdown of VAMP7 (Bal et al 2013). These results support the premise that low-level sustained increases in baseline presynaptic Ca^{2+} triggered by Reelin can selectively mobilize a subset of SVs that are dependent on VAMP7 for their exocytosis.

In central synapses, vesicles that reside within the resting pool, which normally do not respond to AP stimulation (Sudhof, 2000) but may contribute to spontaneous neurotransmitter release (Fredj and Burrone, 2009), are enriched in VAMP7 expression (Hua et al., 2011). The selectivity of Reelin action to VAMP7 suggests that sustained increases in baseline Ca^{2+} levels can specifically mobilize these dormant vesicles and augment spontaneous release. Previous studies have demonstrated that intramolecular binding of the N-terminal longin domain of VAMP7 with its SNARE motif can negatively regulate SNARE

complex formation (Pryor et al., 2008). Accordingly, VAMP7-pHluorin lacking the longin domain has an increased rate of spontaneous exocytosis compared to full-length VAMP7 (Hua et al., 2011). Therefore, downstream components of the Reelin-mediated ApoER2 and VLDLR signaling cascade, such as PI3 kinase, may relieve VAMP7 autoinhibition by its longin domain to promote VAMP7-containing vesicles to a fusion competent state. Alternatively, increases in baseline Ca^{2+} levels may act to overcome autoinhibition of VAMP7 to activate VAMP7-mediated neurotransmission. This reaction may be transduced by a high affinity Ca^{2+} sensor, such as Doc2, that may selectively interact with VAMP7 (Groffen et al., 2010; Pang et al., 2011; Yao et al., 2011). However, our loss-of-function analysis failed to show an impairment in the Reelin-mediated increase in spontaneous neurotransmitter release in cells with reduced levels of all four isoforms of the Doc2 protein family (Doc2A, Doc2B, Doc2G, and rabphilin) (Bal et al 2013; Pang et al., 2011). Our results cannot exclude a potential role for an unidentified alternative Ca^{2+} sensor in transducing slow elevations in baseline Ca^{2+} levels to activation of VAMP7-mediated SV fusion. Indeed, earlier experiments performed at the calyx of Held demonstrated that the increase in baseline vesicular release rate induced by modest rises in presynaptic Ca^{2+} (<400 nM) was relatively unaffected by the loss of synaptotagmin2, which is the primary Ca^{2+} sensor for evoked synchronous neurotransmitter release at this synapse (Sun et al., 2007). Therefore, selective association of VAMP7 driven SNARE complexes with an alternative Ca^{2+} sensor may explain the anomalous behavior of VAMP7 tagged SVs that do not effectively respond to individual APs and require strong stimulation for mobilization (Figure 4.5 and see Ramirez et al. 2012). However, most presynaptic terminals are expected to harbor

multiple Ca^{2+} sensors that can mobilize vesicles in response to distinct forms of stimuli. Accordingly, in several preparations elevation of resting Ca^{2+} augments both spontaneous release and evoked responses to single APs (Awatramani et al., 2005) albeit via different signaling pathways (Virmani et al., 2005; Bouhours et al., 2011; Chu et al., 2012). These earlier results can be reconciled with our observations if Reelin-induced Ca^{2+} signals and subsequent mobilization of VAMP7-enriched vesicles are spatially sequestered within individual presynaptic terminals or selectively localized to a subset of synaptic terminals. We cannot currently exclude either of these scenarios, as the Reelin effect may be partly compartmentalized to synapses that are enriched in VAMP7 such as mossy fiber terminals (Scheuber et al., 2006; Hua et al., 2011), which are present in our culture preparation (Kavalali et al., 1999). Furthermore, it also remains possible that a downstream component of Reelin signaling besides Ca^{2+} may act negatively to suppress the elevation of evoked release probability.

These findings provide new insight into regulation of neurotransmitter release by identifying a physiological neuromodulatory cascade that selectively targets syb2-independent neurotransmission. In view of the abundance of syb2 in central presynaptic terminals, the physiological significance of the residual release remaining after genetic deletion of syb2 has remained elusive (Scales et al., 2001; Schoch et al., 2001). The finding that Reelin signaling can act independent of syb2 function to augment neurotransmitter release strongly suggests that the syb2-independent release is functionally significant. The residual spontaneous neurotransmission present in syb2-deficient synapses could not be explained by the expression of the closely related vesicular SNARE cellubrevin (also called

VAMP3) (Schoch et al., 2001; Deak et al., 2006), although it appears to be partially mediated by *vti1a*, an alternative SNARE molecule localized to SVs (Ramirez et al., 2012). However, in this study, we show that *vti1a*-mediated neurotransmission is largely unresponsive to Reelin induced Ca^{2+} signaling, whereas VAMP7 tagged vesicles robustly respond to the same Ca^{2+} signal. These results are consistent with earlier work suggesting the segregation of vesicles containing *vti1a* to a spontaneously recycling pool and those containing VAMP7 to a resting pool (Hua et al., 2011; Ramirez et al., 2012). The molecular specificity of the actions of Reelin on VAMP7-containing vesicles offers a striking contrast to potentiation of neurotransmitter release in response to other secretagogues such as α -latrotoxin, which could elicit release independent of several key release machinery components including SNAP-25 (Deak et al., 2009) or lanthanides that specifically rely on *syb2* to facilitate the rate of neurotransmitter release at rest (Chung et al., 2008).

The action of neuromodulators is critical in shaping the function of neuronal circuits in multiple species (Bargmann, 2012; Marder, 2012). Although several endogenous neuromodulators can modify all forms of neurotransmitter release, some factors can specifically target AP-independent forms of neurotransmission (Sharma and Vijayaraghavan, 2003; Zucker, 2003; Peters et al., 2010; Ramirez and Kavalali, 2011; Vyleta and Smith, 2011). The present findings indicate that the endogenous neuromodulator Reelin may selectively mobilize a subset of SVs by specifically targeting their SNARE machinery. Therefore, we propose that presynaptic vesicular SNARE heterogeneity forms a molecular substrate for selective neuromodulation and enables regulation of neuronal output without alterations in AP-dependent information processing. Such segregation of AP-dependent and

AP-independent presynaptic regulatory mechanisms may be particularly significant in circumstances where evoked release probability is low (Borst, 2010) and the two types of synaptic signals are difficult to differentiate. Under these circumstances, selective augmentation of spontaneous neurotransmitter release may facilitate neurotrophic, homeostatic or other signaling functions of released neurotransmitter substances without compromising their function in AP-evoked information transfer. Recent studies suggest that the AP-independent forms of neurotransmitter release are critical in the regulation of behavioral outcomes such as nociception, memory processing and response to antidepressants (Autry et al., 2011; Andresen et al., 2012; Jin et al., 2012; Kavalali and Monteggia, 2012; Xu et al., 2012). This premise is consistent with the recent behavioral analysis of VAMP7 knockout mice which revealed a deficit in anxiety-related behaviors (Danglot et al., 2012). In this way, identification of the vesicular release machineries and neuromodulators that specifically modify AP-independent forms of neurotransmission may provide novel avenues to manipulate neurotransmission without altering AP-dependent information processing. These types of approaches provide a promising strategy to uncover the functional roles of these unconventional forms of neuronal communication in the regulation of behavior in normal as well as in disease states.

CHAPTER FIVE

Conclusions and Future Directions

Calcium controls the rate of endocytosis at the single-vesicle level

The data presented here reconciles several previous reports of the kinetics of single-vesicle endocytosis and provides the first optical characterization of the endocytosis of vesicles at rest. This work highlights major kinetic distinctions between stimulation-evoked and spontaneous neurotransmission.

While it is difficult to precisely separate synaptic vesicle endocytosis from reacidification in this optical preparation, one might consider fast kiss-and-run exo-/endocytosis as the population of fusion events that do not manifest a significant fluorescence dwell time. If this interpretation is correct, then fast kiss-and-run-like fusion seems to predominate in low extracellular Ca^{2+} conditions, in synapses that have an intrinsic low release probability and in spontaneous synaptic vesicle fusion. Spontaneous synaptic vesicle fusion seems to occur almost exclusively through a kiss-and-run mechanism. However, there is substantial evidence that vesicles recycling at rest are still capable of taking up large probes such as antibodies. These contradicting lines of evidence may suggest that the fusion pore size is quite dynamic and that rapid endocytosis may still proceed even when the fusion pore is large. In contrast to kiss-and-run fusion, full-collapse fusion becomes more prevalent as stimulation frequency increases, Ca^{2+} concentration increases, as the exocytic load increases, and it is more common in synapses with a higher intrinsic release probabilities.

Together, these observations account for several seemingly disparate findings in the literature.

The work presented here can be used to reconcile previous work that has reported in three (Gandhi and Stevens, 2003), two (Zhu et al., 2009) and one (Balaji and Ryan, 2007) kinetic processes of endocytosis. We can almost exactly reproduce all of the above endocytic kinetics and reconcile the findings as either multiple vesicles fusing (Zhu et al., 2009) or as a bias introduced by selecting only high fusion probability synapses (Balaji and Ryan, 2007) (with the exception of the “stranded” phase of endocytosis observed in Gandhi and Stevens (2003), which we attribute to loss of probe to the cell surface, as it is only thus far reported with sypH). We also show that the rate of reacidification is subject to regulation and it is antagonized by calcineurin activity. Together with the findings that intrinsic release probability sets endocytosis rate, these data agree with and expand on previous work proposing reacidification time as a synapse-dependent property (Gandhi and Stevens, 2003; Granseth et al., 2006).

Our data is also consistent with earlier data that implicates the exocytic load of vesicles as a modulator of the kinetics of endocytosis. When analyzing the fusion of multiple vesicles, we find that the rate of decay of the second event is slower than that of the first. We can also reconcile these earlier studies that concluded that the rate of endocytosis was Ca^{2+} -independent. While we have shown that Ca^{2+} absolutely controls the rate of endocytosis, we also note that there may be a limit to how slow endocytosis can proceed. During 1 Hz stimulation, the endocytosis of each proceeding vesicle fusion event slows, but at high extracellular Ca^{2+} concentrations, the relative deceleration is less than at low extracellular

Ca^{2+} concentrations. Therefore, during intense stimulation, like those used in early experiments, the rate of endocytosis might approach this limit and appear to be constant and relatively slow.

Although our data can reconcile several previous findings, an outstanding question remains: why does endocytosis slow during stimulation? One possibility is that specific release sites competent for one form of fusion over the other are overcome during intense stimulations. Another possibility is that vesicle endocytosis is arrested in preparation for a single massive retrieval of components that could be internalized and redistributed without interfering with ongoing stimulation. Evidence for the first possibility is already present in experiments using 3D microscopy (Zhang et al., 2007). To address the second possibility, one could systematically increase stimulation strength (either by increasing stimulation frequency or extracellular Ca^{2+} concentrations, and thus Ca^{2+} influx) and model the results at the level of the single vesicle similar to what was performed in work described here (Leitz and Kavalali, 2011). This modeling approach does become significantly challenging during intense stimulation as exocytosis and endocytosis increasingly overlap. But during short high frequency stimulations, it may be possible to examine how slow endocytosis becomes and test if some threshold of stimulation triggers an acceleration (a la Klingauf et al., 1999) in endocytosis or a larger single step in endocytosis (bulk endocytosis).

Retrieval of stimulation-evoked vs. spontaneous synaptic vesicles

Our data here highlight a major regulatory difference between vesicles that fuse in response to stimulation and those that fuse spontaneously. While the retrieval of vesicles that

fuse during stimulation is subject to Ca^{2+} regulation, vesicles that fuse spontaneously predominantly use an exceedingly fast kiss-and-run form of fusion that is relatively Ca^{2+} -independent. This divergent kinetic regulation could be explained by previously observed differences in molecular mechanisms of endocytosis between these forms of fusion.

Although the exact mechanism by which calcineurin alters endocytosis is not known, it is likely achieved through action on a variety of proteins (reviewed in Saheki and De Camilli, 2012). One such protein, dynamin is required for stimulation-evoked synaptic vesicle recycling but not recycling of spontaneously fusing vesicles (Chung et al., 2010). It may be interesting to examine if dynamin is a requirement for the endocytosis of all evoked neurotransmission, or if it is only required for endocytosis after full-collapse fusion. If dynamin is involved in the recycling of all evoked fusion neurotransmission, then only stepwise increases in fluorescence will be observed. However, if dynamin is only required for endocytosis after full-collapse fusion, then during stimulation increases in fluorescence should follow one of two waveforms, rapid decay without any dwell time, and step-wise increases in fluorescence due to vesicles that cannot pinch off of the terminal membrane.

We found that vesicles that recycle spontaneously are reacidified much faster than those that recycle during stimulation. Furthermore, reacidification could only be modulated in vesicles that fuse during stimulation. This could be explained by an inherent difference in the synaptic vesicles that recycle spontaneously, the process of fast kiss-and-run fusion, or the relatively low Ca^{2+} influx during spontaneous neurotransmission. If the above dynamin inhibition experiment does suppress only full-collapse fusion, while still permitting fast kiss-and-run fusion, comparing distributions of fluorescence decay times as a function of

extracellular Ca^{2+} between spontaneously recycling vesicles and kiss-and-run vesicles would determine if the relative Ca^{2+} insensitive of fluorescence decay observed during spontaneous vesicle fusion is a property of the vesicles that fuse spontaneously or of the kiss-and-run fusion process itself. To determine if the divergent reacidification times are do to low Ca^{2+} influx, resting cytosolic Ca^{2+} concentrations could be increased through release of internal Ca^{2+} stores. Alternatively, we have shown that reelin acts on internal Ca^{2+} stores to also increase spontaneous neurotransmission (Bal et al., 2013), fluorescence decay times in the presence of reelin might also be augmented. Finally, simply analyzing fluorescence decay times as a function of increasing Ca^{2+} in heavily buffered extracellular solutions (i.e. 50 mM Tris) may also uncover a subtle Ca^{2+} -dependence of reacidification.

While there is no prior direct evidence for such a modulation of reacidification rate, it is not entirely surprising given the vATPase can be activated or inhibited by a variety of cytosolic factors (Forgac, 2007), some of which are Ca^{2+} -sensitive (i.e. calmodulin). Slowing of synaptic vesicle reacidification could be a mechanism to limit neurotransmission during strong stimulations. But another intriguing possibility posits the v-ATPase can directly participate in membrane fusion by interacting with terminal SNARE proteins (Peters et al., 2001; Hiesinger et al., 2005; Poea-Guyon et al., 2013) and it was recently shown that this participation is regulated in a Ca^{2+} -Calmodulin-dependent manner (Wang et al., 2014). In rat hippocampal cultures, specific inactivation of only the V0 subunit of the vATPase using chromaphore-assisted light inactivation (CALI) impaired evoked neurotransmission (Poea-Guyon et al., 2013). A current model places the vATPase as a sensor of vesicle pH where the V1 subunit associates with the vesicle during reacidification and is primarily

dissociated once the vesicle is filled which permits vATPase-based fusion. Interpreting our data in light of this model is difficult, one possibility is that stimulation-evoked fusion is more susceptible to vATPase-based fusion which leads to fewer associated V1 subunits and thus the observed slower rate of reacidification. While this provides a rationale for divergent reacidification rates, it is difficult to reconcile the observed acceleration of reacidification during calcineurin inhibition given this fusion is promoted by Calmodulin which is upstream of calcineurin activation.

Another potential endocytic regulatory target is the vesicle Ca^{2+} sensor syt1. Syt1 is known to play a role in synaptic vesicle endocytosis. Although the precise mechanism of how syt1 regulates endocytosis is unknown, Ca^{2+} itself may be directly involved as early experiments that substitute Sr^{2+} or Ba^{2+} still evoke synaptic vesicle fusion, but endocytosis is severely attenuated. Syt1 can interact with AP2 to recruit clathrin (Artalejo et al., 1995, 1996), but given syt1-deficient cells have enhanced spontaneous neurotransmission, it is possible that endogenous spontaneous vesicle fusion may not utilize syt1.

Finally, synaptic vesicle size could play a passive role in determining vesicle endocytosis mode and could partially account for the variation in vesicle reacidification times we observe. Data from *in vitro* lipid binding assays are consistent with smaller vesicles being more fusogenic (Haque et al., 2001). Furthermore, membrane curvature of smaller vesicles may promote kiss-and-run fusion by producing an energy barrier to full-collapse into the terminal membrane. Although whether synaptic vesicle size correlates with fusion dynamics *in situ* or *in vivo* has yet to be seen and it is possible that the SNARE complex machinery may render small variations in vesicle size irrelevant. Regardless, given synaptic

vesicle radius can vary by ~10%, and volume can vary by a cube of the radius, this could amount to a significant difference in the buffering capability of the vesicle lumen. But how synaptic vesicles might determine and maintain such small size variations during synthesis and maturation is a significant conceptual hurdle. And detailed quantification of synaptic vesicle size could be difficult due to this ultimately small variation in size. To address this possibility, however, one could perform correlative super-resolution imaging of synaptic vesicle markers and high resolution transmission electron microscopy. Similar experiments have been employed to characterize the quantity, variety, and spatial distribution of endocytic proteins in PC12 cells (Sochacki et al., 2014). A simple experiment might be to isolate synaptic vesicles, fluorescently identify vesicles that would predominantly traffic at rest (for instance vti1a- or VAMP7-containing vesicles) and measure vesicle diameter using transmission electron microscopy.

A molecular definition of vesicle pools

Accumulating data, including work here (Bal et al., 2013), supports the hypothesis that there is a molecular heterogeneity among synaptic vesicles that is functionally instructive. But there is substantial evidence that supports the contrasting hypothesis that vesicles that fuse spontaneously are derived from the same pool as vesicles that fuse during stimulation. A parsimonious explanation is that the spontaneous synaptic vesicle pool can be subdivided into several molecularly distinct pools. One subdivision might be according to the Ca^{2+} -sensors used in these processes (which are discussed in chapter 1). The work presented here shows that endocytosis during spontaneous transmission is fundamentally

different in its Ca^{2+} -sensitivity than retrieval during stimulation. But the functional overlap of syt1 and Doc2 family proteins (discussed in chapter 1) will require further research to improve our understanding of the role of these Ca^{2+} sensors in exo-/endocytosis before clear distinctions between vesicle pools can be made.

In addition to triggering fusion, Ca^{2+} might also alter synaptic vesicle trafficking through slower Ca^{2+} -dependent processes downstream of initial influx. For example, it was recently shown in drosophila that formation of a SNARE complex involving the V0a1 subunit of the vATPase is Ca^{2+} -calmodulin dependent (Wang et al., 2014). Embryonic neuromuscular junctions lacking V0a1 have an increased evoked transmission failure rate and reduced excitatory junction currents that rapidly depress upon further stimulation. Moreover, these null mutants have >90% reduction in the frequency of spontaneous miniature excitatory junction currents. Expression of a Ca^{2+} -calmodulin binding-deficient V0 mutant on this null background can rescue the evoked transmission failure rate and ameliorate the excitatory junction current depression during stimulation, but cannot rescue the reduction in frequency of miniature excitatory junction currents (Wang et al., 2014). These data suggest that the calmodulin interaction with V0a1 is required specifically for maintaining neurotransmission. Thus, once Ca^{2+} enters the synaptic terminal, it can act on calmodulin to alter the availability of fusion-competent vesicles rather than directly facilitating fusion. Reelin may operate in an analogous fashion to facilitate spontaneous neurotransmission given that VAMP7 contains an autoinhibitory domain, that when phosphorylated leads to increased exocytosis in COS-7 and hippocampal cells (Burgo et al., 2013). In this case, spontaneous neurotransmission may not be promoted per se, but the

increase in availability of releaseable vesicles results in an increased fusion rate. Thus neurons may be able to modulate different forms of neurotransmission by increasing or decreasing the population of fusion competent vesicles downstream of immediate Ca^{2+} influx.

Indeed, a strong potential molecular definition of vesicle pools might focus on the vSNARE composition of vesicles. VAMP4-containing synaptic vesicles preferentially partake in asynchronous neurotransmission (Raingo et al., 2012) Vti1a seems to be responsible for the high frequency component of spontaneous transmission at rest (Ramirez et al., 2012). VAMP7 specifically targets to vesicles in the resting pool (Hua et al., 2011), but are mobilized in response to presynaptic reelin signaling to enhance spontaneous neurotransmission (presented here Bal et al., 2013). But syb2- containing synaptic vesicles also spontaneously fuse and genetic deletion of syb2 reduces spontaneous transmission in addition to evoked transmission (albeit to different severities). So just how molecularly distinct are synaptic vesicles? One way to directly address this question would be to isolate synaptic vesicles according to SNARE protein composition followed by comparative proteomic analysis. Such an analysis was recently performed to compare glutamatergic and GABAergic enriched synaptic vesicle populations from single rat brains (Gronborg et al., 2010). Comparison revealed that while many proteins were shared among the vesicle populations, some proteins were preferentially found in one of the two populations, including one membrane protein of unknown neuronal function, MAL2 (also called T-cell differentiating protein 2). Applying this technique to different vSNARE populations of

vesicles could significantly advance our understanding synaptic vesicle populations and may implicate as-of-yet uninvolved proteins in the process of spontaneous neurotransmission.

Spontaneous noise and spontaneous signaling

Is all spontaneous neurotransmission relevant to signaling? Homeostatic synaptic plasticity is induced by blocking neurotransmission at rest, but this inhibition is broad in terms of which synaptic vesicles are blocked. Does spontaneous neurotransmission encode information through frequency of neurotransmitter release or through spatial location of release? And do vSNAREs determine either of these properties?

Single-synapse electrophysiological recordings show that spontaneous vesicle fusion rate is not a random Poisson process due to a bursting component of release. This bursting component is the rapid release of 2-7 vesicles within 400 ms, and it is sensitive to bulk increases in Ca^{2+} but independent of Ca^{2+} influx (Abenavoli et al., 2002). Vti1a could be a molecular correlate for this bursting process as vti1a-deficient neurons have a decrease only in a high frequency component of spontaneous neurotransmission. The fluorescence amplitude distributions of spontaneous fusion events shown here also support these findings. This frequency-dependent bursting process is dynamic and open to regulation through changes in intracellular Ca^{2+} and therefore, could be a mechanism by which neurons encode information at rest. However, vti1a knockdown alone does not produce homeostatic synaptic plasticity. VAMP7-containing synaptic vesicles also cycle at rest (Hua et al., 2011), therefore it is possible that VAMP7 and vti1a have redundant roles in spontaneous

neurotransmission. It would be interesting to probe the effect of both *vtil1a* and VAMP7 double knockdown in synaptic scaling.

Information could also be encoded by spatial location of neurotransmitter release. Previous data that spontaneous and evoked neurotransmission activate non-overlapping populations of receptors is a strong indication that information is encoded spatially (Atasoy et al., 2008). Recent advances in super-resolution microscopy could be employed to directly assess the spatial distribution of vSNARE trafficking. Stimulated emission depletion (STED) microscopy is a promising technique that might allow diffraction-unlimited spatial resolution in live cells with high temporal resolution. Dual-color experiments in this system could identify the relative spatial location of fusion between different vSNARE-containing vesicles. Imaging of Ca^{2+} indicators in the postsynaptic terminal using super resolution techniques might also corroborate the observation of non-overlapping receptor populations for evoked and spontaneous neurotransmission.

BIBLIOGRAPHY

Abenavoli, A., Forti, L., Bossi, M., Bergamaschi, A., Villa, A., and Malgaroli, A. (2002). Multimodal quantal release at individual hippocampal synapses: evidence for no lateral inhibition. *J Neurosci* 22, 6336-6346.

Akerboom, J., Chen, T.W., Wardill, T.J., Tian, L., Marvin, J.S., Mutlu, S., Calderon, N.C., Esposti, F., Borghuis, B.G., Sun, X.R., *et al.* (2012). Optimization of a GCaMP calcium indicator for neural activity imaging. *J Neurosci* 32, 13819-13840.

Alabi, A.A., and Tsien, R.W. (2012). Synaptic vesicle pools and dynamics. *Cold Spring Harbor perspectives in biology* 4, a013680.

Alabi, A.A., and Tsien, R.W. (2013). Perspectives on kiss-and-run: role in exocytosis, endocytosis, and neurotransmission. *Annual review of physiology* 75, 393-422.

Alcantara, S., Ruiz, M., D'Arcangelo, G., Ezan, F., de Lecea, L., Curran, T., Sotelo, C., and Soriano, E. (1998). Regional and cellular patterns of reelin mRNA expression in the forebrain of the developing and adult mouse. *J Neurosci* 18, 7779-7799.

Ales, E., Tabares, L., Poyato, J.M., Valero, V., Lindau, M., and Alvarez de Toledo, G. (1999). High calcium concentrations shift the mode of exocytosis to the kiss-and-run mechanism. *Nature cell biology* 1, 40-44.

Almers, W., and Neher, E. (1987). Gradual and stepwise changes in the membrane capacitance of rat peritoneal mast cells. *The Journal of physiology* 386, 205-217.

Andreae, L.C., Fredj, N.B., and Burrone, J. (2012). Independent vesicle pools underlie different modes of release during neuronal development. *J Neurosci* 32, 1867-1874.

Andresen, M.C., Hofmann, M.E., and Fawley, J.A. (2012). Invited Review: The un-silent majority - TRPV1 drives "spontaneous" transmission of unmyelinated primary afferents within cardiorespiratory NTS. *American journal of physiology*.

Aravanis, A.M., Pyle, J.L., and Tsien, R.W. (2003). Single synaptic vesicles fusing transiently and successively without loss of identity. *Nature* 423, 643-647.

Armbruster, M., Messa, M., Ferguson, S.M., De Camilli, P., and Ryan, T.A. (2013). Dynamin phosphorylation controls optimization of endocytosis for brief action potential bursts. *eLife* 2, e00845.

- Armbruster, M., and Ryan, T.A. (2011). Synaptic vesicle retrieval time is a cell-wide rather than individual-synapse property. *Nature neuroscience* *14*, 824-826.
- Artalejo, C.R., Elhamdani, A., and Palfrey, H.C. (1996). Calmodulin is the divalent cation receptor for rapid endocytosis, but not exocytosis, in adrenal chromaffin cells. *Neuron* *16*, 195-205.
- Artalejo, C.R., Henley, J.R., McNiven, M.A., and Palfrey, H.C. (1995). Rapid endocytosis coupled to exocytosis in adrenal chromaffin cells involves Ca²⁺, GTP, and dynamin but not clathrin. *Proceedings of the National Academy of Sciences of the United States of America* *92*, 8328-8332.
- Atasoy, D., Ertunc, M., Moulder, K.L., Blackwell, J., Chung, C., Su, J., and Kavalali, E.T. (2008). Spontaneous and evoked glutamate release activates two populations of NMDA receptors with limited overlap. *J Neurosci* *28*, 10151-10166.
- Autry, A.E., Adachi, M., Nosyreva, E., Na, E.S., Los, M.F., Cheng, P.F., Kavalali, E.T., and Monteggia, L.M. (2011). NMDA receptor blockade at rest triggers rapid behavioural antidepressant responses. *Nature* *475*, 91-95.
- Awatramani, G.B., Turecek, R., and Trussell, L.O. (2005). Staggered development of GABAergic and glycinergic transmission in the MNTB. *Journal of neurophysiology* *93*, 819-828.
- Bal, M., Leitz, J., Reese, A.L., Ramirez, D.M., Durakoglugil, M., Herz, J., Monteggia, L.M., and Kavalali, E.T. (2013). Reelin mobilizes a VAMP7-dependent synaptic vesicle pool and selectively augments spontaneous neurotransmission. *Neuron* *80*, 934-946.
- Balaji, J., and Ryan, T.A. (2007). Single-vesicle imaging reveals that synaptic vesicle exocytosis and endocytosis are coupled by a single stochastic mode. *Proceedings of the National Academy of Sciences of the United States of America* *104*, 20576-20581.
- Bargmann, C.I. (2012). Beyond the connectome: how neuromodulators shape neural circuits. *Bioessays* *34*, 458-465.
- Barrett, E.F., and Stevens, C.F. (1972). The kinetics of transmitter release at the frog neuromuscular junction. *The Journal of physiology* *227*, 691-708.
- Beffert, U., Weeber, E.J., Durudas, A., Qiu, S., Masiulis, I., Sweatt, J.D., Li, W.P., Adelmann, G., Frotscher, M., Hammer, R.E., *et al.* (2005). Modulation of synaptic plasticity and memory by Reelin involves differential splicing of the lipoprotein receptor Apoer2. *Neuron* *47*, 567-579.

- Betz, W.J., and Bewick, G.S. (1992). Optical analysis of synaptic vesicle recycling at the frog neuromuscular junction. *Science (New York, NY)* 255, 200-203.
- Borst, J.G. (2010). The low synaptic release probability in vivo. *Trends in neurosciences* 33, 259-266.
- Bouhours, B., Trigo, F.F., and Marty, A. (2011). Somatic depolarization enhances GABA release in cerebellar interneurons via a calcium/protein kinase C pathway. *J Neurosci* 31, 5804-5815.
- Boyd, I.A., and Martin, A.R. (1956). The end-plate potential in mammalian muscle. *The Journal of physiology* 132, 74-91.
- Bronk, P., Deak, F., Wilson, M.C., Liu, X., Sudhof, T.C., and Kavalali, E.T. (2007). Differential effects of SNAP-25 deletion on Ca²⁺-dependent and Ca²⁺-independent neurotransmission. *Journal of neurophysiology* 98, 794-806.
- Brose, N., Hofmann, K., Hata, Y., and Sudhof, T.C. (1995). Mammalian homologues of *Caenorhabditis elegans* unc-13 gene define novel family of C2-domain proteins. *The Journal of biological chemistry* 270, 25273-25280.
- Burgo, A., Casano, A.M., Kuster, A., Arold, S.T., Wang, G., Nola, S., Verraes, A., Dingli, F., Loew, D., and Galli, T. (2013). Increased activity of the vesicular soluble N-ethylmaleimide-sensitive factor attachment protein receptor TI-VAMP/VAMP7 by tyrosine phosphorylation in the Longin domain. *The Journal of biological chemistry* 288, 11960-11972.
- Burgoyne, R.D. (1995). Fast exocytosis and endocytosis triggered by depolarisation in single adrenal chromaffin cells before rapid Ca²⁺ current run-down. *Pflugers Arch* 430, 213-219.
- Ceccarelli, B., Grohovaz, F., and Hurlbut, W.P. (1979). Freeze-fracture studies of frog neuromuscular junctions during intense release of neurotransmitter. I. Effects of black widow spider venom and Ca²⁺-free solutions on the structure of the active zone. *The Journal of cell biology* 81, 163-177.
- Ceccarelli, B., Hurlbut, W.P., and Mauro, A. (1972). Depletion of vesicles from frog neuromuscular junctions by prolonged tetanic stimulation. *The Journal of cell biology* 54, 30-38.
- Ceccarelli, B., Hurlbut, W.P., and Mauro, A. (1973). Turnover of transmitter and synaptic vesicles at the frog neuromuscular junction. *The Journal of cell biology* 57, 499-524.

- Chen, Y., Beffert, U., Ertunc, M., Tang, T.S., Kavalali, E.T., Bezprozvanny, I., and Herz, J. (2005). Reelin modulates NMDA receptor activity in cortical neurons. *J Neurosci* 25, 8209-8216.
- Cherki-Vakil, R., Ginsburg, S., and Meiri, H. (1995). The difference in shape of spontaneous and unquantal evoked synaptic potentials in frog muscle. *The Journal of physiology* 482 (Pt 3), 641-650.
- Chu, Y., Fioravante, D., Thanawala, M., Leitges, M., and Regehr, W.G. (2012). Calcium-dependent isoforms of protein kinase C mediate glycine-induced synaptic enhancement at the calyx of Held. *J Neurosci* 32, 13796-13804.
- Chung, C., Barylko, B., Leitz, J., Liu, X., and Kavalali, E.T. (2010). Acute dynamin inhibition dissects synaptic vesicle recycling pathways that drive spontaneous and evoked neurotransmission. *J Neurosci* 30, 1363-1376.
- Chung, C., Deak, F., and Kavalali, E.T. (2008). Molecular substrates mediating lanthanide-evoked neurotransmitter release in central synapses. *Journal of neurophysiology* 100, 2089-2100.
- Cousin, M.A., and Robinson, P.J. (2000). Ca²⁺ influx inhibits dynamin and arrests synaptic vesicle endocytosis at the active zone. *J Neurosci* 20, 949-957.
- D'Arcangelo, G., Miao, G.G., Chen, S.C., Soares, H.D., Morgan, J.I., and Curran, T. (1995). A protein related to extracellular matrix proteins deleted in the mouse mutant reeler. *Nature* 374, 719-723.
- Danglot, L., Zylbersztein, K., Petkovic, M., Gauberti, M., Meziane, H., Combe, R., Champy, M.F., Birling, M.C., Pavlovic, G., Bizot, J.C., *et al.* (2012). Absence of TI-VAMP/Vamp7 leads to increased anxiety in mice. *J Neurosci* 32, 1962-1968.
- Deak, F., Liu, X., Khvotchev, M., Li, G., Kavalali, E.T., Sugita, S., and Sudhof, T.C. (2009). Alpha-latrotoxin stimulates a novel pathway of Ca²⁺-dependent synaptic exocytosis independent of the classical synaptic fusion machinery. *J Neurosci* 29, 8639-8648.
- Deak, F., Shin, O.H., Kavalali, E.T., and Sudhof, T.C. (2006). Structural determinants of synaptobrevin 2 function in synaptic vesicle fusion. *J Neurosci* 26, 6668-6676.
- Del Castillo, J., and Katz, B. (1954). Quantal components of the end-plate potential. *The Journal of physiology* 124, 560-573.

- Dittman, J.S., and Regehr, W.G. (1996). Contributions of calcium-dependent and calcium-independent mechanisms to presynaptic inhibition at a cerebellar synapse. *J Neurosci* *16*, 1623-1633.
- Eliasson, L., Proks, P., Ammala, C., Ashcroft, F.M., Bokvist, K., Renstrom, E., Rorsman, P., and Smith, P.A. (1996). Endocytosis of secretory granules in mouse pancreatic beta-cells evoked by transient elevation of cytosolic calcium. *The Journal of physiology* *493* (Pt 3), 755-767.
- Engisch, K.L., and Nowycky, M.C. (1998). Compensatory and excess retrieval: two types of endocytosis following single step depolarizations in bovine adrenal chromaffin cells. *The Journal of physiology* *506* (Pt 3), 591-608.
- Ermolyuk, Y.S., Alder, F.G., Surges, R., Pavlov, I.Y., Timofeeva, Y., Kullmann, D.M., and Volynski, K.E. (2013). Differential triggering of spontaneous glutamate release by P/Q-, N- and R-type Ca²⁺ channels. *Nature neuroscience* *16*, 1754-1763.
- Ertunc, M., Sara, Y., Chung, C., Atasoy, D., Virmani, T., and Kavalali, E.T. (2007). Fast synaptic vesicle reuse slows the rate of synaptic depression in the CA1 region of hippocampus. *J Neurosci* *27*, 341-354.
- Fatt, P., and Katz, B. (1952). Spontaneous subthreshold activity at motor nerve endings. *The Journal of physiology* *117*, 109-128.
- Fernandez-Chacon, R., Konigstorfer, A., Gerber, S.H., Garcia, J., Matos, M.F., Stevens, C.F., Brose, N., Rizo, J., Rosenmund, C., and Sudhof, T.C. (2001). Synaptotagmin I functions as a calcium regulator of release probability. *Nature* *410*, 41-49.
- Forgac, M. (2007). Vacuolar ATPases: rotary proton pumps in physiology and pathophysiology. *Nat Rev Mol Cell Biol* *8*, 917-929.
- Fredj, N.B., and Burrone, J. (2009). A resting pool of vesicles is responsible for spontaneous vesicle fusion at the synapse. *Nature neuroscience* *12*, 751-758.
- Frerking, M., Borges, S., and Wilson, M. (1997). Are some minis multiquantal? *Journal of neurophysiology* *78*, 1293-1304.
- Gad, H., Low, P., Zotova, E., Brodin, L., and Shupliakov, O. (1998). Dissociation between Ca²⁺-triggered synaptic vesicle exocytosis and clathrin-mediated endocytosis at a central synapse. *Neuron* *21*, 607-616.
- Gandhi, S.P., and Stevens, C.F. (2003). Three modes of synaptic vesicular recycling revealed by single-vesicle imaging. *Nature* *423*, 607-613.

Goda, Y., and Stevens, C.F. (1994). Two components of transmitter release at a central synapse. *Proceedings of the National Academy of Sciences of the United States of America* *91*, 12942-12946.

Gracheva, E.O., Hadwiger, G., Nonet, M.L., and Richmond, J.E. (2008). Direct interactions between *C. elegans* RAB-3 and Rim provide a mechanism to target vesicles to the presynaptic density. *Neuroscience letters* *444*, 137-142.

Granseth, B., Odermatt, B., Royle, S.J., and Lagnado, L. (2006). Clathrin-mediated endocytosis is the dominant mechanism of vesicle retrieval at hippocampal synapses. *Neuron* *51*, 773-786.

Groffen, A.J., Martens, S., Diez Arazola, R., Cornelisse, L.N., Lozovaya, N., de Jong, A.P., Goriounova, N.A., Habets, R.L., Takai, Y., Borst, J.G., *et al.* (2010). Doc2b is a high-affinity Ca²⁺ sensor for spontaneous neurotransmitter release. *Science (New York, NY)* *327*, 1614-1618.

Gronborg, M., Pavlos, N.J., Brunk, I., Chua, J.J., Munster-Wandowski, A., Riedel, D., Ahnert-Hilger, G., Urlaub, H., and Jahn, R. (2010). Quantitative comparison of glutamatergic and GABAergic synaptic vesicles unveils selectivity for few proteins including MAL2, a novel synaptic vesicle protein. *J Neurosci* *30*, 2-12.

Haque, M.E., McIntosh, T.J., and Lentz, B.R. (2001). Influence of lipid composition on physical properties and peg-mediated fusion of curved and uncurved model membrane vesicles: "nature's own" fusogenic lipid bilayer. *Biochemistry* *40*, 4340-4348.

Harata, N., Pyle, J.L., Aravanis, A.M., Mozhayeva, M., Kavalali, E.T., and Tsien, R.W. (2001). Limited numbers of recycling vesicles in small CNS nerve terminals: implications for neural signaling and vesicular cycling. *Trends in neurosciences* *24*, 637-643.

Hawkins, R.D. (2013). Possible contributions of a novel form of synaptic plasticity in *Aplysia* to reward, memory, and their dysfunctions in mammalian brain. *Learning & memory (Cold Spring Harbor, NY)* *20*, 580-591.

Heinemann, C., Chow, R.H., Neher, E., and Zucker, R.S. (1994). Kinetics of the secretory response in bovine chromaffin cells following flash photolysis of caged Ca²⁺. *Biophysical journal* *67*, 2546-2557.

Hellwig, S., Hack, I., Kowalski, J., Brunne, B., Jarowyj, J., Unger, A., Bock, H.H., Junghans, D., and Frotscher, M. (2011). Role for Reelin in neurotransmitter release. *The Journal of neuroscience : the official journal of the Society for Neuroscience* *31*, 2352-2360.

- Herz, J., and Chen, Y. (2006). Reelin, lipoprotein receptors and synaptic plasticity. *Nature reviews* 7, 850-859.
- Heuser, J.E., and Reese, T.S. (1973). Evidence for recycling of synaptic vesicle membrane during transmitter release at the frog neuromuscular junction. *The Journal of cell biology* 57, 315-344.
- Heuser, J.E., and Reese, T.S. (1981). Structural changes after transmitter release at the frog neuromuscular junction. *The Journal of cell biology* 88, 564-580.
- Hiesberger, T., Trommsdorff, M., Howell, B.W., Goffinet, A., Mumby, M.C., Cooper, J.A., and Herz, J. (1999). Direct binding of Reelin to VLDL receptor and ApoE receptor 2 induces tyrosine phosphorylation of disabled-1 and modulates tau phosphorylation. *Neuron* 24, 481-489.
- Hiesinger, P.R., Fayyazuddin, A., Mehta, S.Q., Rosenmund, T., Schulze, K.L., Zhai, R.G., Verstreken, P., Cao, Y., Zhou, Y., Kunz, J., *et al.* (2005). The v-ATPase V0 subunit a1 is required for a late step in synaptic vesicle exocytosis in *Drosophila*. *Cell* 121, 607-620.
- Hosoi, N., Holt, M., and Sakaba, T. (2009). Calcium dependence of exo- and endocytotic coupling at a glutamatergic synapse. *Neuron* 63, 216-229.
- Hua, Z., Leal-Ortiz, S., Foss, S.M., Waites, C.L., Garner, C.C., Voglmaier, S.M., and Edwards, R.H. (2011). v-SNARE composition distinguishes synaptic vesicle pools. *Neuron* 71, 474-487.
- Hubel, D.H. (1959). Single unit activity in striate cortex of unrestrained cats. *The Journal of physiology* 147, 226-238.
- Hurlbut, W.P., and Ceccarelli, B. (1974). Transmitter release and recycling of synaptic vesicle membrane at the neuromuscular junction. *Advances in cytopharmacology* 2, 141-154.
- Jahn, R., Lang, T., and Sudhof, T.C. (2003). Membrane fusion. *Cell* 112, 519-533.
- Jin, I., Puthanveetil, S., Udo, H., Karl, K., Kandel, E.R., and Hawkins, R.D. (2012). Spontaneous transmitter release is critical for the induction of long-term and intermediate-term facilitation in *Aplysia*. *Proceedings of the National Academy of Sciences of the United States of America* 109, 9131-9136.
- Kavalali, E.T. (2007). Multiple vesicle recycling pathways in central synapses and their impact on neurotransmission. *The Journal of physiology* 585, 669-679.

- Kavalali, E.T., Chung, C., Khvotchev, M., Leitz, J., Nosyreva, E., Raingo, J., and Ramirez, D.M. (2011). Spontaneous neurotransmission: an independent pathway for neuronal signaling? *Physiology (Bethesda, Md)* 26, 45-53.
- Kavalali, E.T., and Jorgensen, E.M. (2014). Visualizing presynaptic function. *Nat Neurosci* 17, 10-16.
- Kavalali, E.T., Klingauf, J., and Tsien, R.W. (1999). Activity-dependent regulation of synaptic clustering in a hippocampal culture system. *Proceedings of the National Academy of Sciences of the United States of America* 96, 12893-12900.
- Kavalali, E.T., and Monteggia, L.M. (2012). Synaptic Mechanisms Underlying Rapid Antidepressant Action of Ketamine. *The American journal of psychiatry*.
- Klingauf, J., Kavalali, E.T., and Tsien, R.W. (1998). Kinetics and regulation of fast endocytosis at hippocampal synapses. *Nature* 394, 581-585.
- Knuesel, I. (2010). Reelin-mediated signaling in neuropsychiatric and neurodegenerative diseases. *Progress in neurobiology* 91, 257-274.
- Kubo, K., Mikoshiba, K., and Nakajima, K. (2002). Secreted Reelin molecules form homodimers. *Neuroscience research* 43, 381-388.
- Kuo, G., Arnaud, L., Kronstad-O'Brien, P., and Cooper, J.A. (2005). Absence of Fyn and Src causes a reeler-like phenotype. *The Journal of neuroscience : the official journal of the Society for Neuroscience* 25, 8578-8586.
- Kwon, S.E., and Chapman, E.R. (2011). Synaptophysin regulates the kinetics of synaptic vesicle endocytosis in central neurons. *Neuron* 70, 847-854.
- Leitz, J., and Kavalali, E.T. (2011). Ca²⁺(+) influx slows single synaptic vesicle endocytosis. *J Neurosci* 31, 16318-16326.
- Li, Y., and Tsien, R.W. (2012). pHTomato, a red, genetically encoded indicator that enables multiplex interrogation of synaptic activity. *Nature neuroscience* 15, 1047-1053.
- Lou, X., Scheuss, V., and Schneggenburger, R. (2005). Allosteric modulation of the presynaptic Ca²⁺ sensor for vesicle fusion. *Nature* 435, 497-501.
- Marder, E. (2012). Neuromodulation of neuronal circuits: back to the future. *Neuron* 76, 1-11.
- Marks, B., and McMahon, H.T. (1998). Calcium triggers calcineurin-dependent synaptic vesicle recycling in mammalian nerve terminals. *Curr Biol* 8, 740-749.

- Maximov, A., Tang, J., Yang, X., Pang, Z.P., and Sudhof, T.C. (2009). Complexin controls the force transfer from SNARE complexes to membranes in fusion. *Science (New York, NY)* 323, 516-521.
- Melom, J.E., Akbergenova, Y., Gavornik, J.P., and Littleton, J.T. (2013). Spontaneous and evoked release are independently regulated at individual active zones. *J Neurosci* 33, 17253-17263.
- Meng, J., Wang, J., Lawrence, G.W., and Dolly, J.O. (2013). Molecular components required for resting and stimulated endocytosis of botulinum neurotoxins by glutamatergic and peptidergic neurons. *Faseb J* 27, 3167-3180.
- Miesenbock, G., De Angelis, D.A., and Rothman, J.E. (1998). Visualizing secretion and synaptic transmission with pH-sensitive green fluorescent proteins. *Nature* 394, 192-195.
- Miller, T.M., and Heuser, J.E. (1984). Endocytosis of synaptic vesicle membrane at the frog neuromuscular junction. *The Journal of cell biology* 98, 685-698.
- Mozhayeva, M.G., Sara, Y., Liu, X., and Kavalali, E.T. (2002). Development of vesicle pools during maturation of hippocampal synapses. *J Neurosci* 22, 654-665.
- Murthy, V.N., Sejnowski, T.J., and Stevens, C.F. (1997). Heterogeneous release properties of visualized individual hippocampal synapses. *Neuron* 18, 599-612.
- Murthy, V.N., and Stevens, C.F. (1998). Synaptic vesicles retain their identity through the endocytic cycle. *Nature* 392, 497-501.
- Murthy, V.N., and Stevens, C.F. (1999). Reversal of synaptic vesicle docking at central synapses. *Nature neuroscience* 2, 503-507.
- Mutch, S.A., Kensel-Hammes, P., Gadd, J.C., Fujimoto, B.S., Allen, R.W., Schiro, P.G., Lorenz, R.M., Kuyper, C.L., Kuo, J.S., Bajjalieh, S.M., *et al.* (2011). Protein quantification at the single vesicle level reveals that a subset of synaptic vesicle proteins are trafficked with high precision. *J Neurosci* 31, 1461-1470.
- Neher, E., and Marty, A. (1982). Discrete changes of cell membrane capacitance observed under conditions of enhanced secretion in bovine adrenal chromaffin cells. *Proceedings of the National Academy of Sciences of the United States of America* 79, 6712-6716.
- Neher, E., and Zucker, R.S. (1993). Multiple calcium-dependent processes related to secretion in bovine chromaffin cells. *Neuron* 10, 21-30.

- Neves, G., Gomis, A., and Lagnado, L. (2001). Calcium influx selects the fast mode of endocytosis in the synaptic terminal of retinal bipolar cells. *Proceedings of the National Academy of Sciences of the United States of America* *98*, 15282-15287.
- Neves, G., and Lagnado, L. (1999). The kinetics of exocytosis and endocytosis in the synaptic terminal of goldfish retinal bipolar cells. *The Journal of physiology* *515 (Pt 1)*, 181-202.
- Nosyreva, E., Szabla, K., Autry, A.E., Ryazanov, A.G., Monteggia, L.M., and Kavalali, E.T. (2013). Acute suppression of spontaneous neurotransmission drives synaptic potentiation. *J Neurosci* *33*, 6990-7002.
- Pang, Z.P., Bacaj, T., Yang, X., Zhou, P., Xu, W., and Sudhof, T.C. (2011). Doc2 supports spontaneous synaptic transmission by a Ca(2+)-independent mechanism. *Neuron* *70*, 244-251.
- Park, H., Li, Y., and Tsien, R.W. (2012). Influence of synaptic vesicle position on release probability and exocytotic fusion mode. *Science (New York, NY)* *335*, 1362-1366.
- Parsons, T.D., Lenzi, D., Almers, W., and Roberts, W.M. (1994). Calcium-triggered exocytosis and endocytosis in an isolated presynaptic cell: capacitance measurements in saccular hair cells. *Neuron* *13*, 875-883.
- Peled, E.S., Newman, Z.L., and Isacoff, E.Y. (2014). Evoked and spontaneous transmission favored by distinct sets of synapses. *Curr Biol* *24*, 484-493.
- Peng, A., Rotman, Z., Deng, P.Y., and Klyachko, V.A. (2012). Differential motion dynamics of synaptic vesicles undergoing spontaneous and activity-evoked endocytosis. *Neuron* *73*, 1108-1115.
- Pesold, C., Impagnatiello, F., Pisu, M.G., Uzunov, D.P., Costa, E., Guidotti, A., and Caruncho, H.J. (1998). Reelin is preferentially expressed in neurons synthesizing gamma-aminobutyric acid in cortex and hippocampus of adult rats. *Proc Natl Acad Sci U S A* *95*, 3221-3226.
- Peters, C., Bayer, M.J., Buhler, S., Andersen, J.S., Mann, M., and Mayer, A. (2001). Trans-complex formation by proteolipid channels in the terminal phase of membrane fusion. *Nature* *409*, 581-588.
- Peters, J.H., McDougall, S.J., Fawley, J.A., Smith, S.M., and Andresen, M.C. (2010). Primary afferent activation of thermosensitive TRPV1 triggers asynchronous glutamate release at central neurons. *Neuron* *65*, 657-669.

- Phillips, C.G., Harnett, M.T., Chen, W., and Smith, S.M. (2008). Calcium-sensing receptor activation depresses synaptic transmission. *J Neurosci* *28*, 12062-12070.
- Poea-Guyon, S., Ammar, M.R., Erard, M., Amar, M., Moreau, A.W., Fossier, P., Gleize, V., Vitale, N., and Morel, N. (2013). The V-ATPase membrane domain is a sensor of granular pH that controls the exocytotic machinery. *The Journal of cell biology* *203*, 283-298.
- Polo-Parada, L., Bose, C.M., and Landmesser, L.T. (2001). Alterations in transmission, vesicle dynamics, and transmitter release machinery at NCAM-deficient neuromuscular junctions. *Neuron* *32*, 815-828.
- Pratt, K.G., Zhu, P., Watari, H., Cook, D.G., and Sullivan, J.M. (2011). A novel role for γ -secretase: selective regulation of spontaneous neurotransmitter release from hippocampal neurons. *J Neurosci* *31*, 899-906.
- Pryor, P.R., Jackson, L., Gray, S.R., Edeling, M.A., Thompson, A., Sanderson, C.M., Evans, P.R., Owen, D.J., and Luzio, J.P. (2008). Molecular basis for the sorting of the SNARE VAMP7 into endocytic clathrin-coated vesicles by the ArfGAP Hrb. *Cell* *134*, 817-827.
- Qiu, S., Zhao, L.F., Korwek, K.M., and Weeber, E.J. (2006). Differential reelin-induced enhancement of NMDA and AMPA receptor activity in the adult hippocampus. *The Journal of neuroscience : the official journal of the Society for Neuroscience* *26*, 12943-12955.
- Raimondi, A., Ferguson, S.M., Lou, X., Armbruster, M., Paradise, S., Giovedi, S., Messa, M., Kono, N., Takasaki, J., Cappello, V., *et al.* (2011). Overlapping role of dynamin isoforms in synaptic vesicle endocytosis. *Neuron* *70*, 1100-1114.
- Raingo, J., Khvotchev, M., Liu, P., Darios, F., Li, Y.C., Ramirez, D.M., Adachi, M., Lemieux, P., Toth, K., Davletov, B., *et al.* (2012). VAMP4 directs synaptic vesicles to a pool that selectively maintains asynchronous neurotransmission. *Nature neuroscience* *15*, 738-745.
- Ramaswami, M., Krishnan, K.S., and Kelly, R.B. (1994). Intermediates in synaptic vesicle recycling revealed by optical imaging of *Drosophila* neuromuscular junctions. *Neuron* *13*, 363-375.
- Ramirez, D.M., and Kavalali, E.T. (2011). Differential regulation of spontaneous and evoked neurotransmitter release at central synapses. *Current opinion in neurobiology* *21*, 275-282.

- Ramirez, D.M., and Kavalali, E.T. (2012). The role of non-canonical SNAREs in synaptic vesicle recycling. *Cellular logistics* 2, 20-27.
- Ramirez, D.M., Khvotchev, M., Trauterman, B., and Kavalali, E.T. (2012). Vti1a identifies a vesicle pool that preferentially recycles at rest and maintains spontaneous neurotransmission. *Neuron* 73, 121-134.
- Regehr, W.G., Delaney, K.R., and Tank, D.W. (1994). The role of presynaptic calcium in short-term enhancement at the hippocampal mossy fiber synapse. *J Neurosci* 14, 523-537.
- Renger, J.J., Egles, C., and Liu, G. (2001). A developmental switch in neurotransmitter flux enhances synaptic efficacy by affecting AMPA receptor activation. *Neuron* 29, 469-484.
- Richards, D.A. (2009). Vesicular release mode shapes the postsynaptic response at hippocampal synapses. *The Journal of physiology* 587, 5073-5080.
- Richards, D.A., Bai, J., and Chapman, E.R. (2005). Two modes of exocytosis at hippocampal synapses revealed by rate of FM1-43 efflux from individual vesicles. *The Journal of cell biology* 168, 929-939.
- Rouze, N.C., and Schwartz, E.A. (1998). Continuous and transient vesicle cycling at a ribbon synapse. *J Neurosci* 18, 8614-8624.
- Rudolph, S., Overstreet-Wadiche, L., and Wadiche, J.I. (2011). Desynchronization of multivesicular release enhances purkinje cell output. *Neuron* 70, 991-1004.
- Ryan, T.A., Reuter, H., Wendland, B., Schweizer, F.E., Tsien, R.W., and Smith, S.J. (1993). The kinetics of synaptic vesicle recycling measured at single presynaptic boutons. *Neuron* 11, 713-724.
- Ryan, T.A., Smith, S.J., and Reuter, H. (1996). The timing of synaptic vesicle endocytosis. *Proceedings of the National Academy of Sciences of the United States of America* 93, 5567-5571.
- Sabatini, B.L., and Regehr, W.G. (1996). Timing of neurotransmission at fast synapses in the mammalian brain. *Nature* 384, 170-172.
- Saheki, Y., and De Camilli, P. (2012). Synaptic vesicle endocytosis. *Cold Spring Harbor perspectives in biology* 4, a005645.
- Sankaranarayanan, S., and Ryan, T.A. (2000). Real-time measurements of vesicle-SNARE recycling in synapses of the central nervous system. *Nature cell biology* 2, 197-204.

- Sankaranarayanan, S., and Ryan, T.A. (2001). Calcium accelerates endocytosis of vSNAREs at hippocampal synapses. *Nature neuroscience* 4, 129-136.
- Sara, Y., Virmani, T., Deak, F., Liu, X., and Kavalali, E.T. (2005). An isolated pool of vesicles recycles at rest and drives spontaneous neurotransmission. *Neuron* 45, 563-573.
- Scales, S.J., Finley, M.F., and Scheller, R.H. (2001). Cell biology. Fusion without SNAREs? *Science (New York, NY)* 294, 1015-1016.
- Scheuber, A., Rudge, R., Danglot, L., Raposo, G., Binz, T., Poncer, J.C., and Galli, T. (2006). Loss of AP-3 function affects spontaneous and evoked release at hippocampal mossy fiber synapses. *Proceedings of the National Academy of Sciences of the United States of America* 103, 16562-16567.
- Schoch, S., Deak, F., Konigstorfer, A., Mozhayeva, M., Sara, Y., Sudhof, T.C., and Kavalali, E.T. (2001). SNARE function analyzed in synaptobrevin/VAMP knockout mice. *Science (New York, NY)* 294, 1117-1122.
- Sharma, G., and Vijayaraghavan, S. (2003). Modulation of presynaptic store calcium induces release of glutamate and postsynaptic firing. *Neuron* 38, 929-939.
- Smith, C., and Neher, E. (1997). Multiple forms of endocytosis in bovine adrenal chromaffin cells. *The Journal of cell biology* 139, 885-894.
- Sochacki, K.A., Shtengel, G., van Engelenburg, S.B., Hess, H.F., and Taraska, J.W. (2014). Correlative super-resolution fluorescence and metal-replica transmission electron microscopy. *Nature methods* 11, 305-308.
- Soriano, E., and Del Rio, J.A. (2005). The cells of cajal-retzius: still a mystery one century after. *Neuron* 46, 389-394.
- Sudhof, T.C. (2000). The synaptic vesicle cycle revisited. *Neuron* 28, 317-320.
- Sudhof, T.C. (2004). The synaptic vesicle cycle. *Annual review of neuroscience* 27, 509-547.
- Sudhof, T.C. (2013). Neurotransmitter release: the last millisecond in the life of a synaptic vesicle. *Neuron* 80, 675-690.
- Sudhof, T.C., and Rothman, J.E. (2009). Membrane fusion: grappling with SNARE and SM proteins. *Science (New York, NY)* 323, 474-477.

- Sun, J., Pang, Z.P., Qin, D., Fahim, A.T., Adachi, R., and Sudhof, T.C. (2007). A dual-Ca²⁺-sensor model for neurotransmitter release in a central synapse. *Nature* 450, 676-682.
- Sun, J.Y., Wu, X.S., and Wu, L.G. (2002). Single and multiple vesicle fusion induce different rates of endocytosis at a central synapse. *Nature* 417, 555-559.
- Sun, T., Wu, X.S., Xu, J., McNeil, B.D., Pang, Z.P., Yang, W., Bai, L., Qadri, S., Molkenkin, J.D., Yue, D.T., *et al.* (2010). The role of calcium/calmodulin-activated calcineurin in rapid and slow endocytosis at central synapses. *J Neurosci* 30, 11838-11847.
- Sutton, M.A., Ito, H.T., Cressy, P., Kempf, C., Woo, J.C., and Schuman, E.M. (2006). Miniature neurotransmission stabilizes synaptic function via tonic suppression of local dendritic protein synthesis. *Cell* 125, 785-799.
- Sutton, M.A., and Schuman, E.M. (2005). Local translational control in dendrites and its role in long-term synaptic plasticity. *Journal of neurobiology* 64, 116-131.
- Sutton, M.A., Taylor, A.M., Ito, H.T., Pham, A., and Schuman, E.M. (2007). Postsynaptic decoding of neural activity: eEF2 as a biochemical sensor coupling miniature synaptic transmission to local protein synthesis. *Neuron* 55, 648-661.
- Takamori, S., Holt, M., Stenius, K., Lemke, E.A., Gronborg, M., Riedel, D., Urlaub, H., Schenck, S., Brugger, B., Ringler, P., *et al.* (2006). Molecular anatomy of a trafficking organelle. *Cell* 127, 831-846.
- Teng, H., and Wilkinson, R.S. (2005). Clathrin-mediated endocytosis in snake motor terminals is directly facilitated by intracellular Ca²⁺. *The Journal of physiology* 565, 743-750.
- Thomas, P., Lee, A.K., Wong, J.G., and Almers, W. (1994). A triggered mechanism retrieves membrane in seconds after Ca²⁺-stimulated exocytosis in single pituitary cells. *The Journal of cell biology* 124, 667-675.
- Thomas, P., Surprenant, A., and Almers, W. (1990). Cytosolic Ca²⁺, exocytosis, and endocytosis in single melanotrophs of the rat pituitary. *Neuron* 5, 723-733.
- Thomas, P., Wong, J.G., and Almers, W. (1993). Millisecond studies of secretion in single rat pituitary cells stimulated by flash photolysis of caged Ca²⁺. *The EMBO journal* 12, 303-306.

- Torri-Tarelli, F., Grohovaz, F., Fesce, R., and Ceccarelli, B. (1985). Temporal coincidence between synaptic vesicle fusion and quantal secretion of acetylcholine. *The Journal of cell biology* *101*, 1386-1399.
- Trommsdorff, M., Gotthardt, M., Hiesberger, T., Shelton, J., Stockinger, W., Nimpf, J., Hammer, R.E., Richardson, J.A., and Herz, J. (1999). Reeler/Disabled-like disruption of neuronal migration in knockout mice lacking the VLDL receptor and ApoE receptor 2. *Cell* *97*, 689-701.
- Turrigiano, G. (2012). Homeostatic synaptic plasticity: local and global mechanisms for stabilizing neuronal function. *Cold Spring Harbor perspectives in biology* *4*, a005736.
- van den Bogaart, G., and Jahn, R. (2011). Counting the SNAREs needed for membrane fusion. *Journal of molecular cell biology* *3*, 204-205.
- Van der Kloot, W. (1996). Spontaneous and unquantal-evoked endplate currents in normal frogs are indistinguishable. *The Journal of physiology* *492 (Pt 1)*, 155-162.
- Van Hook, M.J., and Thoreson, W.B. (2012). Rapid synaptic vesicle endocytosis in cone photoreceptors of salamander retina. *J Neurosci* *32*, 18112-18123.
- Vardjan, N., Stenovec, M., Jorgacevski, J., Kreft, M., and Zorec, R. (2007). Subnanometer fusion pores in spontaneous exocytosis of peptidergic vesicles. *J Neurosci* *27*, 4737-4746.
- Virmani, T., Ertunc, M., Sara, Y., Mozhayeva, M., and Kavalali, E.T. (2005). Phorbol esters target the activity-dependent recycling pool and spare spontaneous vesicle recycling. *J Neurosci* *25*, 10922-10929.
- von Gersdorff, H., and Matthews, G. (1994). Inhibition of endocytosis by elevated internal calcium in a synaptic terminal. *Nature* *370*, 652-655.
- Vyleta, N.P., and Smith, S.M. (2011). Spontaneous glutamate release is independent of calcium influx and tonically activated by the calcium-sensing receptor. *J Neurosci* *31*, 4593-4606.
- Walter, A.M., Haucke, V., and Sigrist, S.J. (2014). Neurotransmission: spontaneous and evoked release filing for divorce. *Curr Biol* *24*, R192-194.
- Wan, Q.F., Vila, A., Zhou, Z.Y., and Heidelberger, R. (2008). Synaptic vesicle dynamics in mouse rod bipolar cells. *Visual neuroscience* *25*, 523-533.

- Wan, Q.F., Zhou, Z.Y., Thakur, P., Vila, A., Sherry, D.M., Janz, R., and Heidelberger, R. (2010). SV2 acts via presynaptic calcium to regulate neurotransmitter release. *Neuron* *66*, 884-895.
- Wang, D., Epstein, D., Ossama, K., Sankaranarayanan, S., Williamson, R.W., Fayyazuddin, A., Quioco, F.A., and Hiesinger, P.R. (2014). Ca²⁺/calmodulin regulates SNARE assembly and spontaneous neurotransmitter release via v-ATPase subunit V0a1. *Cell Biol.*
- Washbourne, P., Thompson, P.M., Carta, M., Costa, E.T., Mathews, J.R., Lopez-Bendito, G., Molnar, Z., Becher, M.W., Valenzuela, C.F., Partridge, L.D., *et al.* (2002). Genetic ablation of the t-SNARE SNAP-25 distinguishes mechanisms of neuroexocytosis. *Nature neuroscience* *5*, 19-26.
- Watanabe, S., Rost, B.R., Camacho-Perez, M., Davis, M.W., Sohl-Kielczynski, B., Rosenmund, C., and Jorgensen, E.M. (2014). Ultrafast endocytosis at mouse hippocampal synapses. *Nature* *504*, 242-247.
- Wierda, K.D., and Sorensen, J.B. (2014). Innervation by a GABAergic neuron depresses spontaneous release in glutamatergic neurons and unveils the clamping phenotype of synaptotagmin-1. *J Neurosci* *34*, 2100-2110.
- Wu, L.G., and Betz, W.J. (1996). Nerve activity but not intracellular calcium determines the time course of endocytosis at the frog neuromuscular junction. *Neuron* *17*, 769-779.
- Wu, W., Xu, J., Wu, X.S., and Wu, L.G. (2005). Activity-dependent acceleration of endocytosis at a central synapse. *J Neurosci* *25*, 11676-11683.
- Wu, X.S., McNeil, B.D., Xu, J., Fan, J., Xue, L., Melicoff, E., Adachi, R., Bai, L., and Wu, L.G. (2009). Ca²⁺ and calmodulin initiate all forms of endocytosis during depolarization at a nerve terminal. *Nature neuroscience* *12*, 1003-1010.
- Xu, J., Pang, Z.P., Shin, O.H., and Sudhof, T.C. (2009). Synaptotagmin-1 functions as a Ca²⁺ sensor for spontaneous release. *Nature neuroscience* *12*, 759-766.
- Xu, W., Morishita, W., Buckmaster, P.S., Pang, Z.P., Malenka, R.C., and Sudhof, T.C. (2012). Distinct neuronal coding schemes in memory revealed by selective erasure of fast synchronous synaptic transmission. *Neuron* *73*, 990-1001.
- Yamashita, T., Hige, T., and Takahashi, T. (2005). Vesicle endocytosis requires dynamin-dependent GTP hydrolysis at a fast CNS synapse. *Science (New York, NY)* *307*, 124-127.

- Yao, C.K., Lin, Y.Q., Ly, C.V., Ohshima, T., Haueter, C.M., Moiseenkova-Bell, V.Y., Wensel, T.G., and Bellen, H.J. (2009). A synaptic vesicle-associated Ca²⁺ channel promotes endocytosis and couples exocytosis to endocytosis. *Cell* *138*, 947-960.
- Yao, J., Gaffaney, J.D., Kwon, S.E., and Chapman, E.R. (2011). Doc2 is a Ca²⁺ sensor required for asynchronous neurotransmitter release. *Cell* *147*, 666-677.
- Zhang, Q., Cao, Y.Q., and Tsien, R.W. (2007). Quantum dots provide an optical signal specific to full collapse fusion of synaptic vesicles. *Proceedings of the National Academy of Sciences of the United States of America* *104*, 17843-17848.
- Zhang, Q., Li, Y., and Tsien, R.W. (2009). The dynamic control of kiss-and-run and vesicular reuse probed with single nanoparticles. *Science (New York, NY)* *323*, 1448-1453.
- Zhang, W., Wang, D., Volk, E., Bellen, H.J., Hiesinger, P.R., and Quirocho, F.A. (2008). V-ATPase V0 sector subunit a1 in neurons is a target of calmodulin. *The Journal of biological chemistry* *283*, 294-300.
- Zhou, P., Pang, Z.P., Yang, X., Zhang, Y., Rosenmund, C., Bacaj, T., and Sudhof, T.C. (2013). Syntaxin-1 N-peptide and Habc-domain perform distinct essential functions in synaptic vesicle fusion. *The EMBO journal* *32*, 159-171.
- Zhu, Y., Xu, J., and Heinemann, S.F. (2009). Two pathways of synaptic vesicle retrieval revealed by single-vesicle imaging. *Neuron* *61*, 397-411.
- Zucker, R.S. (2003). Can a synaptic signal arise from noise? *Neuron* *38*, 845-846.
- Zucker, R.S., and Regehr, W.G. (2002). Short-term synaptic plasticity. *Annual review of physiology* *64*, 355-405.